NBS SPECIAL PUBLICATION 400-50

U.S. DEPARTMENT OF COMMERCE / National Bureau of Standards

Semiconductor Measurement Technology:

Reliability Technology for Cardiac Pacemakers III

A Workshop Report

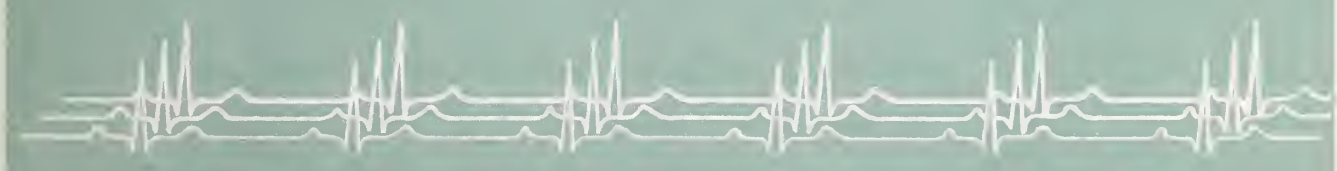

NATIONAL BUREAU OF STANDARDS

The National Bureau of Standards[1] was established by an act of Congress March 3, 1901. The Bureau's overall goal is to strengthen and advance the Nation's science and technology and facilitate their effective application for public benefit. To this end, the Bureau conducts research and provides: (1) a basis for the Nation's physical measurement system, (2) scientific and technological services for industry and government, (3) a technical basis for equity in trade, and (4) technical services to promote public safety. The Bureau's technical work is performed by the National Measurement Laboratory, the National Engineering Laboratory, and the Institute for Computer Sciences and Technology.

THE NATIONAL MEASUREMENT LABORATORY provides the national system of physical and chemical and materials measurement; coordinates the system with measurement systems of other nations and furnishes essential services leading to accurate and uniform physical and chemical measurement throughout the Nation's scientific community, industry, and commerce; conducts materials research leading to improved methods of measurement, standards, and data on the properties of materials needed by industry, commerce, educational institutions, and Government; provides advisory and research services to other Government Agencies; develops, produces, and distributes Standard Reference Materials; and provides calibration services. The Laboratory consists of the following centers:

Absolute Physical Quantities[2] — Radiation Research — Thermodynamics and Molecular Science — Analytical Chemistry — Materials Science.

THE NATIONAL ENGINEERING LABORATORY provides technology and technical services to users in the public and private sectors to address national needs and to solve national problems in the public interest; conducts research in engineering and applied science in support of objectives in these efforts; builds and maintains competence in the necessary disciplines required to carry out this research and technical service; develops engineering data and measurement capabilities; provides engineering measurement traceability services; develops test methods and proposes engineering standards and code changes; develops and proposes new engineering practices; and develops and improves mechanisms to transfer results of its research to the utlimate user. The Laboratory consists of the following centers:

Applied Mathematics — Electronics and Electrical Engineering[2] — Mechanical Engineering and Process Technology[2] — Building Technology — Fire Research — Consumer Product Technology — Field Methods.

THE INSTITUTE FOR COMPUTER SCIENCES AND TECHNOLOGY conducts research and provides scientific and technical services to aid Federal Agencies in the selection, acquisition, application, and use of computer technology to improve effectiveness and economy in Government operations in accordance with Public Law 89-306 (40 U.S.C. 759), relevant Executive Orders, and other directives; carries out this mission by managing the Federal Information Processing Standards Program, developing Federal ADP standards guidelines, and managing Federal participation in ADP voluntary standardization activities; provides scientific and technological advisory services and assistance to Federal Agencies; and provides the technical foundation for computer-related policies of the Federal Government. The Institute consists of the following divisions:

Systems and Software — Computer Systems Engineering — Information Technology.

[1]Headquarters and Laboratories at Gaithersburg, Maryland, unless otherwise noted; mailing address Washington,D.C. 20234.
[2]Some divisions within the center are located at Boulder, Colorado, 80303.

The National Bureau of Standards was reorganized, effective April 9, 1978.

Semiconductor Measurement Technology:

Reliability Technology for Cardiac Pacemakers III — A Workshop Report

Report of a Workshop
Held at the National Bureau of Standards
Gaithersburg, MD, October 19-20, 1977

Harry A. Schafft, Editor

Electron Devices Division
Center for Electronics and
Electrical Engineering
National Engineering Laboratory
National Bureau of Standards
Washington, DC 20234

U.S. DEPARTMENT OF COMMERCE, Juanita M. Kreps, Secretary

Jordan J. Baruch, Assistant Secretary for Science and Technology

NATIONAL BUREAU OF STANDARDS, Ernest Ambler, Director

Issued June 1979

Library of Congress Catalog Card Number: 78-600158

National Bureau of Standards Special Publication 400-50
Nat. Bur. Stand. (U.S.), Spec. Publ. 400-50, 134 pages (June 1979)
CODEN: XNBSAV

U.S. GOVERNMENT PRINTING OFFICE
WASHINGTON: 1979

For sale by the Superintendent of Documents, U.S. Government Printing Office, Washington, D.C. 20402

Stock No. 003-003-02076-1 Price $4.50

Semiconductor Measurement Technology:

Reliability Technology for Cardiac Pacemakers III

— A Workshop Report —

Harry A. Schafft, Editor

Table of Contents

PREFACE

The workshop on reliability technology for cardiac pacemakers was conducted as part of the Semiconductor Technology Program in the Electron Devices Division of the National Bureau of Standards (NBS).

The Semiconductor Technology Program serves to focus NBS efforts to enhance the performance, interchangeability, and reliability of discrete semiconductor devices and integrated circuits through improvements in measurement technology for use in specifying materials in national and international commerce and for use by industry in controlling device fabrication processes. Its major thrusts are the development of carefully and well-documented test procedures and associated technology and the dissemination of such information to the electronics community. Application of the output by industry will contribute to higher yields, lower cost, and higher reliability of semiconductor devices. The output provides a common basis for the purchase specifications of government agencies which will lead to greater economy in government procurement. In addition, improved measurement technology will provide a basis for controlled improvements in fabrication processes and in essential device characteristics.

Essential assistance to the Program is received from the semiconductor industry through cooperative experiments and technical exchanges. NBS interacts with industrial users and suppliers of semiconductor devices through participation in standardizing organizations; through direct consultations with device and material suppliers, government agencies, and other users; and through symposia and workshops. Progress reports have been regularly prepared for issuance in the NBS Special Publication 400- subseries. Progress briefs are issued in the NBSIR series to describe the work in the Semiconductor Technology Program on a periodic basis and also list new reports as they become available. More detailed reports such as state-of-the-art reviews, literature compilations, and summaries of technical efforts conducted within the Program are issued as these activities are completed. Reports of this type which are published by NBS also appear in the Special Publicaiton 400- subseries.

Semiconductor Measurement Technology:

Reliability Technology for Cardiac Pacemakers III

— A Workshop Report —

Harry A. Schafft, Editor

Abstract: The workshop, third in a series, served as a forum for pacemaker manufacturers and other interested parties to address technical questions relevant to the enhancement and assurance of cardiac pacemaker reliability. Extended summaries are provided of 27 talks and of eight sets of group encounter discussions on the following topic areas: microcalorimetric measurements to evaluate nondestructively batteries used in pacemakers; qualification procedures, end-of-life prediction, and neutron radiography interrogation of lithium-based batteries; measurement of moisture; moisture effects on the reliability of pacemakers and components; electrostatic-induced damage to semiconductor devices; procurement of high reliability semiconductor components; automated testing of pacemakers; actuarial analyses of lead and pacemaker failures; pacemaker case welding processes; surface contamination measurements; corrosion and accelerated tests for metallic materials; and conformal coatings for pacemaker applications.

Key Words: Automated testing; batteries; cardiac pacemakers; contamination; corrosion; electrostatic-induced damage; hermeticity; hybrid devices; leak testing; measurement technology; microcalorimetry; moisture; nondestructive testing; pacemaker leads; process control; reliability; semiconductor devices; welding.

1. INTRODUCTION

The third workshop on reliability technology for cardiac pacemakers was held on October 19-20, 1977 at the National Bureau of Standards, Gaithersburg, Maryland, in response to continued strong interest in such workshops by the pacemaker community.

The NBS-sponsored workshop was designed to provide a forum for pacemaker manufacturers and other interested parties to address the following technical questions relevant to the enhancement and assurance of cardiac pacemaker reliability:

- microcalorimetric measurements of batteries
- battery evaluation, characterization, and quality control
- moisture measurement and control
- electronic parts and systems procurement, quality assurance, and testing
- materials and assembly processes

These topics were addressed by a total of 27 papers in five sessions.

The format of the workshop consisted of two series of presentations in which speakers were provided time in joint meetings to discuss their work in highlight form. Each series was followed by group encounters where speakers were provided time to respond to questions and to provide more details of their work in small groups. Speakers in each series were divided appropriately into four speaker groups to visit, in turn, the four groups into which the remaining participants were divided. Highlights of these encounters were summarized at a final joint meeting by scribes who accompanied the speaker groups.

The workshop was attended predominantly by technical representatives of pacemaker manufacturers, manufacturers of batteries used in pacemakers, and suppliers of materials, components, and services to the pacemaker community. Also among the attendees, which totaled 157, were representatives of the Food and Drug Administration and other industrial and governmental organizations concerned with reliability.

Highlights of the presentations and group encounters are given in the next section of this report followed by extended summaries of the presentations in each of the five sessions. These summaries were prepared by the authors of the presentations. Their technical accuracy is the responsibility of the authors. Summaries of the group encounters, written by the scribes who accompanied the speaker groups, complete the report proper. The workshop program and credits are included in Appendix A.

Certain commercial materials and equipment have been identified by the authors of the extended summaries and the scribes in order to specify usage adequately. This identification does not imply recommendation or endorsement by the National Bureau of Standards, nor does it imply that the materials and equipment are necessarily the best available for the purpose.

2. HIGHLIGHTS

Microcalorimetry is a new, potentially powerful nondestructive measurement tool to evaluate the design, behavior, and quality of batteries for use in cardiac pacemakers. Discussion of this tool, begun by Prosen and Colbert of NBS at the previous workshop,[1] was continued by them and others in the present one. Several special microcalorimeters were described and measurement results reported. Absolute measurements of less than 5 μW with precisions of better than 1.0 μW were reported. The use of these instruments to measure internal leakage, corrosion reactions, and other chemical and electrochemical reactions were discussed. While microcalorimetry is well-suited to study different construction and designs and to determine effects of fabrication changes, it is not suited for screen testing because of the length of time to make measurements.

The prediction of the life of lithium-iodine cells was discussed with much interest because of their growing use in pacemakers and because of problems with developing adequate accelerated tests and in predicting the end-of-life characteristics of these cells. Gerrard of Medtronic, Inc., described a computer simulation model for lithium-iodine battery longevity projection which was devised from and is calibrated by accelerated test data from individual cells. Schneider of the Catalyst Research Corporation described methods to approximate nominal battery run-down curves. In doing so, he cautioned that the use of high current drains and high temperatures as stress tests to predict end of life are not satisfactory because such stresses introduce reactions that are not present at 37°C. Furthermore, a model used to determine the life of such cells subjected initially to high current drains followed by typical pacemaker current drains may provide optimistic estimates. The sharpness of the

[1] Schafft, H. A., Ed, *Semiconductor Measurement Technology:* Reliability Technology for Cardiac Pacemakers II — A Workshop Report, NBS Special Publication 400-42 (August 1977).

knee of the voltage versus time plots of such cells near end of life, and hence the warning time available to physicians, remains an area of contention. Schneider called for improved circuit designs to provide adequate warning of end of life, even for worst case conditions.

Other lithium-based batteries are also in use. As well as the lithium-iodine cell, the lithium-thionyl chloride and the lithium-silver chromate cells were discussed in papers describing steps used to assure their quality.

Kraus of the Catalyst Research Corporation reported that the corrosive effects of the iodine poly-2-vinylpyridine (P2VP) depolarizer complex material in lithium-iodine cells are affected by moisture.

A new tool to view the depletion of lithium-iodine cells was proposed by Garrett of NBS. He showed preliminary results of using thermal neutron radiography to view cell interiors nondestructively. He reported seeing the development of nonuniform structures in the electrolyte with use, and a relationship between the degree of battery depletion and the extent of darkened areas observable in neutron radiographs. The absorption characteristics of thermal neutrons are such that the electrolyte in the lithium-based cells can be viewed even though it is encased in a stainless steel jacket — a task impossible for x-rays. X-rays have been been used extensively to determine the depletion of mercury-based cells. These cells are now being rapidly replaced by lithium-based cells as the typical power source for pacemakers.

Moisture, its measurement, efforts to eliminate it, and its effects inside pacemakers and semiconductor components were discussed by a number of speakers. Thomas of RADC gave an invited overview paper in which he described various aspects and problems in the accurate measurement of moisture, mentioned work in the field, and described the methods for measuring moisture in semiconductor components which have been incorporated in MIL-STD 883B and will be in force in 1978.

While maximum allowed limits on moisture content to be specified in MIL-STD 38510 are 5,000 ppm_v for integrated circuits and 6,000 ppm_v for hybrid circuits, speakers and attendees maintained that much lower limits are needed to achieve pacemaker reliability goals.

In the face of these measurement needs, Perkins of Rockwell International presented early results of an interlaboratory experiment that show severe deficiencies in the precision of moisture content measurements with mass spectrometers. Early results indicate over one order of magnitude variability in measurements of special packages sealed with moisture at levels ranging from 1,000 to 10,000 ppm_v that had been sent to prominent laboratories involved in moisture analysis.

Hasegawa described the capabilities of the NBS humidity laboratory and discussed NBS' responsibility for disseminating standards for humidity measurement and for providing calibration services.

Ferreira of Telectronics Ltd. reported the results of gas analyses of various makes of hermetically sealed pacemakers and cited the importance of removing the moisture from compo-

nent parts and sealing in a dry environment to assure that moisture is not sealed inside the pacemaker.

Wilary of Medtronic Inc. described baking procedures and process changes for reducing moisture levels in hermetically sealed pacemakers and the use of the mass spectrometer and moisture sensors to evaluate materials and processing changes to reduce moisture content.

Regarding moisture which may penetrate hermetic packages through leaks after assembly, Der Marderosian of Raytheon described analyses which indicate that the moisture ingress rate is from two to three orders of magnitude less than for the standard air leak rate in the range from 10^{-1} to 10^{-5} atm·cm^3/s. Also, his data suggest that the leak rate specifications specified by the military for semiconductor components may be too lenient for high reliability applications.

The procurement and assurance of high reliability electronic parts for pacemakers remain subjects of critical concern. Gerz of the Cordis Corporation outlined basic considerations for the design, procurement, and testing of hybrid circuits. The need for close communication between circuit vendor and user, as can be achieved in a captive line and less so in a dedicated line, was cited as critical because of the need for the vendor to report every significant processing change. Test methods in MIL-STD 883 are relied on heavily in qualification and acceptance testing. Gerz also described burn-in tests that require zero failures after a 120- to 240-hour test in order to qualify a production lot of hybrid semiconductor circuits.

The importance of building-in rather than testing-in reliability in circuits produced on a normal production line was also stressed by Blanco of SGS-ATES SpA, an Italian integrated circuit manufacturer.

An additional dimension to obtaining high reliability components was also discussed: component vendors are reluctant to sell their products to pacemaker manufacturers if they are to be part of pacemakers implanted in humans. The fear of legislative, regulatory, and legal consequences of pacemaker failure in the present environment interferes with the availability of such components and the adequate utilization of modern electronic technology by pacemaker manufacturers.

Design and economic aspects in developing automated test systems for pacemakers were incorporated into design guidelines by Meyering of Motorola (formerly with Custom Devices). As an example in the use of these guidelines, he described a calculator-based system for testing pacemakers which he built. The use of microprocessors in such a system is not now economical because of the tremendous hidden costs in software development.

Static electricity can cause not only immediate device failure but also latent damage which can degrade device performance or cause premature failure during operation. This was the message that Walker of the Reliability Analysis Center (RAC) had to offer. He also discussed latent failure mechanisms and precautions in design, packaging, and handling of semiconductor components. Both MOS and bipolar components are susceptible to electrostatic-

induced damage. For guidance in protection from electrostatic degradation, references were made to appropriate MIL-STD 38510 slash sheets and a future monograph from RAC on the subject.

Factors to consider in the selection and in the use of a process for welding cardiac pacemaker enclosures were discussed at length by Bangs of the IIT Research Institute and by Llewellyn of Ebtec Corporation. The laser, electron beam, plasma arc, and gas tungsten arc processes were reviewed. Important factors to consider in choosing which to use are the joint design and the ability to control alignment during welding. The biggest problem cited in making a good weld is the compositional variability of the materials being welded. The importance of controlling the welding process is the more critical because there is no satisfactory means of nondestructively testing the pacemaker weld after it is made.

Pertinent to good welding as well as adhesive bonding and encapsulation is contamination of the surfaces involved. Gilman of Medtronic, Inc. discussed the measurement of surface contamination using a contact-angle goniometer to determine the types of contamination present and the wettability of the surfaces to be encapsulated. Because it is impossible to prevent the adsorption of water vapor and organic contaminants from the air to reduce wettability of the surface, processes and adhesives must be designed in such a way to insure wettability of the surface to the adhesive at the time of encapsulation.

The results of testing a number of materials for use as conformal coatings of electronic components in hermetically sealed pacemaker cases were described by Thornton of Cardiac Pacemakers, Inc. The reason for the interest in conformal coatings is in avoiding the filling of pacemaker interiors with epoxy to serve as a barrier to water vapor. The material Parylene C, a monochlorinated xylene with chlorine substituted in one of the alkyl positions, was found to be the most acceptable coating with performance comparable to epoxy potting. The most prevalent failure mode of polymeric conformal coatings was felt to be a lack of adequate adhesion to the substrate. A method was described in the group encounters for applying Parylene C which would minimize adhesion problems.

The susceptibility to corrosion of various implant metals used for pacemaker cases was discussed by Schaldach and Thull of The University of Erlangen-Nürnberg. They suggested that at the present time the use of the cobalt-nickel-based stainless steel alloy MP-35N is a superior choice over the use of titanium. The importance of the influence of material contaminants on a metal's performance in a corrosive environment and the need to eliminate or reduce such contaminants were stressed repeatedly in discussions.

3. EXTENDED SUMMARIES OF WORKSHOP PAPERS

3.1 Session I Microcalorimetric Measurements

3.1.1 Pacemaker Battery Microcalorimetry

William S. Holmes
Wilson Greatbatch Ltd.
10,000 Wehrle Drive
Clarence, NY 14031
(716) 759-6901

Tests of batteries fall into two classes, destructive and nondestructive. The former, while useful, are last-resort investigations which foreclose further studies of battery performance. Until quite recently, the latter were confined to the use of x-rays, external-case visual examination, and electrical measurements. With the application of microcalorimetry to battery studies by Prosen[1] of NBS and Berger[2] of NIH, however, we have a potentially powerful new tool for studying battery behavior. Internal leakage, corrosion reactions, and other chemical or electrochemical reactions can be assessed by a microcalorimeter. The limits to the information one can secure through measurement of endothermic or exothermic heats of reaction are imposed by the stability and sensitivity of the calorimeter and the ability of the experimenter to design test sequences which permit the separation of different reactions.

The calorimeter we use isolates a copper battery test chamber inside a massive aluminum heat sink. Bismuth telluride thermoelectric module sensors[3] couple the test chamber to the heat sink and thereby measure the heat flow from the battery to the heat sink via the copper test chamber. This assembly is decoupled thermally from the environment by alternate layers of insulation and heavy aluminum shells. The temperature of the shell closest to the heat sink is maintained at 37°C ± 0.005°C. Electrical output of the bismuth telluride sensors is amplified for display on an ink-pen strip chart recorder. When the thermally sealed calorimeter has stabilized with no specimen in the test chamber and a baseline established, a prewarmed battery is lowered into the test chamber, and the heat sink and shells are thermally sealed again using aluminum plugs. Upon recovery from the insertion transient, the inked trace exhibits an offset from the baseline, which through previous calibrations can be converted to microwatts of dissipation. Sensitivities of less than 1 μW and absolute accuracies of less than 5 μW are possible.

---

[1]Prosen, E. J., Goldberg, R. N., Staples, B. R., Boyd, R. N., and Armstrong, J. P., Microcalorimetry Applied to Biochemical Processes, *Thermal Analysis: Comparative Studies on Materials*, H. Kambe and T. D. Gern, Eds, pp. 253-289 (Kodansha Ltd. and John Wiley and Sons, Tokyo and New York, 1974).

[2]Private communication.

[3]Cambion 801-2001-01.

The WGLtd. 752 pacemaker battery contains two lithium-iodine cells which function in parallel and are encapsulated in a pair of halar[4] cups which are heat sealed into a closed package. Cyanoacrylate adhesive is used in the sealing process. The resultant sealed package is potted in polyester resin and cemented with epoxy into a stainless steel can. After lead attachment, a stainless steel top is welded onto the can. The iodine of the electrochemical cell is reacted with poly-2-vinylpyridine (P2VP). The iodine reacts chemically with the P2VP in the lithium coating for a while after being poured into the cell.

In order to separate the heat contributions of the components of the WGLtd. 752 battery, a series of partial batteries was constructed as listed in table 1. Dissipation measurements show that a normal WGLtd. 752 dissipates 60 to 85 μW, of which 10 to 15 μW can be ascribed to electrochemically inactive iodine-P2VP reactions, and 17 to 30 μW to other electrochemically inactive components, leaving 15 to 60 μW to be accounted for by internal electrical leakage or by other heat generation mechanisms.

Table 1. Dissipation Measurements of Completed and Partial Batteries.

Construction	Serial Number	Date of Assembly	Date of Measurement	Dissipation μW
Iodine/P2VP complex only in heat-sealed cup in welded can (WGLtd. 752)	10796	29 July 76	5 Aug 76	10
	10797	29 July 76	5 Aug 76	15
	10798	29 July 76	5 Aug 76	15
No Iodine/P2VP complex; all else as normal battery (WGLtd. 752)	10790	29 July 76	16 Aug 76	29.5
	10791	29 July 76	19 Aug 76	21.5
	10792	29 July 76	25 Aug 76	17
Normal WGLtd. 752	11585	12 Mar 76	26 July 76	80
	11585	12 Mar 76	28 July 76	80
	11540	12 Mar 76	30 July 76	60
	9960	28 Feb 76	9 Aug 76	85
	11393	4 Mar 76	11 Aug 76	75
Lithium uncoated; all else as normal battery (WGLtd. 752)	10781	29 July 76	17 Aug 76	25.5
	10782	29 July 76	23 Aug 76	17
	10783	29 July 76	27 Aug 76	15
Polyester Only	2.2 grams	19 July 76	23 July 76	55
Epoxy Only	3 drops	17 July 76	20 July 76	26

[4]One of the few plastic materials that does not become highly conductive in the presence of iodine.

Studies have also been made of the heat evolution of batteries in the calorimeter under a variety of load conditions. This approach necessitates the installation of very fine wires leading from the battery to external loads and to measurement instruments. The thermodynamics of a battery in an isothermal constant pressure situation are described by the Gibbs free energy, G, defined as:

$$\Delta G = \Delta H - T\Delta S \ ,$$

where: H = enthalpy,
T = temperature, and
S = entropy.

From this relation, one can derive the relation for the measured heat, Q_m:

$$Q_m = T\Delta S + \Delta G + I^2Rt + \Delta H_{SD} + Q_i \ ,$$

where: I = current,
R = external load,
t = time,
ΔH_{SD} = heat of self-discharge, and
Q_i = other reactions.

For a unit time and known constants including heat of reaction for lithium-iodine, one can obtain:

$$\Delta H_{SD} + Q_i = Q_m - (2.82738 - E)I \ ,$$

where: E = voltage at battery terminals under load.

The results of load experiments on a WGLtd. 752 type battery are presented in table 2. The indicated loads are applied while the battery is in the calorimeter, each for a time sufficient for the battery to reach thermal stability. The results are consistent with expected levels of dissipation for the iodine/P2VP complex plus the polyester resin, the epoxy resin, and the cyanoacrylate adhesive. They also indicate that it is possible to identify an internal high resistance short if it generates in excess of about 50 μW. This would correspond to an internal current of approximately 18 μA which should be compared to a pacemaker drain of approximately 27 μA. From a practical point of view, however, this type of measurement is useful mostly as a research tool (1) to identify faults in preproduction prototypes immediately after fabrication and (2) to confirm conjectures based on electrical measurements prior to destructive analysis.

A larger number (67) of WGLtd. 755s have been measured after at least four months of test.[5] All measurements were made with the battery under no load. This permits the characterization of the distribution of dissipation for normal WGLtd. 755 batteries. Table 3 shows the dissipation distribution of these bat-

[5]The interior volume of the case is filled with electrolyte to form a grounded case type battery.

teries. The spread in values is far in excess of the measurement uncertainty so we conclude that the battery design exhibits this much variation in dissipation.

From the work completed to date, it can be concluded that a large amount of heat is dissipated from the lithium-iodine battery chemicals early in its life but that most of this heat comes from chemical as opposed to electrochemical reactions. The microcalorimeter can usefully screen battery prototypes and serve as a pre-destructive analysis guide for battery dissection. As a research tool, it can be used to study dynamics of battery loading effects, although we have yet to carry out more than cursory work in this area.

Table 2. Loaded Battery (model 752, serial number 14) Calorimetric Study.

R (kΩ)	E (V)	Q_m (μW)	$\Delta H_{SD} + Q_s$ (μW)
Open Circuit	2.803	20.0	20.0
100	2.779	19.6	18.5
50	2.757	20.0	16.1
20	1.697	40.0	22.4
10	2.568	85.0	18.4

Table 3. WGLtd. 755 Dissipation Distribution

Dissipation Ranges (μW)	Number of Batteries
-5 to 0	2
> 0 to 10	12
>10 to 20	16
>20 to 30	11
>30 to 40	11
>40 to 50	8
>50 to 60	2
>60 to 70	0
>70 to 80	2
>80 to 90	0
>90 to 100	1
>100	2

3.1.2 The Characterization of Internal Power Losses in Pacemaker Batteries by Calorimetry

L. D. Hansen
Thermochemical Institute
and Department of Chemistry
Brigham Young University
Provo, UT 84602
(801) 374-1211 x4795

R. M. Hart
Tronac, Inc.
1804 South Columbia Lane
Orem, UT 84057
(801) 224-1131

One of the limits on the operational life of pacemakers is the battery which is used as a power source. All batteries are subject to internal self-discharge which, in turn, limits or shortens the life of the batteries. This self-discharge can result from three processes: (1) migration and direct chemical combination of anode or cathode substances, (2) spontaneous decomposition of the anode or cathode, and (3) reaction of the anode or cathode with contaminant gases or some battery component that was supposedly inert. The rates of these self-discharge processes can be dependent on or independent of the current being drawn from the battery. Since self-discharge is essentially a chemical reaction occurring inside the battery, it can be measured and studied by determining the rate of heat production of the battery in a calorimeter.[1-5] The possibility also exists for developing the calorimetric method into a nondestructive quality control test to eliminate batteries with abnormally high self-discharge rates.

The purposes of this paper are: (1) to describe a calorimeter which was designed specifically for studying pacemaker batteries, (2) to give a thermodynamic basis for determining the dependence of the rate of self-discharge on electrical current in the battery, and (3) to present some of the results which have been obtained on various types of batteries.

The calorimeter used is a twin cell differential heat flow instrument[6] as shown in figure 1. The calorimeter has a peak-to-peak noise level of less than 0.3 μW, a time constant of 6 min, and a precision better than 1 μW for a battery measurement. The calorimeter consists of an aluminum block about 6 in. (15 cm) wide, 7 in. (18 cm) high, and 12 in. (30 cm) long with a tapered channel about 4 in. (10 cm) wide, 4 in. (10 cm) deep, and 10 in. (25 cm) long cut into it; four wedges of 1-in. (2.5-cm) thick aluminum, which are placed in the channel;

---

[1]Prosen, E. J., and Colbert, J. C., Microcalorimetric Study of Cardiac Pacemakers and Batteries, *Semiconductor Measurement Technology:* Reliability Technology for Cardiac Pacemakers II — A Workshop Report, NBS Special Publication 400-42, pp. 16-18 (August 1977).

[2]Thorin, A., and Lodin, A., Siemens-Elema AB, S-17194 Solna, Sweden, paper presented at Tokyo in March 1976; private communication.

[3]Anon., Evaluation of Pacemaker Battery Parameters by Microcalorimetry, report issued by Wilson Greatbatch Ltd., Clarence, NY, 1977.

[4]Untereker, D. R., and Owens, B. B., Medtronics, Inc., private communication.

[5]Gibbard, H. F., *J. Electrochem. Soc.* 125, 353-358 (1978).

[6]Commercially available from Tronac, Inc.

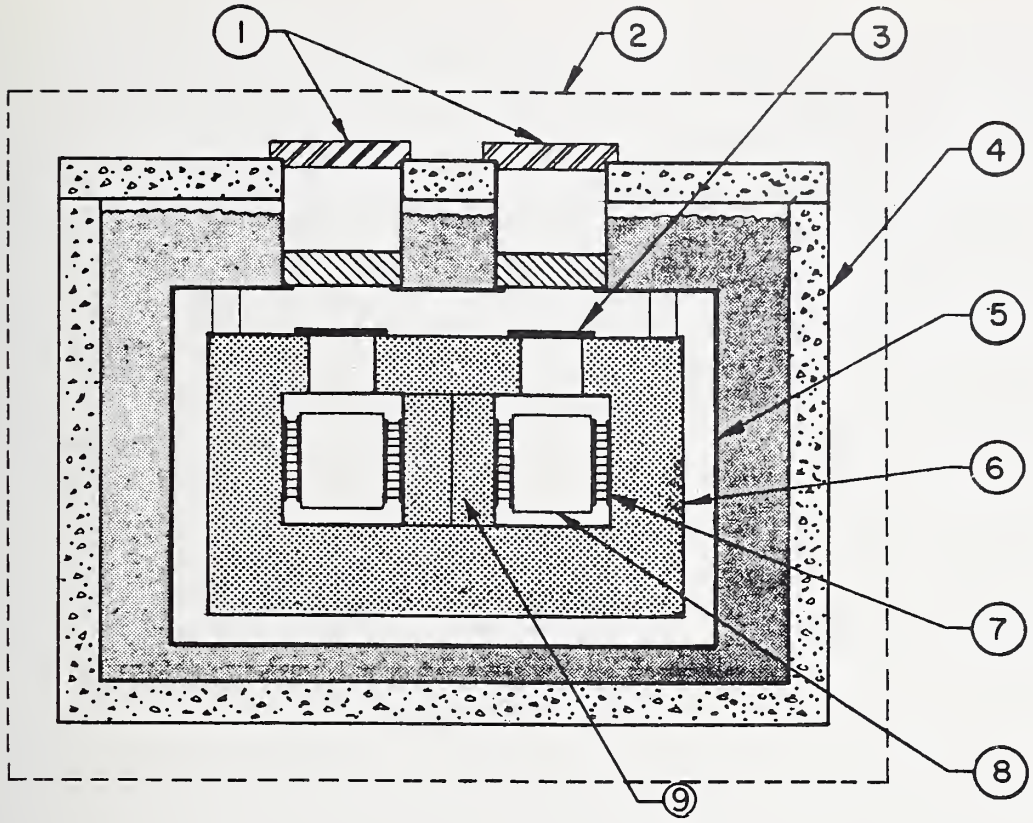

Figure 1. Schematic of Tronac battery calorimeter. (1) access tubes, with top cover and bottom thermal conducting plug, (2) temperature-controlled air bath with electronics inside, (3) covers on block compartments, (4) temperature-controlled water bath, (5) watertight stainless steel box, (6) aluminum heat sink block suspended by bolts at four corners, (7) thermoelectric sensors, (8) battery holder, and (9) one of four aluminum wedges placed in tapered channel.

and four thermoelectric measuring devices,[7] which are mounted on the aluminum wedges, together with two battery holders made of thin aluminum, and a cover plate with access holes to the two battery holders. The large aluminum block assembly, suspended by four 0.25-in. (0.8-cm) bolts in the center of a watertight box, is submerged in a water bath[8] controlled at 37°C to ±0.0002°C. Two pipes, sealed around holes in the box cover, give access through the water bath to the battery holders. During a measurement, the holes in the box cover and the battery holders are covered with 0.060-in. (1.5-mm) thick aluminum plates to prevent heat transfer by air currents.

The outputs from the two sets of thermoelectric devices are connected with opposing polarities so that the effects of any temperature fluctuations in the block will be canceled in the output. The difference in the output voltages of the two compartments, which is proportional to the difference in the rates of

[7]Cambion model 1052.

[8]Tronac model 405.

heat production in the two compartments, is filtered with a simple RC filter (time constant = 6 min), amplified by an amplifier,[9] and recorded on a strip chart recorder. Typically, the recorder is run at 2 in./h and 100 mV full scale, and the amplifier is adjusted for a gain of 3×10^4. Peak-to-peak baseline noise was found to be about ±0.1 μW if the heat capacity of the compartment used as a reference was carefully adjusted by an aluminum block to be the same as the compartment containing a battery.

Calibrations were done in two ways. In most cases, a 1-kΩ resistor mounted in the battery holder was used to provide a known rate of heat to the cell. In one case, the 1-kΩ resistor was mounted directly on a battery. There was no significant difference in the results. Calibrations were done at heater powers of 20, 137, and 184 μW. Again, there was no significant difference in the output voltage per microwatt of heat input. The calibration constant is believed to be accurate to about 2 percent at the lowest heater power and to about 1 percent at the higher ones. The heater and standard resistor voltages were measured with a digital voltmeter.[10] The results from a sample set of calibration runs are given in table 1.

Measurements of open circuit heat production of batteries were made by equilibrating the batteries for 8 to 12 h in the space above the measurement compartment, placing a battery in a compartment, waiting (usually about one hour) until any heat stored in the battery (because of a temperature difference) has dissipated totally as shown by a flat baseline, and then removing the battery. The

[9]Keithley model 150B.

[10]Data Precision model 3500 (5-1/2 digit); a Tronac 450EC board was used as a power supply.

Table 1. Sample Calibration Runs.
Displacement from Baseline in Microvolts[+]

Heater Power = 19.77 μW	Heater Power = 19.81 μW
Left Side	Right Side
3408	3149
3399	3153
3410	3139
3402	3140
3404	3144
3405	
Average 3405 ± 2[*]	3145 ± 3[*]

[+]Corrected to sensor outputs. Data in this table were collected digitally with a DVM.

[*]Standard deviation with respect to the mean.

difference in the measured rate of heat output from a given compartment before and after removal of the battery is then the heat output of the battery. Tests using an aluminum block in place of a battery showed that the reproducibility of this procedure was better than ±1 μW.

Measurements of heat dissipation in batteries under discharge were made by electrically connecting the battery to a resistor outside the calorimeter with two wires.[11] The wires were placed in good thermal contact with the calorimeter block to prevent thermal leakage from outside the calorimeter.

For an experiment on an ideal battery where the battery is in a calorimeter and connected electrically to a load resistor outside the calorimeter, the first law of thermodynamics states that

$$\Delta E = Q - W \ , \tag{1}$$

where: ΔE = internal energy change,

Q = heat produced in the calorimeter, and (2)

$W = I^2Rt$ = electrical energy dissipated in the resistor when the battery is sealed so that $P\Delta V$ work is zero. (3)

Substituting eq (3) into eq (1) and taking the derivative with respect to time, we have

$$\frac{d\Delta E_1}{dt} = \frac{I\Delta E_1}{F} = q - I^2R \tag{4}$$

where I is the current through the resistor, F is the Faraday constant, ΔE_1 is the total energy change per equivalent of current-producing reaction under the conditions extant in the battery, q is the rate of heat production in the battery, and R is the load resistance value. For a real battery with more than one reaction occurring and less than 100-percent current-producing efficiency of the main reaction, it is necessary to add a term to the left side of eq (4) for each extra reaction and for that part of the main reaction that does not produce current:

$$\frac{I\Delta E_1}{F} + \frac{d\Delta E_2}{dt} + \frac{d\Delta E_3}{dt} + \ . \ . \ . = q - I^2R \ . \tag{5}$$

Rearranging eq (5) so that all known terms are on the right side gives

$$P_{internal} = q - I^2R - \frac{I\Delta E_1}{F} \tag{6}$$

where $P_{internal}$ is the sum of the unknown derivative terms. The behavior of $P_{internal}$ as a function of the current can tell much about the nature of the

[11] Number 40 AWG.

unknown processes in a battery as will be shown in the following discussion of microcalorimetric measurement results.

The results obtained for a series of open circuit heat measurements on batteries of various kinds, shapes, and sizes are given in table 2. These results clearly show the capabilities of the calorimeter as well as the reproducibility of open circuit heat production in a set of supposedly identical batteries.

Calorimetric measurements of open circuit heat production of batteries may not accurately reflect that a primary chemical reaction is occurring in the battery with a consequent loss in ampere-hours available. Any process, such as crystal growth, evaporation of liquids, curing of plastics and cements, and mechanical strain release can produce a change in the total energy content of the battery and, hence, an output signal to the calorimeter. These changes are usually not significant in determining battery life, although they can lead to mechanical failure of some battery component. Calorimetric experiments can be conducted to determine the magnitude and source of most of these effects by measuring the heat output of each of the battery components separately. Open cir-

Table 2. Open Circuit Battery Measurements.

Battery Type	Capacity (A-h)	Voltage (V)	Power,[a] (μW)	No. in Sample
Mercury, HgO-Zn, Pacemaker Set I	1	1.4	4.1 ± 0.1	2
Mercury, HgO-Zn, Pacemaker Set II	1	1.4	7.5 ± 0.3	2
Alkaline, MnO_2-Zn, Penlight	2	1.5	46 ± 2	2
Mercury, HgO-Zn, Penlight	2	1.4	68 ± 5	2
Carbon-Zinc, Penlight	1	1.5	15	1
Silver-Oxide-Zinc Watch Battery Set I	0.16	1.5	7 ± 1	8
Silver-Oxide-Zinc Watch Battery Set II	0.16	1.5	10.2 ± 0.4	3
Silver-Oxide-Zinc Watch Battery Set III	0.16	1.5	13 ± 1	5
Lithium-Iodine, Pacemaker Set I	1.2	2.7	5 ± 1	2
Lithium-Iodine, Pacemaker Set II	1.5	2.7	30 ± 5	2
Lithium-Iodine, Pacemaker Set III	3.0	2.7	6 ± 2	2

[a]Deviations are the standard deviation of the mean between batteries.

cuit heat production is also typically a function of age as shown in figure 2, and this must be taken into account in interpreting these kinds of data.

Representative results of measurements of heat production for three different types of batteries under discharge are given in table 3. The data from table 3 were used to calculate values of $P_{internal}$ [eq (6)] which were then plotted as shown in figure 3.

Because $P_{internal}$ represents the chemical or stored energy dissipated as heat by all reactions that do not produce current, a line with a slope equal to zero, as in the lithium-iodine system, shows that all such processes are independent of the current. The slope of zero also proves that all of the current-producing reactions have been accounted for properly by the one assumed reaction with a current efficiency of 100 percent in the lithium-iodine battery. The non-zero intercept is thus probably due to processes, as mentioned above, which do not cause a loss in total available current.

The silver oxide-zinc battery becomes slightly more efficient in the use of total stored energy as the current increases, while the mercury oxide-zinc battery apparently rapidly loses energy efficiency as the current increases, as can be seen in figure 3. Both of these effects are probably due to changes in current-producing reactions, since intermediate oxidation states are possible for mercury and silver. The linearity of the curve for the mercury oxide-zinc battery at the higher currents suggests that either the ΔE_1 value is in error by about 4 percent, which is unreasonable for these substances, or that we have not fully accounted for the battery reactions which produce current.

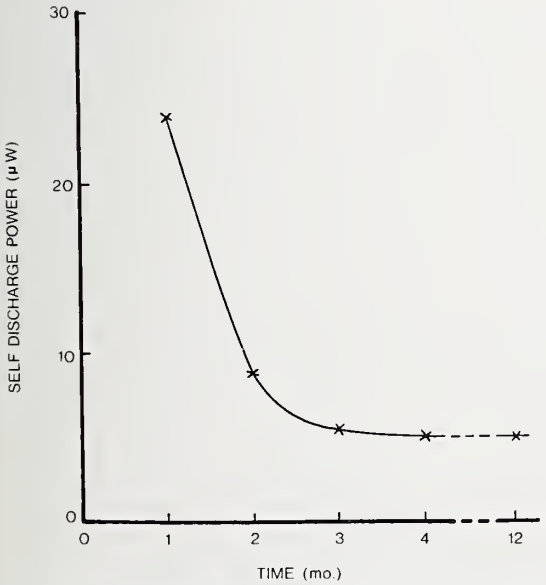

Figure 2. Effect of aging on open circuit heat production from lithium-iodine batteries.

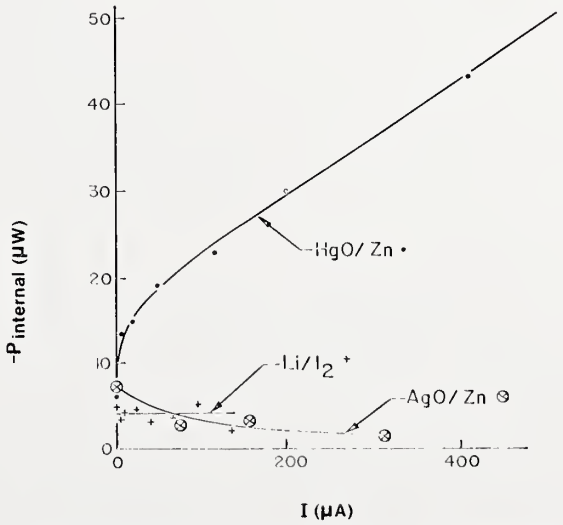

Figure 3. Plots of $P_{internal}$ against current being drawn from the battery. [See text, eq (6).]

Table 3. Heat Dissipation from Batteries under Discharge.

Battery	Voltage (V)	Current (μA)	Load Resistor (kΩ)	Rate of Heat[a] Production (μW)
Lithium-Iodine:	2.8093	-	open circuit	-
$Li + 1/2\ I_2 = LiI$	2.7955	4.9	566	-1.25
ΔE = -272 kJ/equivalent	2.7816	10.2	273	-0.63
	2.7526	21.3	129	1.25
	2.7056	39.8	68.04	2.50
	2.6344	67.4	39.10	11.3
	2.5682	94.4	27.20	24.0
	2.4615	137	17.97	46.0
Silver Oxide-Zinc:	1.5810	-	open circuit	-
AgO + Zn = Ag + ZnO	1.5614	78	20.0	9.5
ΔE = -168 kJ/equivalent	1.5610	156	10.01	24.3
	1.5580	311	5.01	51.6
Mercury Oxide-Zinc:	1.3996	-	open circuit	-
HgO + Zn = Hg + ZnO	1.3690	5.1	273	7.2
ΔE = -129 kJ/equivalent	1.3896	20.4	68.04	7.9
	1.3780	50.7	27.20	11.6
	1.3701	114.9	11.92	13.5
	1.3629	197	6.93	18.5
	1.3578	407	3.34	28.5
	1.3533	752	1.80	43.5

[a]Values given in this column are the actual measured differences between the rate of heat production with the external load resistor open circuit heat production rate. To get the total heat production rate for calculation of $P_{internal}$, open circuit heat production values of 5, 7, or 6 μW must be added for the lithium-iodine, silver oxide-zinc, or mercury oxide-zinc battery, respectively.

Further evidence that more than one current-producing reaction is involved in the silver oxide-zinc battery was observed in the calorimetric data produced during the transient from zero to 150 μA of discharge as shown in figure 4. The shoulder on the curve clearly shows that an additional reaction occurs at the higher current after depletion of some intermediate component.

In summary, data plotted as shown in figure 3 can be used to show that all current dependent battery processes have been correctly described (slope = zero) or that they have not. In the latter case, the form of the curve suggests the nature of the remaining processes.

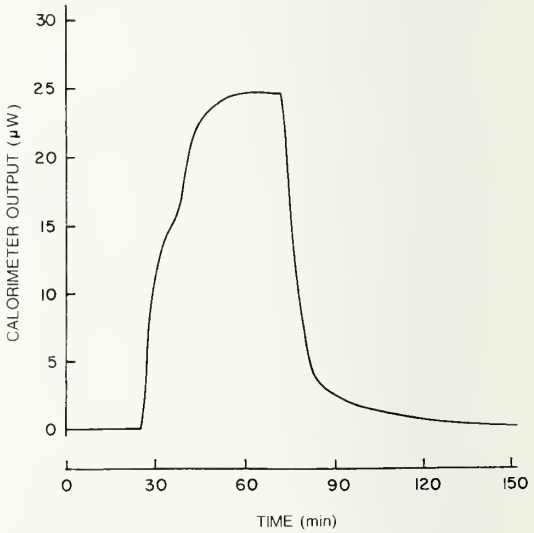

Figure 4. Actual calorimeter output for a silver oxide-zinc battery. From 0 to 28 min the battery circuit was open. At 23 min, a 10-Ω resistor was connected across the battery. The circuit was opened at 70 min. Power dissipation is relative to the baseline with the battery in the calorimeter with wires attached but with the circuit open.

3.1.3 Microcalorimetry: A Tool for the Assessment of Self-Discharge Processes in Batteries

D. F. Untereker and B. B. Owens
Medtronic, Inc.
Minneapolis, MN 55418
(612) 574-3090

The determination of self-discharge processes is of considerable importance to both manufacturers and users of batteries. This is particularly true in the medical device field where unique high energy density cells are being qualified for long-term human use. The classical methods for obtaining such data involve determining relative capacities before and after storage. The problem with such experiments for long-lived batteries is that the storage periods involved are excessively long and are subject to a variety of complex variables. Also, this experimental approach does not take into account any effect of load on the rate of self-discharge processes. It is, therefore, very desirable to obtain estimates of the rates of parasitic processes on a short-term basis rather than to rely solely on experiments such as those described above. Calorimetry has been proposed as a good method for obtaining estimates of these processes and has recently shown much promise.[1,2,3] One main objective is to present some data and show how it may be interpreted in a fairly simple manner. Some of the text and figures below have been abstracted from other papers.[4]

The data presented in this paper were obtained with a Tronac Model 351RA Microwattmeter. This calorimeter is a differential heat conduction type instrument and has a short-term noise level of about 0.2 μW and a long-term stability of about 1 μW. The construction and performance of this instrument are described more fully elsewhere.[5]

A simple experimental procedure was used to obtain data. The first step was to pre-equilibrate the battery. This was done in two stages. First, the battery was placed in an air bath (37 ± 0.5°C) which surrounds the calorimeter. After equilibrium was established, the battery was moved into thermal contact with the water bath in which the calorimeter block is submerged. This bath was held to a fixed temperature with a tolerance of ±0.0002°C. Following this sec-

---

[1]Prosen, E. J., and Colbert, J. C., *Semiconductor Measurement Technology:* Reliability Technology for Cardiac Pacemakers II — A Workshop Report, NBS Special Publication 400-42, pp. 16-18 (August 1977).

[2]Greatbatch, W., Wilson Greatbatch Ltd., Clarence, New York, private communication (1976).

[3]Hart, R. M., and Hansen, L. D., this publication, pp. 10-16.

[4]Untereker, D. F., and Owens, B. B., Calorimetric Investigations of Li/I_2 Cardiac Pacemaker Batteries, Abstract No. 24, 152nd National Electrochemical Society Meeting, Atlanta, Georgia, October 1977, p. 65.

[5]Untereker, D. F., Use of a Microcalorimeter for Analysis of Load Dependent Processes Occurring in a Primary Battery, to be published.

ond pre-equilibration step, the battery could be placed inside the calorimeter measurement cavity with minimal disturbance to the calorimeter. A typical experiment including battery insertion, settling, battery removal, and subsequent return to baseline generally required three hours or less.

In some experiments reported here, the battery was discharged at a fixed rate while calorimeter measurements were obtained. To do this, fine wires were soldered to the battery's terminals before the experiment was begun. Once the battery was in place, these wires were run through the air bath to two feed-throughs leading outside of the calorimeter. From these points, external load resistors could be connected to the battery and its load voltage monitored. A Keithley Model 150 B microvoltmeter was used to monitor changes in the thermopile voltages. The output of the microvoltmeter was recorded on a strip chart recorder for a permanent record.

The type of calorimeter used for these experiments yields data in terms of heat flux rather than heat. Each of the thermodynamic quantities may readily be converted to an equivalent rate form if the rate is assumed to be measured by the current in the external wire. Then, for example, the power in watts is given by:

$$P = \frac{4.18\ \Delta H\ i}{nF}$$

where ΔH is the change in enthalpy or heat of reaction in calories per mole, i is the current in amperes, n is the number of electrons transferred in equivalents per mole, F is the Faraday constant in coulombs per equivalent, and 4.18 (joules per calorie) represents the mechanical equivalent of heat. Other thermodynamic quantities may be calculated analogously.

The calibration of the calorimeter was done via a 1-kΩ resistor which is imbedded in the battery cell holder between the thermopiles. For our calorimeter, the calibration factor is 8.45 μW/μV at 37°C. This calibration factor turns out to be independent of the thermal conductivity and heat capacity of the battery and battery holder.

In a search of the existing literature, we have not seen a discussion of the thermodynamics involved in calorimetric battery experiments such as that presented here and by Greatbatch.[2] The equations presented here are reasonably simple and can be readily derived from basic thermodynamics for a system at constant temperature. Because thermodynamic equations are strictly applicable only to systems at equilibrium, allowances must be made for the errors which develop as a result of the nonequilibrium situation which arises when current is drawn from a cell or parasitic processes occur.

Consider the chemical reaction $mM + nX \rightarrow M_mX_n$. From the first law of thermodynamics $\Delta U = w + q$, where ΔU is the internal energy change, w is the work done, and q is the energy transferred, or the heat. If M and X are combined directly

in the calorimeter, w can only be the mechanical work allowed by the nature and the geometry of the system and is nearly zero if all reactants and products are condensed phases. Now consider the same chemical and geometrical system except that M and X are constrained in such a way that the only path for formation of $M_m X_n$ is via electron transport through a wire external to the calorimeter. When an external resistance is placed in series with this wire, electrical work may be performed external to the calorimeter. If ΔU is fixed by the reaction taking place and work is being performed outside the calorimeter, less heat must appear inside the calorimeter. The question then becomes how ΔU is divided between q and w. As will be seen below, there is a theoretical minimum for q, and the observed proportioning will be determined by kinetic as well as thermodynamic characteristics.

For any system, the maximum amount of external work is done when the process is carried out reversibly. Thus, the minimum heat must be produced under reversible conditions. The equations for the second law of thermodynamics defining free energies in terms of ΔU or ΔH and entropy, S, turn out to express the necessary relationships because the change in the Helmholtz function, ΔA, and the Gibbs function, ΔG, are equal to the reversible electrical work a system is capable of, holding temperature and volume or pressure, respectively, constant, namely, $\Delta A = \Delta U - T\Delta S$ and $\Delta G = \Delta H - T\Delta S$.

A rearrangement of the last equation summarizes this when pressure is constant, $\Delta H = \Delta G + T\Delta S$. Thus, $T\Delta S$ is the minimum heat generated during the electrochemical formation process. When polarization or irreversibility comes into play, q is greater than $T\Delta S$ so w (irreversible) becomes less than ΔG. The extra energy will eventually be given off as heat; however, it may be temporarily stored. There can also be losses in the battery from its own internal resistance. At true steady-state conditions, all of these losses may be lumped together since they all affect the battery by reducing its output voltage.

As pointed out above, irreversible effects lead to a reduction in the load voltage on a cell. Since a cell's current-voltage curve relates its voltage to its rate of reaction, this curve is the keystone to calculating how power is proportioned between useful external energy and internal heat.

Figure 1 shows these relationships at steady state. In this example, ΔH is more exothermic than ΔG. In order to make the units consistent, this curve is plotted as nFE versus i/nF rather than the more familiar E versus i. For a cell run at E_L and i_L, where L stands for loaded, the shaded and crosshatched areas in figure 1 show the internal and external power dissipation. It is obvious that the minimum internal power is $4.18\ T\Delta S\ (i/nF)$ even if the cell reaction is carried out reversibly.

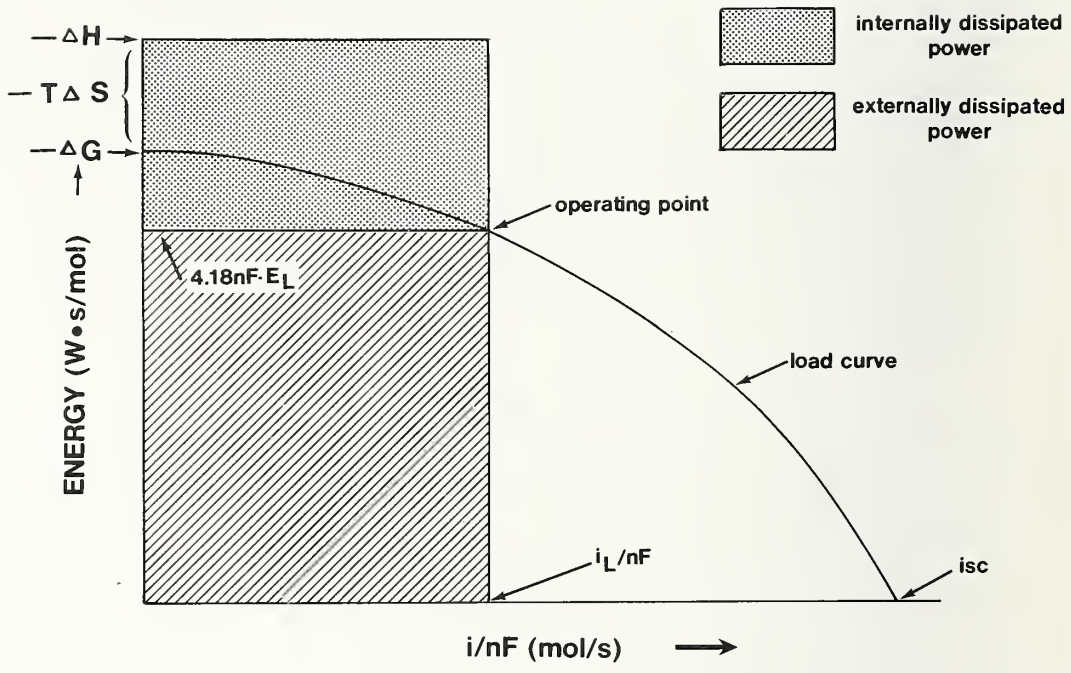

Figure 1. Partitioning of total power between internal and external dissipation in an ideal battery.

This discussion has only covered the behavior of a cell where there are no parasitic reactions occurring. As seen in figure 1, the internal heat produced in a cell in which no parasitic reactions occur always goes to zero as $i \to 0$. Therefore, the presence of internal power dissipation when $i = 0$ is proof of the occurrence of some parasitic process.

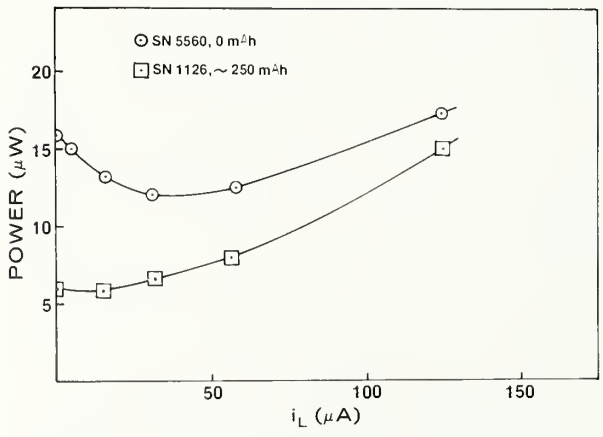

Figure 2. Measured internal power dissipation versus load current for two Wilson Greatbatch Ltd. model 755 batteries. One battery (SN5560) had not been discharged; the other had been discharged to about 10 percent of its rated capacity.

Experiments of the sorts described earlier were performed on batteries based on lithium-iodine chemistry. The data of figure 2 are for two Wilson Greatbatch Ltd. model 755 batteries. One of these batteries (SN5560) had not been discharged, while the other (SN1126) had been discharged to about 10 percent of its rated capacity. The dissipation versus load current plot is curved in each case and both appear to have minima. The relative dissipations seem plausible as the new cell would be expected to have a higher

output than the partially discharged cell because the latter should have a much thicker product layer of lithium-iodine and thus be less subject to further self-discharge, assuming the direct combination of lithium and iodine were responsible for much of the calorimetric output.

The next two figures show the effect of correcting the raw data for known current-dependent variables. It turns out that for the lithium-iodine system, ΔS is very small (0.1 k cal/K·mol), and the entropy correction is negligible in the range shown. However, these batteries are inherently resistive and, since other polarization effects should also take the form of potential drops, a single correction was made by subtracting $i\Delta E$, where ΔE is the difference between E_L at the measured current and E_{ocv}, the open circuit potential. The corrected data for the new battery became nearly horizontal after an initial dip, as shown in figure 3. The same correction for the slightly discharged cell yields a line not nearly so horizontal, as shown in figure 4. At the present time, we do not know if all the observed differences are indicative of the states of discharge or whether some might be artifacts of the batteries themselves. Hansen and Hart have shown that the lithium-iodine reaction is essentially 100-percent current-efficient,[3] and this leads us to speculate that the observations of the initial dip may really be due to changes in the rate of self-discharge because of a competition of the chemical and electrochemical mechanisms. Such a mechanism would be expected to be much more noticeable on a new cell where the protective lithium-iodine layer is very thin. It seems likely from these preliminary experiments that most of the calorimetric output observed in the model 755 battery is due to self-discharge and that at least early in life its rate is quite dependent upon current. The positive slopes in figures 3 and 4 indicate there is something happening that we do not understand.

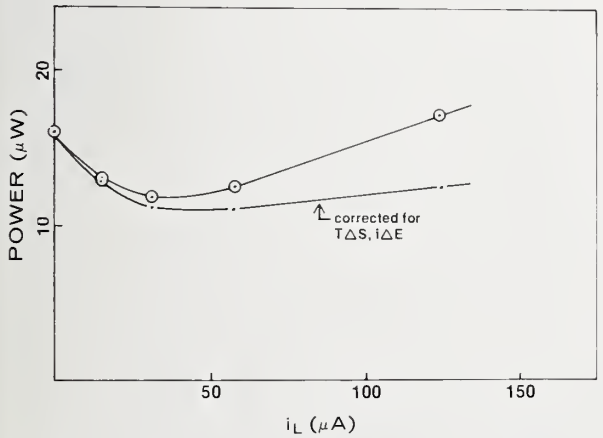

Figure 3. Measured and corrected (for known current-dependent variables) internal power versus load for one Wilson Greatbatch Ltd. model 755 battery (SN5560).

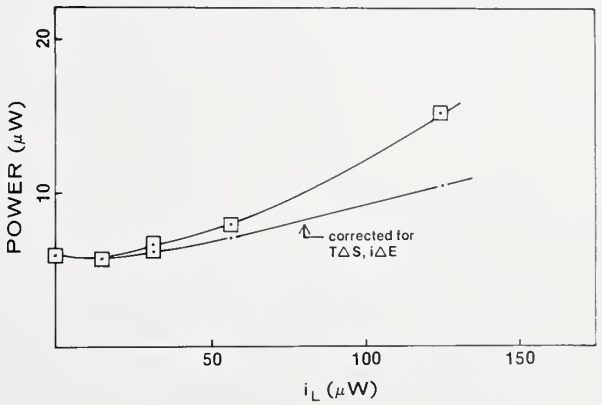

Figure 4. Measured and corrected (for known current-dependent variables) internal power versus load for one Wilson Greatbatch Ltd. model 755 battery (SN1126).

Because a main purpose of using microcalorimetric measurements is to estimate self-discharge rates, we wished to determine how self-discharge might change during the life of a battery. We stated above that discharge is expected to be high initially in the lithium-iodine system and then decrease with time and discharge depth. If this is true, the shape of this curve must be known as a function of time and discharge. The effect of discharge depth was investigated using a set of rapidly discharged Wilson Greatbatch Ltd. model 742 batteries. These batteries are not directly comparable to the model 755 cells already discussed because their designs are quite different and they are even subject to different accompanying parasitic reactions. Nevertheless, the basic chemistry is the same and the results should be indicative of this generic type of battery.

A group of 21 batteries was discharged to different depths. The 742 battery has a rated capacity of 1000 mAh and the data cover the full range of useful life. The calorimetric outputs, measured under open circuit conditions, are shown in figure 5. As expected, the data show a high initial output which, under these conditions, falls to about 10 percent of its initial level by 40 percent of discharge. We believe that there are significant contributions to the heat output of this battery from other parasitic reactions early in its life, but, if we ignore these and assume all of the heat output in figure 5 is due to self-discharge, we can integrate under this curve to obtain a fractional total loss of energy during battery life. The number obtained from figure 5 is a 12-percent total loss which is approximately the loss specified by the manufacturer. While the experiment described above has real-time uncertainties built into it from the accelerated discharge of the batteries, the shape of the curve indicates that calorimetric measurements from batteries discharged to 30 percent of capacity or even less may be able to be used to obtain total self-discharge estimates in the lithium-iodine system with a reasonable precision.

In summary, we have found that microcalorimetry is a good tool for assessing parasitic reactions in small battery systems. A first-order thermodynamic treatment accounts for most of the energy exchanges observed between the lithium-iodine system and its surroundings. However, there still appear to be some data which are not completely explained by the simple treatment. Even so, the lithium-iodine system seems to be particularly amenable to meaningful calorimetric measurements since it appears that the rate

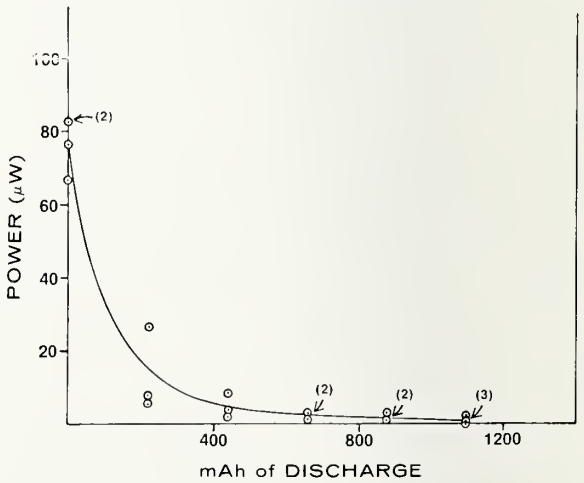

Figure 5. Calorimetric data for 21 Wilson Greatbatch Ltd. model 742 batteries discharged at a rate of 1 mA at 60°C to different depths.

of self-discharge decreases very rapidly and may fall to a relatively insignificant level after about 30 percent of discharge.

The test results from lithium-iodine batteries (subjected to accelerated discharge conditions) indicate that the average loss rate would be equivalent to about 1 percent per year when the batteries are discharged at normal pacing rates.

3.1.4 A Microcalorimeter for Measuring Characteristics of Pacemaker Batteries[1]

Edward J. Prosen and Jennifer C. Colbert
Center for Thermodynamics and Molecular Science
Chemical Thermodynamics Division
National Bureau of Standards
Washington, DC 20234

A microcalorimeter has been designed and constructed to measure the self-discharge (or shelf-life) of pacemaker batteries under load and to measure the energy dissipation of the completed pacemaker. The design is based on the previous work reported[2] using our earlier NBS biological microcalorimeter which could handle only small camera and watch batteries.

The calorimeter is of the heat conduction type and employs a substitution and guarding principle. The earlier microcalorimeters[3] consist of a single heat sink or block whereas the pacemaker calorimeter contains three block sections as shown in figure 1. These three blocks, made of aluminum, are in good thermal contact. The center block contains the measuring compartment, and the end blocks serve as the guarding compartments. Each compartment contains an aluminum reaction vessel (not shown) of size 7.93 by 6.66 by 2.85 cm. The various vessels can contain batteries, a pacemaker, or a dummy.

The blocks are surrounded by an inner and an outer aluminum can (shield). The inner shield is wrapped with both a heater and a Wheatstone bridge (one arm of which is nickel wire) which controls the temperature of the shield to approximately ±0.001°C. The temperature of the

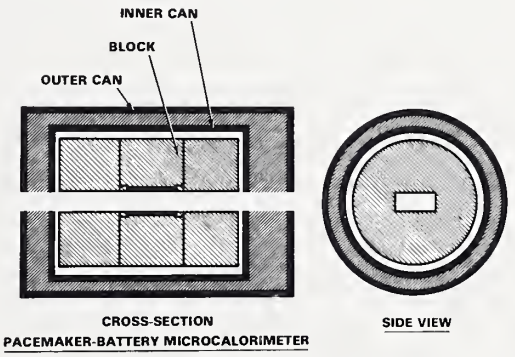

Figure 1. Cross-sectional schematic of pacemaker calorimeter. The calorimeter is approximately 30 cm in diameter and 46 cm in length.

---

[1]This work is supported by the Nondestructive Evaluation Program, National Measurement Laboratory, National Bureau of Standards.

[2]Prosen, E. J., and Colbert, J. C., Microcalorimetric Study of Cardiac Pacemakers and Batteries, Nat. Bur. Stand. NBSIR 77-1310 (September 1977).

[3]Prosen, E. J., Design and Construction of the NBS Clinical Microcalorimeter, Nat. Bur. Stand. Report 73-179 (April 1973).

blocks, which are separated from the inner shield by a 1.0-cm air-gap, is thus constant to about 1 μ°C after an overnight equilibration period. The 5-cm space between the inner and outer shield, including the ends of the shield, are filled with polyurethane foam. The entire pacemaker calorimeter is enclosed in a temperature-controlled air bath. The air temperature is maintained at approximately 30°C (±0.02°C) and the block temperature at 32°C. For future measurements, the block temperature will be controlled at 37°C. Any temperature between 20 and 40°C can conveniently be used.

The calorimeter always contains three vessels, i.e., one in each block. The center vessel will initially contain a dummy which generates no heat. The vessels in the two guarding blocks contain power cells or pacemakers to be tested. All vessels contain a small amount of hydrocarbon oil (Due Seal Pump Oil "A") to improve thermal contact between the sample and vessel.

Once equilibrium is attained, the vessels are pushed to new positions, i.e., a vessel containing an active sample (power cells or a pacemaker) is pushed into the center block. The dummy vessel is placed in one end block and the second active sample in the other end block. Differences in signal output are a measure of the power output from the active samples. This arrangement minimizes shifts due to temperature differences in the vessels and gives good baseline stability.

Under ideal conditions, the instrument detectability is expected to be 0.1 μW. This has not yet been attained on active samples in this new instrument. Our reproducibility is presently about 1 μW.

In making the measurements, the thermodynamic equation which follows explains the quantities being measured per unit of time.

$$\Delta G = \Delta H - T\Delta S$$

or

$$\Delta H = \Delta G + T\Delta S \ ,$$

where ΔG, ΔH, and ΔS are the changes of the Gibbs energy, enthalpy, and entropy, respectively, and T is the absolute temperature. It is assumed that the reactions take place at constant temperature and pressure.

If an open-circuited power cell alone is placed in the calorimeter, then the self-heating or "self-discharge" power is measured by the calorimeter. Side reactions, such as corrosion of the metal components, may account for some of this self-heating.

If the power cell has a resistor placed across it and both the power cell and resistor are in the calorimeter, then the heat evolved, $q = -\Delta H$ is measured by the calorimeter. "Self-discharge" may also be occurring.

If a load (resistor) is placed across the power cell with the load outside the calorimeter, with small copper leads[4] connecting it to the power cell in the calorimeter, then the heat evolved, $q = -T\Delta S$, is measured by the calorimeter. The usable energy, ΔG, is measured electrically by measuring the current and voltage across the external resistor and the time. Each of these quantities is measured as a function of time. Thus, power rather than energy is measured. The quantities being measured are shown schematically in figure 2.

The literature value of the $T\Delta S$ quantity for the reaction $Li(c) + 1/2\ I_2(c) \rightarrow LiI(c)$, where (c) signifies condensed phase, proves to be very small, -0.22 kJ/mol[5] compared to ΔH, -273.6 kJ/mol.[5]

Alkaline, mercury-zinc, and lithium-iodine power cells were tested for their self-discharge and load characteristics and the results follow.

The open-circuit calorimetric output of 8 alkaline batteries contained together in the calorimeter, with each battery producing approximately 56 μW, is shown in figure 3. This calorimeter has a calibration constant of 4.9

[4]No. 32 AWG was used.

[5]Values for the formation of lithium-iodine were provided by Richard Schumm, NBS Thermodynamic Data Evaluation Center.

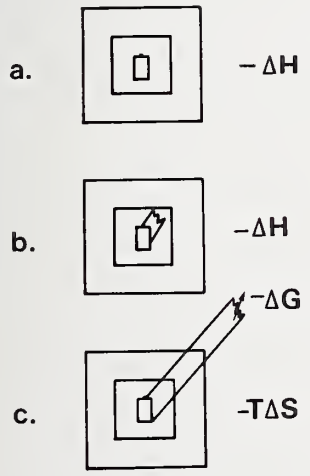

Figure 2. Schematic diagram showing thermodynamic quantities which are measured for: a) battery in calorimeter with no load; $-\Delta H$ is measured by calorimeter; b) battery with load inside calorimeter, $-\Delta H$ measured by calorimeter; and c) battery in calorimeter, load outside calorimeter; $-T\Delta S$ is measured by calorimeter, $-\Delta G$ is dissipated in the load outside the calorimeter.

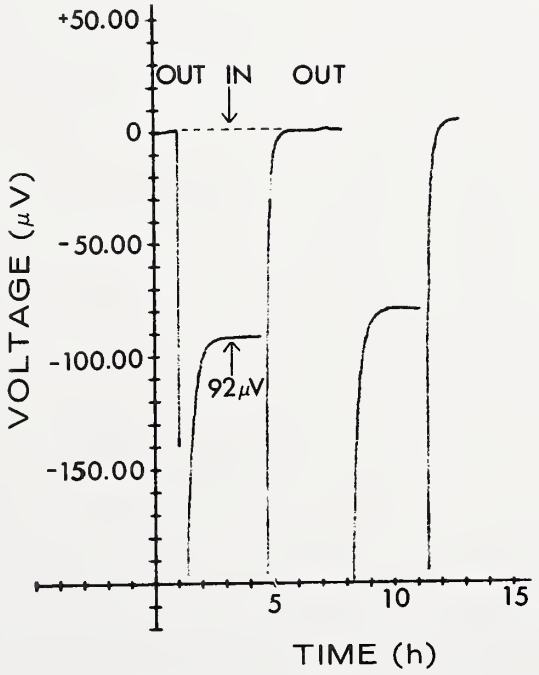

Figure 3. Microcalorimetric output voltage versus time for 8 separate open-circuit batteries in and out of the microcalorimeter. A sensor output voltage of 92 μV is indicated which corresponds to 451 μW or about 56 microwatts per battery.

μW/μV, this value was used in calculating the power and energy quantities in the test. In figure 4, the open-circuit discharge of 16 mercury batteries is given; each battery produces about 5.8 μW. The four lithium-iodine batteries tested under open-circuit conditions indicate approximately 0 ± 5 μW of power as shown in figure 5. One battery subjected to a 100-kΩ load inside the calorimeter dissipates about 73.5 μW of power, as shown in figure 6. This is approximately equal to the value obtained by calculating the power dissipated in the load and assuming that TΔS is zero: $W_{calc} = E^2/R$ (where E = voltage and R = resistance) = $(2.75)^2/100200$ = 75.5 μW. Measurements have not as yet been made on batteries under external load.

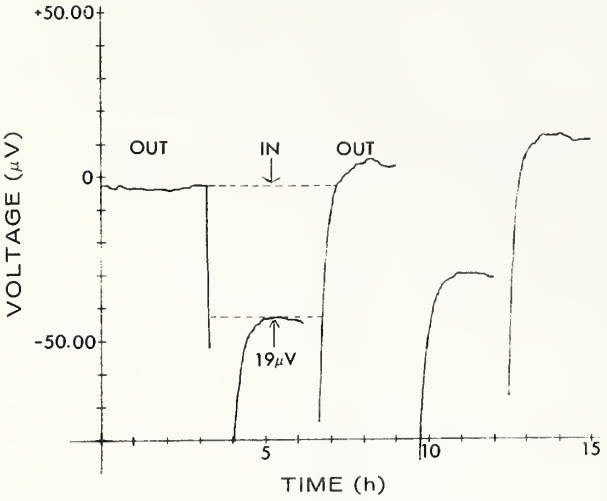

Figure 4. Microcalorimetric output voltage versus time for 16 separate open-circuit mercury batteries in and out of the microcalorimeter. A sensor output voltage of 19 μV is indicated which corresponds to 93 μW or about 5.8 microwatts per battery.

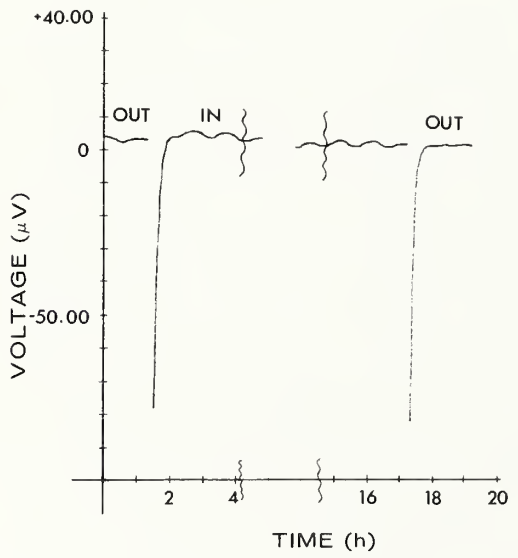

Figure 5. Microcalorimetric output voltage versus time for 4 lithium-iodine batteries (open circuit and previously discharged for 10 months through 100 kΩ). A sensor output voltage of ±1 μV is indicated which corresponds to ±5 μW for the four batteries or ±1 microwatt per battery.

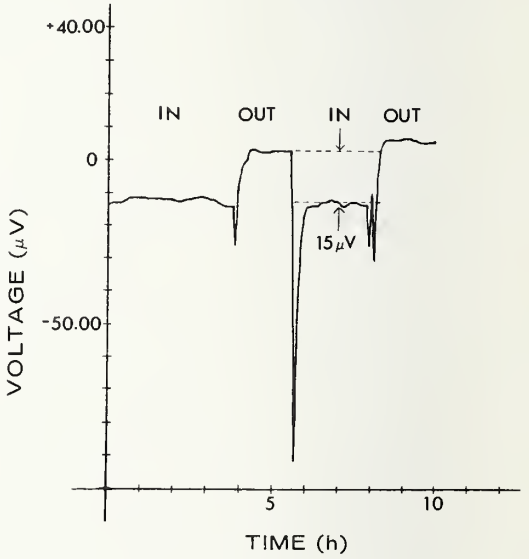

Figure 6. Microcalorimetric output voltage versus time for 1 lithium-iodine battery (under load of 100 kΩ in the microcalorimeter). A sensor output voltage of 15 μV is indicated which corresponds to 73.5 μW of power.

3.2 Session II Battery Characterization and Quality Control

3.2.1 End-of-Life Characteristics of the Lithium-Iodine Cell

A. A. Schneider and F. E. Kraus
Catalyst Research Corporation
1421 Clarkview Road
Baltimore, MD 21209
(301) 296-7000

The end-of-life characteristics of the lithium-iodine cell have become a subject of considerable interest to both the pacemaker designer and doctor, now that this cell has come to be so widely used. Unfortunately, the first lithium-iodine production pacemaker cell will not run down under normal drain for several years, so today's pacemakers have to be designed to provide adequate warning of end-of-life without knowledge of the nominal rundown curve. To obtain an approximation to the nominal rundown curve, three methods have been considered and are discussed below.

The first method involves accelerated discharge of production cells at high currents and, perhaps, also at high temperatures. Many such tests have been run by producers of the lithium-iodine cell and by pacemaker manufacturers themselves. Our results show, however, that such accelerated discharge disturbs the chemistry of the cell.

The following equations show the electrochemical discharge reaction for the lithium-iodine cell, where P2VP is an abbreviation for poly-2-vinylpyridine, the organic component of the organic/iodine complex depolarizer.

$$2Li = 2Li^{+} + 2e^{-} \quad \text{at the anode}$$

$$2Li^{+} + 2e^{-} + P2VP\cdot nI_2 = P2VP\cdot(n-1)I_2 + 2LiI \quad \text{at the cathode}$$

$$2Li + P2VP\cdot nI_2 = P2VP\cdot(n-1)I_2 + 2LiI \quad \text{net reaction}$$

Consider the reaction at the interface between the lithium iodide electrolyte and the $P2VP\cdot nI_2$ depolarizer. To support the reduction, iodine must diffuse from the depolarizer bulk to the interface. If the discharge is accelerated to, for example, 5 to 10 times normal pacemaker rates, the layer of the depolarizer adjacent to the lithium iodide becomes so depleted of iodine that its resistivity rises prematurely and does not return to normal values, even if the load is removed from the cell for several months. The result is that such experiments predict a cell rundown with a very gentle slope near end-of-life, with plenty of time for elective replacement. Even at discharges of only three times the normal rate, where such a resistive layer does not seem to form, the character of the lithium-iodine layer is altered. There are, however, other ways of approximating end-of-life which do not encounter these difficulties.

The second method involves the construction of cells which are normal in every aspect except that the depolarizer contains a deficiency of iodine. Because these cells contain only a thin layer of lithium-iodine, their resistance

is essentially determined by the resistance of the depolarizer. One can, from a series of such cells, plot depolarizer resistances ranging from that found in fresh cells to that found in spent cells. Such a plot is shown in figure 1. If the behavior is projected to actual cells and the resistance of the lithium-iodine layer is also considered, curves of the type shown in figure 2 are produced. The linear region of these curves corresponds to an accumulation of lithium iodide according to the above equations. The "knee" region corresponds to an iodine depletion phenomenon in the polarizer, seen in the exponential region of figure 1 where the iodine content is between one and two molecules for each monomer unit of P2VP. These curves show a much sharper decline in the "knee" area than those generated by accelerated discharges. Even so, there is still adequate warning time available to allow for convenient elective replacement of the pacemaker.

The method of detecting the end-of-life, however, becomes an important factor. For example, in figure 3 two discharge curves are shown for the 802/23 cell: one at 50 μA, the other at 15 μA. If a 1.9-V cell output is assumed to be the warning point in the pacemaker, the cell under lighter load gives much less warning than the cell under heavier drain. The cell under lighter load undergoes considerably more discharge before the voltage sensing circuit detects its condition; by that time, it is on a steeper decline path. If, however, cell internal resistance rather than cell voltage is detected by the pacemaker circuit, the cell at 15 μA would exhibit a much less steep end-of-life

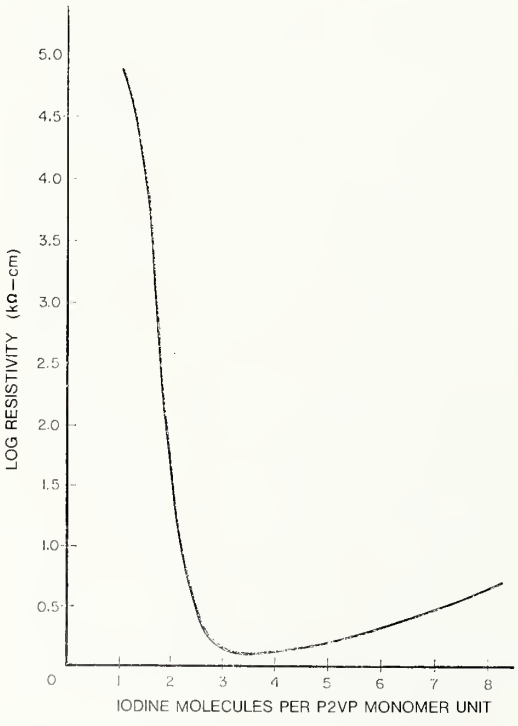

Figure 1. Depolarizer resistivity as a function of iodine content.

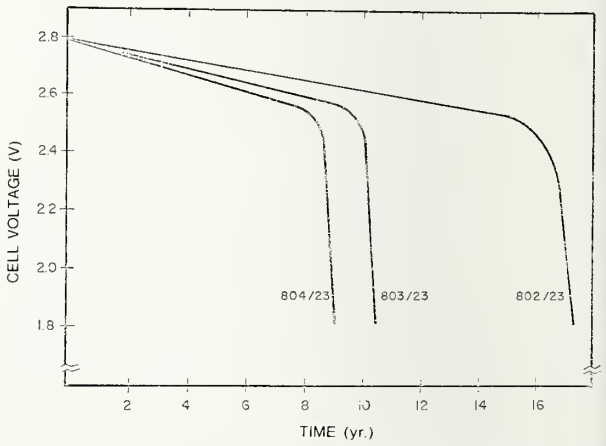

Figure 2. Projected discharge curves showing linear and "knee" region of three cell types. Cells are loaded with a resistance of 190 kΩ.

curve. At low currents, plots of resistance versus time give more warning than plots of voltage versus time.

Voltage sensing is even more complex when two cells are used in series at low drains. The probability that both cells are of identical capacity is small. The cell with the smaller capacity may be in a very steep portion of the discharge curve before the voltage sensing circuit detects a drop in the sum of both cell voltages. Certainly, voltage sensing can be used, but the parameters of cell behavior and pacemaker behavior must be well-matched and well-understood. Cell resistance rather than cell voltage seems to be a better warning indicator, particularly with the new, thin, large-area cells which generally have steeper end-of-life slopes.

The third method is to build cells with the normal iodine content but with much thinner depolarizer layers. These cells are run down at normal loads but reach end-of-life much sooner than cells with normal thickness. Discharge curves for two such cells, each with only one of their two cathodes loaded, are shown in figures 4 and 5. These are 702E cells whose capacities are 0.5 rather than 4 ampere hours. Normal cell load is 50 kΩ,[1] no more than a factor of two above standard pacemaker loads. These cells do exhibit the "knee" predicted by analysis of the second method. In fact, if 702E cell performance is estimated by the second method, the end-of-life section of the curve, shown in figure 6, is remarkably similar to the curves of figures 4 and 5. Corroboration by the real data of figures 4 and 5 suggests that the predictions of the

[1]A 100-kΩ resistor is placed in series with each of the two cathodes to develop a load resistance of 50 kΩ to the cell.

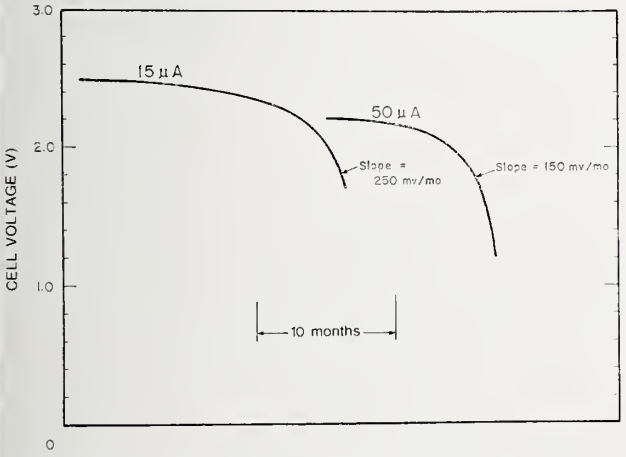

Figure 3. Projected end-of-life curves for the 802/23 cell based on resistance of depolarizer. Significantly different rates of decay of cell voltage are shown at 1.9 V for two typical cell currents. Horizontal scales of the two curves are the same but shifted to facilitate comparison.

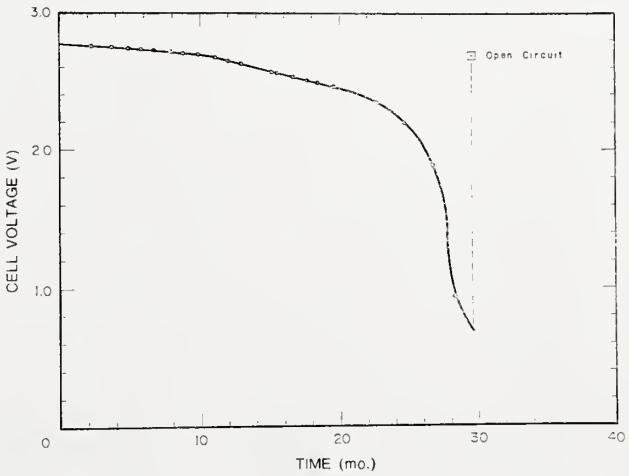

Figure 4. Discharge under a 100-kΩ load to one of the two cathodes of a special 702E cell (30A) constructed with 1/8 the normal depolarizer thickness.

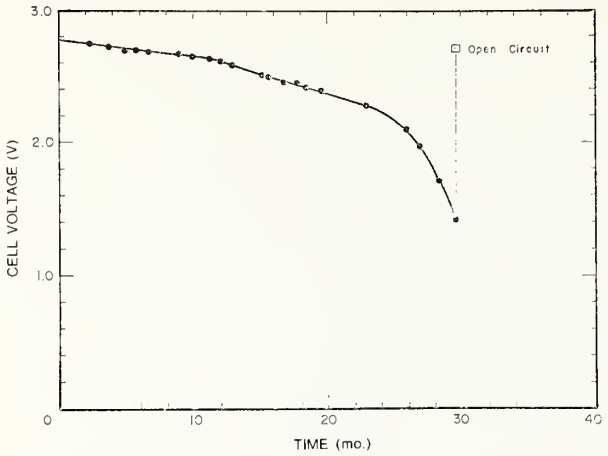

Figure 5. Discharge under a 100-kΩ load to one of the two cathodes of a special 702E cell (30B) constructed with 1/8 the normal depolarizer thickness.

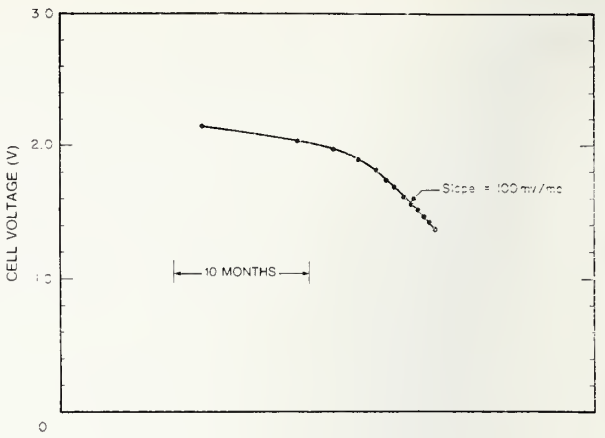

Figure 6. Projected end-of-life curve for a 702E cell, calculated using the data of figure 1. Cell load resistance is 50 kΩ.

second method should not be ignored; pacemaker manufacturers must deal with the "knee" effect and design their warning circuitry accordingly.

In summary, the reliability of the lithium-iodine cell has been demonstrated time and again. The time has come to focus not on reliability but on pacemaker circuit designs which provide adequate warning of end-of-life. The lithium-iodine system is not like other batteries and must be well-understood by the circuit designer to provide adequate warning. With proper circuit design, however, adequate warning can certainly be achieved, even under worst-case conditions.

3.2.2 Statistical Projections of Battery Longevity from Accelerated Discharge Data on Lithium-Iodine Power Cells

Douglas J. Gerrard,[1] Boone B. Owens, and Keith Fester
Medtronic, Inc.
3055 Old Highway Eight
Minneapolis, MN 55440
(612) 574-3095

A computer simulation model for use in lithium-iodine battery longevity projection has been devised from and is calibrated by accelerated test data from individual cells. The model incorporates the essential relationship between battery load voltage and the actual operating current of a functioning cardiac pacemaker.

Unlike mercury-zinc power cells, which maintain a relatively small and constant source impedance, R_{DC}, lithium-iodine batteries exhibit a continuously rising impedance throughout service life. The level depends not only upon the charge

[1]Now with Intermedics, Inc., P. O. Box 617, Freeport, TX 77541, (713) 233-8611, x150.

state, Q, of battery discharge, but also on the current drain, I, and the sequence of drains employed to achieve the given discharge state. A longevity model of a lithium-iodine powered pacemaker must therefore characterize the relationship between R_{DC}, I, and Q before it may properly incorporate the effect of pacemaker circuitry on current drain — hence, on generator life.

Accelerated test data[2] from type 742 batteries, on which the model was generated, are provided in figure 1. Here, the mean of the observed battery voltage drops, ΔV, is plotted against the charge delivered, Q, for various current drains. The number of cells tested under each of the different constant resistive loads, R_L, to achieve the indicated current levels, is listed in table 1. Voltage drop is defined as the estimated initial battery open-circuit voltage, V_{OC}, less the observed battery voltage, V_L. On the higher current drain tests, the curves indicate that distinctively different stages occur in the life of a 742 battery: a gently rising exponential increase, followed by a relatively linear increase, and completed with a sharp upswing in voltage drop. This pattern is amplified in figure 2 where ln ΔV is shown in relation to Q and I. Here, not only the aforementioned stages may be observed, but also a distinctive period at the beginning of battery life.

[2]Provided by the Power Sources Test and Evaluation Department of Medtronic.

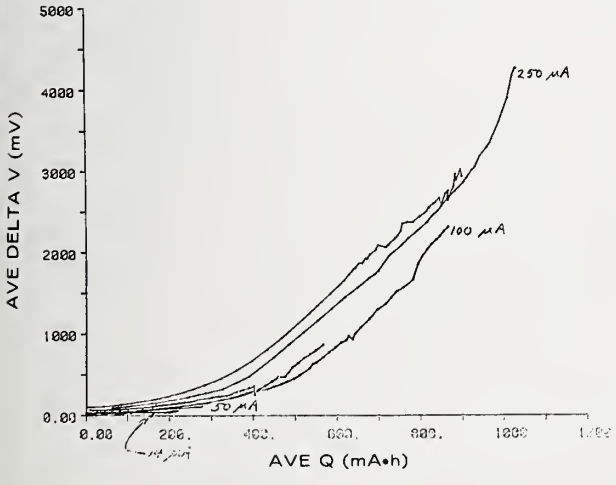

Figure 1. Average of the observed battery voltage drops, ΔV, plotted against the average delivered charge, Q, for different current drains of type 742 batteries.

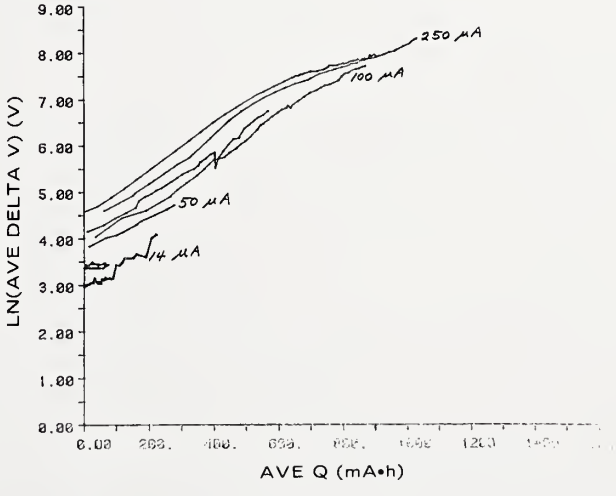

Figure 2. Logarithm of the average of the observed battery voltage drop, ΔV, plotted against the average delivered charge, Q, for different current drains of type 742 batteries.

Table 1. Number of Type 742 Cells Tested Under Different Constant Resistive Loads to Achieve Indicated Current Levels for Accelerated Test Data.

Number of Cells	Resistive Load (kΩ)	Nominal Drain (μA)
9	22.1	250
10	22.6	250
9	54.9	100
10	54.9	100
10	54.9	100
10	110	50
34	402	14
230	402	14
100	402	14

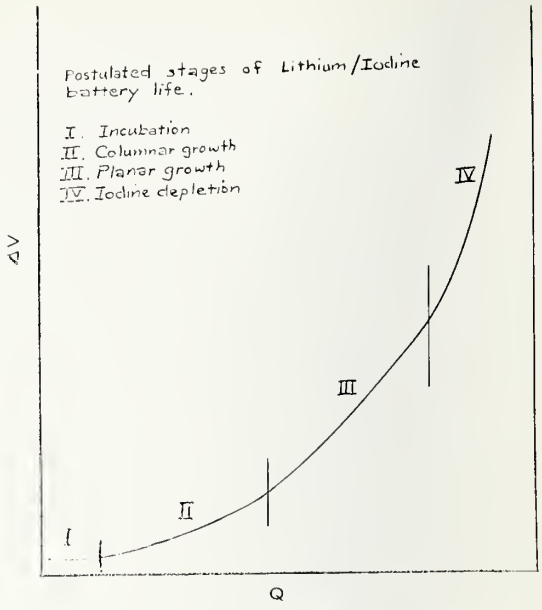

Figure 3. Illustration of the four postulated stages of life of a 742 battery described by the battery voltage drop, ΔV, as a function of delivered charge, Q.

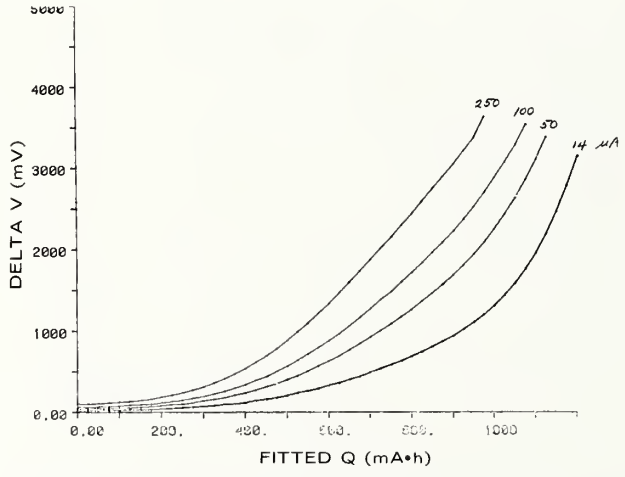

Figure 4. Dependence of battery voltage drop, ΔV, on delivered charge, Q, for different current drains as predicted by simulation model.

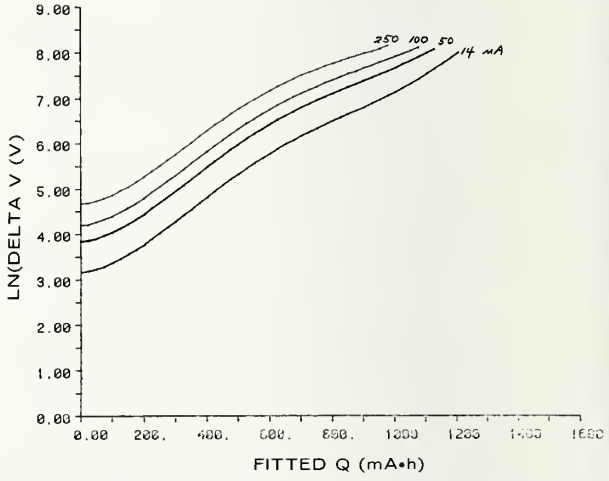

Figure 5. Dependence of the logarithm of of the battery voltage drop, ΔV, on delivered charge, Q, for different current drains as predicted by simulation model.

The four stages suggested by figures 1 and 2 and illustrated in figure 3 are postulated to be:

I. A period of incubation or stabilization,

II. A period of electrolyte columnar growth,

III. A period of electrolyte planar growth, and

IV. A period of severe iodine depletion within the cathode.

These stages, it should be emphasized, are a simplification of the actual complex changes occurring within the cell. However, they may be shown to have some basis in theory, and offer something more than a purely empirical rationale for mathematical model selection.

With respect to the effect of current drain, the pattern of curves as shown suggests a log-log relationship between ΔV and I. Independent current and voltage scans of other lithium-iodine cells substantiated this behavior, within the range of accelerated tests shown. From these considerations, the following mathematical model was selected and fitted to the data, using least squares:

$$\ln \Delta V = \beta \ln I + P_4(Q) \ , \tag{1}$$

where, for fixed load data,

$$I = (V_{OC} - \Delta V)/R_L \ , \tag{2}$$

and

$$P_4(Q) = \alpha + \gamma Q + \delta Q^2 + \varepsilon Q^3 + \lambda Q^4 \ . \tag{3}$$

Excellent agreement with the data was indicated by a correlation coefficient 0.9972 and by visual inspection of the fitted curves. (See figs. 4 and 5.) Consequently, eq (1) was incorporated into the simulation model to represent 742 battery behavior.

In the computer model, the beginning of pacemaker service life is defined as the maximum shelf-life of the generator. Knowing the current drain due to the timing and sensing circuits, the amount of charge removed during this early period may be used to calculate ΔV_0, the voltage drop at time zero. This becomes the initialization point for the computer simulator.

The elapsed times corresponding to successive stages in pacemaker life are then obtained by invoking the argument that because $I = dQ/dt$, $t = \int dQ/I$. If I were constant or expressable as an explicit function of Q, t might be derivable in closed form. But for the Xyrel pacemaker series, I may be obtained only by an iterative convergent procedure for each new value of ΔV. Consequently, t must be approximated by the relationship:

$$t = \sum_{\Delta V} \Delta Q/I \ , \tag{4}$$

in which ΔQ is the difference between successive positive real roots of eq (1) and I is the mean current drain during each increment.

In pacemaker models 5972 and 5973, the circuit is designed to maintain approximately constant energy by means of pulse-width stretching in response to load voltage. The current drain is therefore a nontrivial function of ΔV as illustrated in figure 6.

At each new time t, the energy output of the generator may be computed from the relationship:

$$E = \frac{C\ V_O^2}{2}\left\{1 - \exp\left(-\frac{2PD}{R_L C}\right)\right\} \qquad (5)$$

in which C is the capacitance of the output capacitor; PD is the pulse duration; R_L is the assumed electrode/tissue interface impedance; and V_O is the voltage accumulated on the output capacitor at the end of its recharge cycle, and is an elaborate function of pulse period, pulse duration, and the R_{DC} of the battery, which also must be obtained by iteration.

The computer model developed in this way is now able to show the manner in which battery and circuit parameters change with time under various electrode/tissue interface impedances. It is therefore able to generate a profile of pacemaker energy output throughout battery service life. This, considered in relation to energy stimulation thresholds to control the heart rate, observed in typical clinical study groups, ultimately enables the prediction of exit block[3] risk levels throughout the theoretical life of the pacemaker.

As an example of the use of this model, the calculation of energy output over time of the 5973 pacemaker is shown in figure 7 with and without the pulse-width-stretching feature. Superimposed on this plot are estimated percentiles

[3]Inability of the pacemaker to control the heart rate.

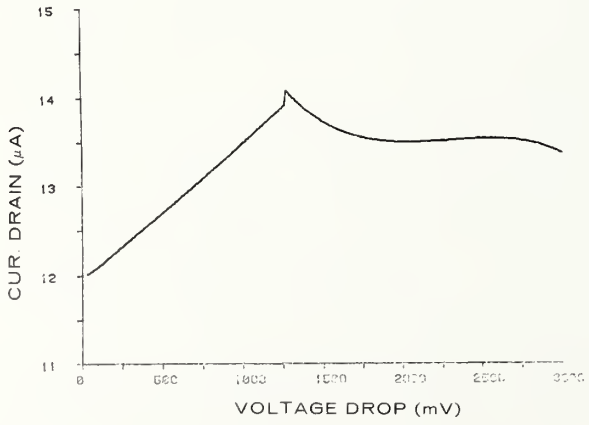

Figure 6. Current drain as a function of battery voltage drop for pacemaker models 5972 and 5973.

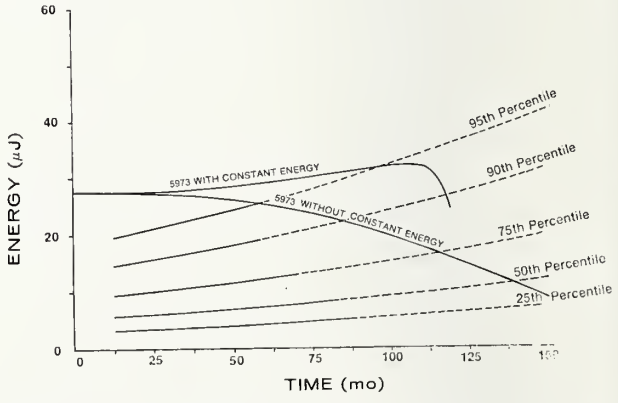

Figure 7. Calculated energy output over time of the 5973 pacemaker with and without pulse-width stretching feature. Superimposed are estimated percentiles of patient energy thresholds for effective unipolar pacemaker control of heart rate.

of patient energy thresholds, based upon actual clinical data from a series of different pacemaker follow-up centers. Although rate change, triggered by the reduction of battery voltage below a predetermined level, will occur earlier in the system employing energy compensation, its purpose of minimizing the risk of exit block during use is readily apparent in the illustration.

3.2.3 Qualification Procedures for Lithium-Iodine Pacemaker Cells and Cell Components

F. E. Kraus, M. V. Tyler, and A. A. Schneider
Catalyst Research Corporation
1421 Clarkview Road
Baltimore, MD 21209
(301) 296-7000

Catalyst Research Corporation lithium-iodine cells intended for pacemaker power source applications are subjected to an extensive design qualification protocol. This qualification program consists of material compatibility testing, on-going long-term monitoring of electrical performance, and environmental qualification testing. The purpose of this program is to determine the existence of any failure mechanisms inherent in the design or induced by exposure to environmental extremes. This paper will discuss the procedures and test parameters used in the qualification program.

All materials which are currently being used in the lithium-iodine cells and any materials which are proposed for use in these cells are studied to determine compatibility with the iodine-P2VP[1] charge transfer complex. Samples are placed in glass-stoppered test tubes containing a small amount of the complex and a piece of lithium metal. The sealed tubes are incubated at 37°C and at 60°C.

Two classes of materials are included in the qualification: metals and insulating materials. The surface resistance of the nonconductors is measured before immersion and after the complex is removed. These specimens are also inspected for changes in appearance, color changes, brittleness, etc. The metals are inspected using visible light microscopy, metallographic techniques, and scanning electron microscopy.

Environmental qualification procedures for pacemaker cells involve the selection of 32 cells from a single lot of cells at the completion of preliminary electrical tests but prior to the start of normal 45- or 60-day electrical tests. The remaining cells in the lot are subjected to the normal electrical test. The sample is divided into two 12-unit subsamples and one 8-unit subsample. One 12-unit subsample is exposed to 2,000-G shocks (6 times), 16.9-G RMS random vibration (6 h), 36-G repetitive bumps (4,000 times), and thermal cycles

[1]Abbreviation for poly-2-vinylpyridine.

between -40°C and +60°C (10 times). Prior to and after each test, the cells are inspected for insulation resistance and hermeticity, as well as for alteration of internal structure (radiographic inspection). Electrical properties at 37°C under a 100-kΩ load are also measured. Continuous monitoring of voltage dropout is employed throughout the vibration, bump, and shock tests.

The second 12-unit subsample is stored for eight weeks at 60°C under no electrical load. Periodic measurements are made of the electrical properties at 37°C under a 100-kΩ load. This subsample is also checked for insulation resistance, hermeticity, and internal integrity.

The 8-unit subsample is subjected to long-term life testing at 37°C and 60°C.

At the completion of these tests, each of the two 12-unit subsamples is divided into three groups of four units each. The first group is life-tested at 60°C under a 1-kΩ load, the second group is life-tested at 37°C under a 100-kΩ load, and the final group undergoes a post mortem examination.

The remaining cells of the lot from which the test sample was taken are subjected to the normal 45- or 60-day electrical test at 37°C under a 100-kΩ load. The test data from these cells serve as a data base for the evaluation of the data from the qualification sample.

Corrosion testing, which has been a part of the efforts to check for material compatibility, has shown that the results can be very dependent on environmental factors. It is well known that the more cold working that a stainless steel alloy receives, the greater will be the reduction in corrosion resistance. One sample of 304 stainless steel from a pacemaker cell case exposed to depolarizer for four months exhibited general corrosion in the corners only. In other words, only those areas which had been most severely cold worked had corroded. The corrosion rate was at least 0.56 mils per year (mpy) (14 μm/yr).

The other environmental factor which seems to have a considerable effect on the corrosion of metals by the depolarizer complex material is moisture. Results previously reported indicated that the iodine-P2VP complex material caused extensive pitting corrosion on 304 stainless steel with a rate on the order of 1 mpy (25 μm/yr). Recent results have indicated that the type but not the rate of corrosion is sensitive to moisture content.

Several samples of 304 stainless steel pacemaker cell cases which were immersed in depolarizer for four months at 37°C yielded rates of corrosion which varied from 0.70 to 1.8 mpy (18 to 46 μm/yr), with the average being 1 mpy (25 μm/yr). This corrosion was an uneven though general surface attack on the metal; pitting corrosion was not found.

A number of experimental batteries were constructed with the 304 stainless steel case used as a cathode current collector. The interior of the case was,

therefore, in intimate contact with the corrosive depolarizer. The batteries were stored on open circuit at 37°C for one year. At the end of this time, one of the batteries underwent a post mortem examination and the case was examined metallographically. The interior surface of the case exhibited intergranular corrosion over the entire area of the case. The average rate of the intergranular attack was 1 mpy (25 μm/yr).

The cause for the disparity between the current results and those obtained previously is believed to be moisture. In the first set of results, samples which were immersed in depolarizer with a piece of lithium exhibited less extensive corrosion than did those without lithium. The lithium partially desiccated the depolarizer, thus reducing the amount of corrosion. In this second set of data, there is evidence that the presence or absence of moisture influences the type of corrosion which is caused by the depolarizer. The outer surface of the case used as a cathode current collector exhibited pitting corrosion with a rate of 1.2 mpy (30 μm/yr). The outside of the case was exposed to iodine vapor with approximately 1-percent relative humidity and with short-term excursions to higher humidities. This seems to indicate that the presence of some minimum concentration of moisture is necessary for pitting corrosion to occur, but not for the other types of corrosion.

Another indication that moisture is responsible for the observed effects is the behavior of titanium in the two tests. In the early, presumably "wetter" test, titanium samples showed only surface etching; there was no appreciable removal of material. In the second set of tests, the depolarizer caused removal of large amounts of material, producing holes in some spots. The rate of corrosion was in excess of 30 mpy (762 μm/yr). This is believed to be moisture-related, since it is well known that titanium is corroded severely by dry chlorine, but not by moist chlorine gas. These results indicate strongly that the second set of corrosion tests was performed under "drier" conditions, although the concentration of water which would constitute "wet" conditions is completely unknown.

The following conclusions can be drawn from the data. The corrosive properties of the iodine-P2VP complex material are sensitive to moisture. In 304 stainless steel, pitting occurs in "moist" conditions, while general and intergranular corrosion are found under "dry" conditions. The rate of corrosion of 304 stainless steel has been found to be approximately 1 mpy (25 μm/yr) regardless of the moisture content.

3.2.4 Lithium-Thionyl Chloride Battery for Implantable Cardiac Pacemakers

J. Epstein and A. Lombardi
Power Systems Center
GTE Laboratories, Inc.
40 Sylvan Road
Waltham, MA 02154
(617) 890-8460

Three things must be considered in developing a power source for any application, especially one as critical as an implantable life-sustaining device: first, the choice of the type of power source, whether it be electrochemical, nuclear, or some other system; second, the design of the package to contain this system so that the efficiency of energy conversion is maximized and the operation of the device is not interrupted; and third, a quality control program to insure that the materials and assembly procedures are consistent with a prescribed set of standards.

For an energy source to meet the requirements of an implantable medical device, it must have the following characteristics: an energy density higher than, and an internal power loss rate lower than, those systems currently in use.

The capacities of three lithium-thionyl chloride cells after storage at room temperature for eighteen months are shown in table 1, while the capacities of another three cells after storage at 72°C are shown in table 2.

Although at this time there are not sufficient data available to support this claim with confidence, a trend is developing from the data in table 2 that indicates that the self-discharge rate or rather the rate of internal capacity loss is not constant. The energy densities of a typical lithium-thionyl chloride cell are 272 Wh/kg and 0.8 Wh/cm^3, making this system the highest energy density battery available.

Another characteristic of this battery system which makes it attractive is the ease of fabrication of the electrode materials. Both the cathode and anode are comprised of soft materials which are easily made to conform to almost any shape. The depolarizer is a liquid which will readily fill all the voids not filled by the anode and cathode.

The ability of this system to withstand both thermal and physical shock and vibration is superior to most other systems due also to the physical nature of the materials. Table 3 lists physical tests which a typical pacemaker cell can survive.

Other aspects of the design of this system include: the design of the packaging which precludes the possibility of a spontaneous reaction if the cell should be short-circuited, the selection of construction materials with respect to their compatibility with the active materials in the system, and the selection of the shape and positioning of the electrodes and current collectors to obtain maximum capacity at low rates of discharge.

Table 1. Capacities of Three Lithium-Thionyl Chloride Cells After Storage at Room Temperature.

Cell Number	Discharge Current, mA	Capacity, Ah
1	10	1.76
2	10	1.73
3	10	1.70

Table 2. Capacities of Three Lithium-Thionyl Chloride Cells After Storage at 72°C.

Months on Storage	Discharge Current, mA	Capacity, Ah
2	10	1.48
4	10	1.40
6	10	1.38

Table 3. Stress Tests and Conditions for Lithium-Thionyl Chloride Cells.

1.	Paint Shaker	- 5 h at approximately 45 Gs at 12 Hz
2.	Pressure Test	- 4 atm
3.	4-G Vibration	- at 20, 500, and 20 Hz
4.	Thermal Cycling	- from -40°C to +72°C; 2 cycles with 2 h at each temperature
5.	Drop Test	- 4500 Gs, one drop
6.	50-G Shock Test	- 3000 shocks
7.	545-G Shock Test	- 96 shocks

3.2.5 The SAFT Lithium Battery — Quality System

G. Lehmann and J. P. Rivault
SAFT Departement Piles
Rue G. Leclanché
86009 Poitiers, France
(49) 41.35.02

To assure the reliability of lithium-silver-chromate cells for pacemakers, SAFT has a quality system with the following characteristics: an organization structure where every operator is quality-minded; strict control procedures and tests for raw materials, parts, and finished products; acquisition and processing of control and test data for continuous evaluation of product quality; and close two-way technical relationships with customers to provide assistance and to improve battery quality and reliability.

A cell registration system is used to assure traceability of each cell and its components. These data, which have previously been recorded manually, are now being entered automatically into the registration system with a computer. Each cell manufactured in a given batch (one day's production) is numbered and has an identification sheet. As an example of one of the actions adopted to avoid risk of human error, the weights of all the cell components are recorded on the identification sheet. After the cell is assembled, the sum of the component weights is compared to the weight of the completed cell to insure that no component has been excluded.

To assure the quality of the cells which are shipped to customers, tests are performed 24 hours and 4 weeks after manufacture and prior to shipment.

At 24 hours after manufacture, the physical and electrical characteristics of each cell are measured. Then, out of each batch a sample of cells is selected to be discharged under an accelerated discharge rate of 200 μA and a pacemaker rate of 10 μA. These tests are performed instead of, for example, discharging all cells for one month under a low drain, because experience has shown that the behavior of the sample is representative of the cells in the batch. There is another reason for sample testing. The open-circuit voltage of an undischarged cell which is greater than 3.45 V will decrease to a level of 3.30 V after one-percent discharge. Therefore, by using an acceptance level of 3.45 V, the customer can be assured that the cell has not been previously discharged.

Four weeks after manufacture, the cell sample being discharged under accelerated and pacemaker rates is tested to check for abnormal behavior. Abnormal values of cell voltage and impedance for cells discharged under accelerated rates have been detected on occasion (about twice a year). This has led to batch rejection even though no abnormal behavior had been detected in cells discharged under pacemaker rates.

Prior to shipment, the cells are subjected to final checks (electrical characteristics tests, visual inspection, etc.). The characteristics of each cell are supplied to the customers so that they may compare them with the results of their incoming inspection tests.

The discharge tests of the samples from each batch are continued until the cells are discharged. The results of these tests are used to update cell reliability data and to improve the efficiency of the screen tests used.

3.2.6 The Observation of Electrolyte Phenomena in Lithium-Iodine Pacemaker Batteries With Neutron Radiographic Interrogation

Donald A. Garrett and Martin Ganoczy
Center for Materials Science
Reactor Radiation Division
National Bureau of Standards
Washington, DC 20234
(301) 921-3634

Thermal neutron radiography has been established in the field of nondestructive evaluation as a useful and complementary method to those of x- and gamma radiography. The differences in the absorption characteristics of x-rays and thermal neutrons, illustrated graphically in figure 1, demonstrate many areas in which thermal neutron images can provide data not possible with x-ray techniques. For example, most heavy elements are relatively transparent to thermal neutrons as compared to x-rays. One can easily inspect reasonable thicknesses

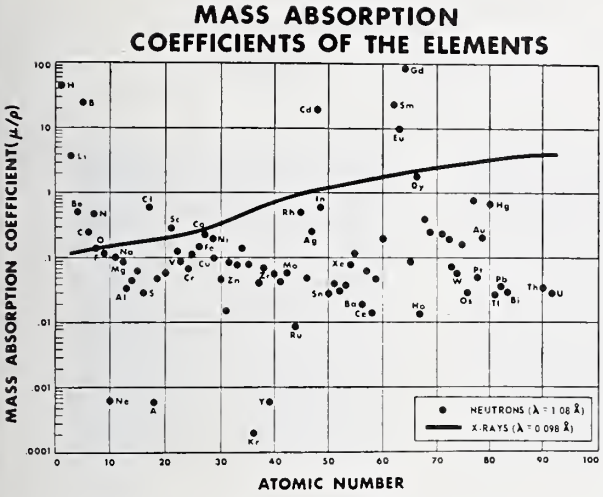

Figure 1. Mass absorption coefficients of the elements as a function of atomic number.

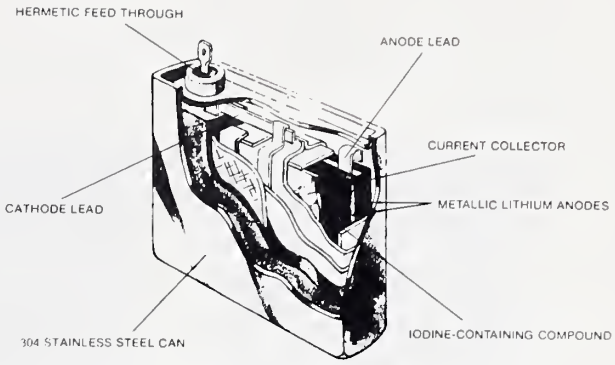

Figure 2. Schematic diagram of lithium-iodine pacemaker battery.

of such materials with neutrons, and it is possible to image some light materials when combined in an assembly with heavy materials, such as stainless steel.

As part of a cooperative effort between NBS and the Food and Drug Administration (FDA), a number of lithium-iodine batteries,[1] such as used in cardiac pacemakers, have been subjected to thermal neutron radiographic interrogation. The intent of this investigation was to determine the physical processes occurring in the electrolyte during battery depletion. The purpose of this report, at this early stage of the investigation, is only to document observations. No effort has been made yet to employ three-dimensional laminography or destructive testing.

X-radiography could not be used to examine these batteries because of the stainless steel encasement and electrodes used. Construction details of the batteries are illustrated in figure 2. Neutrons are capable of penetrating the case and electrodes, and, at the same time, they are capable of imaging the physical state of the low atomic number poly-2-vinylpyridine and lithium components of the battery.

Five separate batteries were subjected to neutron radiography. Neutron radiographs of batteries depleted for 0, 10, 28, 68, and 102 percent of the predicted battery lifetime are illustrated in figures 3 through 7, respectively. An apparent electrolyte migration was observed with increased battery depletion. Indeed, there appears to be a correlation between the radiographic density, i.e., increased neutron transmission through the battery, with increasing battery depletion as illustrated in figure 8. Although a separate battery was used for each depletion time period, the indications are that this correlation is real.

[1]Provided by FDA.

Several phenomena may be taking place with depletion to account for these observations. One may be the formation of gas pockets in the poly-2-vinylpyridine. Another may be the selective depletion of the lithium metal electrode. It should be noted that more experimentation must be conducted to explain the observed phenomena.

Figure 3. Neutron radiograph of a lithium-iodine battery with 0-percent depletion.

Figure 4. Neutron radiograph of a lithium-iodine battery with 10-percent depletion.

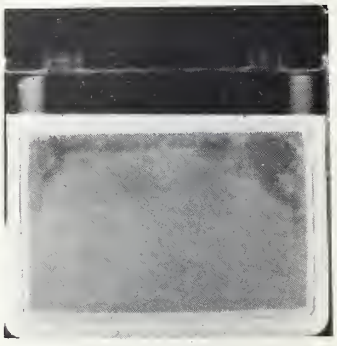

Figure 5. Neutron radiograph of a lithium-iodine battery with 28-percent depletion.

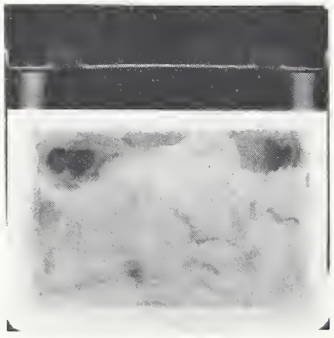

Figure 6. Neutron radiograph of a lithium-iodine battery with 68-percent depletion.

Figure 7. Neutron radiograph of a lithium-iodine battery with 102-percent depletion.

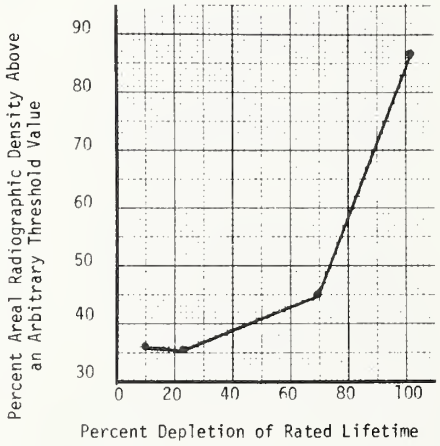

Figure 8. Percent of areal radiographic density (above an arbitrary threshold value) as a function of percent-depletion of rated lifetime.

3.3 Session III Moisture and Reliability

3.3.1 Moisture Measurements and Reliability — An Overview

Robert W. Thomas
Rome Air Development Center
RBRM
Griffiss Air Force Base, NY 13441

The correlation of moisture content with device reliability ultimately rests with the accuracy of the moisture measurement, locating the source of moisture, and a detailed understanding of the failure mechanisms which may be involved. Because of the large amount of research going on at the present time, it is appropriate that an overview be given to establish the current state-of-the-art in this field. The overview will be followed by projection into the future of the trends in moisture measurement.

Mass spectrometry is one of the oldest techniques used to measure moisture in integrated circuits. The RADC system has been in operation over 7 years and has analyzed over 10,000 parts. Mass spectrometers are known for giving reproducible results. Besides moisture, they also provide useful information on other gases within the package. Commercial equipment is now available that operates either in the batch mode or rapid cycle manner.[1] The biggest problem yet to be resolved is the transferability of mass spectrometer analyses. Because of differences in system configuration and calibration techniques, it has been very difficult to obtain correlation of gas analyses performed by different spectrometers on packages containing similar quantities of moisture. Attempts will be made to correct this problem through the use of round-robin correlation standards. The interpretation of the mass spectrometer data is also complicated by the outgassing of the package walls or other moisture-containing materials such as desiccants from within the cavity. Until the rapid cycle system was developed, the analysis was slow, requiring an overnight bakeout before analysis was possible.

The carrier gas system was developed primarily for large hybrid packages such as cardiac pacemakers. The package is punctured in two places and purged with a nitrogen carrier gas. Moisture picked up by the carrier gas is measured by a moisture sensor and integrated electronically to compute the moisture content of the package. Since the detector is relatively inexpensive compared to a mass spectrometer and no vacuum pumps are required, the total carrier gas system costs less than 25 percent of the mass spectrometer system. The interpretation of the results is also easier since the purge gas is at atmospheric pressure. This factor, plus a lower analysis temperature, decreases the outgassing from the cavity walls and organics (if present). The disadvantages of the system are that the technique does not work well for packages of less than 0.1-cm^3 volume. Also,

[1] Pernicka Corp., 1065 W. Maude, Suite 301, Sunnyvale, CA. (408) 735-0220.

since the sensor detects only moisture, other gaseous components cannot be evaluated.

Several types of moisture sensors are available which allow direct measurement of moisture by sealing the sensor inside the package. The surface conductivity sensor,[2] using interdigitated aluminum conductors, will withstand cerdip seal temperatures but has the disadvantage that, as yet, it provides only a qualitative measurement. The aluminum oxide sensors[3,4] have the advantage of being able to be calibrated for quantitative measurement, but will not yet survive the cerdip sealing cycle without degradation.

Many methods of calibration have been investigated. For day-to-day mass spectrometer system checks, the use of a large number of TO-18 cans sealed under controlled conditions was found to be very useful. For many years, RADC has used a molecular beam generation system. Even though costly, it proved to be an accurate method to establish sensitivity factors for moisture, oxygen, argon, and carbon dioxide. Moisture mixtures can also be generated by reacting hydrogen and oxygen over a hot platinum membrane. Commercial equipment is available which uses this technique. Research grade mixtures of moisture are also available. These seem to be most stable in the moisture range of 100 to 500 ppm. At higher or lower moisture content, the moisture content of the gas cylinders apparently does not remain stable. Other techniques are the two-temperature bath-bubbler with dilution flow, salt solutions, teflon capsules containing water, and packages containing moisture sensors.

Correlation experiments[5] were performed four years ago. At that time, agreement between laboratories was very poor, with results sometimes as great as two orders of magnitude apart. More recently in 1976, another round robin[6] was conducted which indicated that the spread had decreased to less than one order of magnitude for packages containing 800 ppm moisture.

RADC is now developing moisture standards for use in calibrating mass spectrometer and carrier gas systems. These standards are solder-sealed, side-brazed ceramic packages containing a moisture sensor for monitoring moisture

---

[2]Der Marderosian, A., Experimental and Theoretical Analysis of the Rate of Water Vapor Penetration Into Non-Hermetic Enclosures, this publication, pp. 56-60.

[3]Kovac, M., Chleck, D., and Goodman, P., A New Moisture Sensor for "In Situ" Monitoring of Sealed Packages, *15th Annual Proceedings, Reliability Physics*, Las Vegas, Nevada, April 12-14, 1977, pp. 85-91.

[4]Kovac, M., Performance Characteristics of Al_2O_3 Moisture Sensor Inside Sealed Hybrid Packages, *International Symposium on Microelectronics*, Baltimore, Maryland, October 24-26, 1977, pp. 249-252.

[5]Meyer, D. E., and Thomas, R. W., Moisture in SC Packages, *Solid State Technology* 17, 56-59 (1974).

[6]RADC Internal Reports (1976); data available upon request from author.

content. The sensor will be calibrated at RADC before opening and checked by the National Bureau of Standards after opening to provide traceability.

Polymer seals have been investigated thoroughly[7,8] during the last 3 years. It can be stated unequivocally now that polymer-sealed packages are not hermetic with respect to moisture.[9]

Work has progressed in the moisture characterization of organic materials. It has been shown that, by using adequate cure and bakeout conditions, the package ambients can be kept dry.[10]

A large amount of work is currently going on in a number of laboratories[11] to characterize moisture sensors. When this work is complete, there will be a very valuable technique available for measuring not only moisture content of hybrid packages but also leak rate.

Studies are planned using an ultra-sensitive microbalance to make direct measurements of surface isotherms for moisture. The results of these experiments will greatly aid in the interpretation and understanding of moisture analysis. Recently, contract work[12] has been initiated to establish failure threshold for moisture. This will provide the needed hard data for new LSI technology as well as sensitive CMOS hybrids.

In-house work at RADC on the gettering capability of several desiccants is now underway. Tentative results indicate that desiccants release moisture into the cavity at 100°C if the water content in the desiccant is greater than 10 percent.

Basic research is planned on the bonding mechanisms of moisture at surfaces, within organic die attach adhesives, and at surface discontinuities.

The military standard for microcircuits was published on 30 August 1977.[13] Method 1018 of that standard sets forth procedures which may be used to measure moisture in microcircuits. Maximum water content was established at 6000 ppm_v for hybrids, 5000 ppm_v for ICs, and 1000 ppm_v for desiccated parts, all measured

---

[7]Traeger, R., Hermeticity of Polymeric Lid Sealants, *Proc. 26th Electronic Components Conf.*, San Francisco, California, April 26-28, 1976, pp. 361-367.

[8]Thomas, R., Moisture, Myths and Microcircuits, *IEEE Trans. Parts, Hybrids, and Packaging* PHP-12, 167-171 (1976).

[9]Perkins, K., Moisture Measurement Studies, this publication, pp. 60-65.

[10]Messinger, C., Improved Reliability Through Dry and Hermetic Microcircuit Packaging, *Proc. 27th Electronic Components Conf.*, Arlington, Virginia, May 16-18, 1977, pp. 172-174.

[11]Bell Labs, Autonetics, Analog Devices (work in progress).

[12]Kovac, M., Effect of Ambients on Microelectronic Components, AF30602-75-C-0118, University of South Florida.

[13]Method 1018, MIL-STD-883B, Test Methods and Procedures for Microelectronics, August 30, 1977.

at equilibrium at 100°C. Reducing the maximum allowed level of water content further right now would force cerdips out of the military product lines. It is anticipated that cerdips will soon become available with moisture contents of less than 500 ppm_v.

The most important problem to be solved at this time is the transferability of moisture measurement technology throughout the industry. RADC is making every effort to develop accurate moisture standards for the analytical labs. It is highly desirable that the National Bureau of Standards become actively involved to insure traceable standards for the future.

3.3.2 Overview of Methods for Reducing Moisture Levels in Hermetically Sealed Pulse Generators

Frank J. Wilary and Arthur W. Burnham
Medtronic, Inc.
3055 Old Highway Eight
Minneapolis, MN 55418
(612) 574-3157

Hermetically sealed pulse generators, powered by lithium cells, consist of three hermetically sealed parts: the battery, the electronic circuitry, and the pulse generator package. Each part requires different processing and methods for controlling the internal moisture content.

The lithium battery is assembled in a dry room or a glove box under carefully controlled conditions. Use of this battery type provides the advantage of having a built-in moisture getter, the lithium anode. In general, the methods and processes used for controlling moisture inside the lithium battery are well developed and defined. Methods for monitoring the moisture content in the assembly area include the dew point hygrometer for dry rooms and gas chromatography for inside glove boxes.

The second part of the pulse generator, the electronic circuitry, is contained in its own hermetically sealed package. To achieve a moisture content of less than 1000 ppm requires that the circuitry be sealed in an inert-gas glove box subsequent to a high temperature (150°C) vacuum baking procedure. Levels of total moisture content, as measured with a mass spectrometer, have ranged from 200 to 600 ppm. When a lower baking temperature of 125°C was used, coupled with exposure to the room environment, the total moisture content measured ranged from 800 to 5400 ppm.

The pulse generator package is the third part of the hermetically sealed pulse generator. The package typically contains discrete components, feedthroughs (to the external lead and to the electronic circuitry), and soldered or welded connections, which are all susceptible to moisture-induced failure. For this reason, it is important to control moisture levels here as well. However, the extensive use of moisture-absorbing polymers and encapsulants inside

the package and the limits on the maximum allowed temperature (to protect the battery) make it difficult to achieve low levels of moisture by vacuum baking.

Two methods[1] have been used to monitor water content inside hermetically sealed pulse generators. They involve the use of a moisture sensor inside the pulse generator package to measure the vapor phase content and the use of a mass spectrometer to measure the total moisture content at 100°C.

The effects of different baking times and processing changes on the total moisture and the vapor phase contents inside pulse generator packages are provided in table 1. These types of data have proven very useful in evaluating materials and processing changes made to reduce water content inside research model pulse generators. Such changes have involved the elimination of potting compounds, the use of vacuum baking in controlled atmospheres, and the use of moisture getters. Use of these studies coupled with an understanding of the design factors and kinetics involved can result in the determination of a safe water content level for a given pulse generator system.

Table 1A. Total Water Content Versus Bake Time at 135°F (57.2°C) for Pulse Generator Package.

Vacuum Bake Time, h	Total Water Content, mg
0	6.0
0.167	2.4
4	1.45
4-18-4[a]	0.71
22	0.524
22[b]	0.125

[a]Three bake periods with assembly operations after the first and second periods.

[b]Improved transfer step from assembly to sealing and control of environment.

Table 1B. Vapor Phase Water Content Versus Bake Time at 135°F (57.2°C) for Pulse Generator Package.

Vacuum Bake Time, h	Range of Vapor Phase Water Content at 23°C, ppm
0	3,700 to 12,250
4	1,800 to 3,600
22[c]	30 to 460
22[d]	<2.5 to 50

[c]Potting compound used to anchor discrete components and electronic circuitry.

[d]Clip used to hold discrete components and electronic circuitry.

[1]Method 1018, MIL-STD-883B, Test Methods and Procedures for Microelectronics (August 31, 1977).

3.3.3 The Effects of Moisture on the Reliability of Implantable Pacemakers

Lloyd A. Ferreira[1]
Telectronics Proprietary Ltd.
8560 Main Street
Williamsville, NY 14221
(716) 631-0360

Moisture has been a focal point of attention in pacemaker reliability studies because it has been responsible for a variety of failure modes in high reliability products.[2] In combination with various other contaminants (halides, reactive metals, phosphates, etc.), it guarantees some of the most bizarre failures imaginable. It is virtually impossible to eliminate contaminants during manufacture; therefore, the removal of moisture at manufacture and the protection against its intrusion after implant would make the single greatest contribution to pacemaker reliability.

Consider a typical hermetically sealed pacemaker of contemporary design. It can be simplified into three hermetic metal containers which have moisture trapped in them and seals through which moisture can enter. The basic building block for each of these three containers is a metallic conductor fused to a cylindrical insulator feed-through (usually ceramic) for electrical access to the container interior. In the complete pacemaker, this gives us at least six sources of moisture as indicated in figure 1, or more in the case of bipolar pacemakers and multiterminal electronics packages and batteries.

---

[1]Present address: Intermedics, Inc., P. O. Box 617, 240 Tarpon Inn Village, Freeport, TX 77541.

[2]MacGregor, D. C., M.D., Noble, E. J., M.D., Morrow, J. D., M.D., Scully, H. E., Covvy, H. D., MSc, Goldman, B. S., M.D., Management of a Pacemaker Recall, *J. Thoracic and Cardiovascular Surgery* 74, 657-667 (1977).

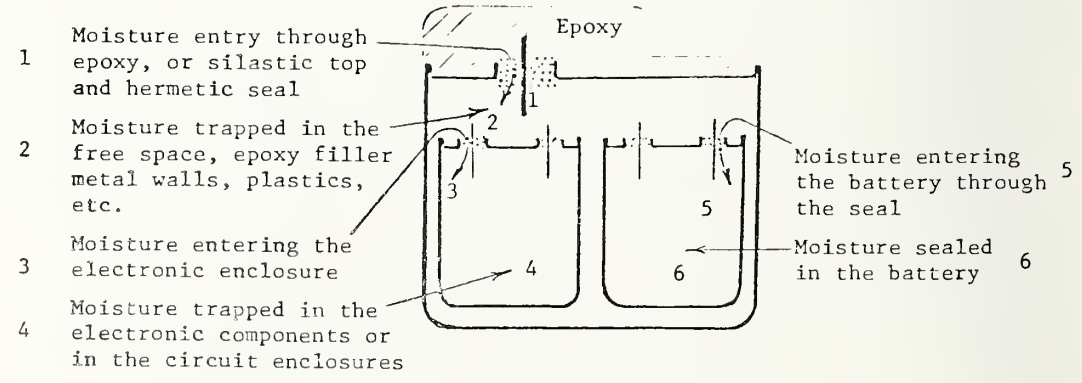

Figure 1. Sources of moisture in a typical pacemaker.

A study was made to determine the efficaciousness of hermetically sealing pulse generators. A comparison was made of 107 epoxy encapsulated pulse generators (Model P7, 1968) with 88 hermetically sealed pulse generators (Model P9, 1971). Both generators used identical monolithic integrated circuits and mercury-zinc cells. All units were mature human implants supplied to three hospitals over a period of three years,[3] randomly selected from a production series of 1,257 pacemakers.

Both sets of units showed good reliability to 33 months, with the oldest survivors in use for 51 and 54 months, respectively. Survival data for these units are shown in table 1. As may be observed, the gain in reliability and longevity is negligible and could be attributed to improved quality control techniques rather than to hermetic sealing. The incidence of electronic failure was not significantly different between the two units, probably a direct result of having all active components housed in the one hermetically sealed monolithic integrated circuit used in both units.

Why did hermetic sealing and the exclusion of body fluids not significantly improve the performance of these units? One reason, obviously, is the operating life limitation of the mercury-zinc battery; but the other is that these units (in spite of the inclusion of moisture getters and a claimed hermetic seal of 1×10^{-7} atm·cm^3/s) were always operating in an environment saturated with moisture, due in part to moisture vented from the nonhermetic cell,[4] but largely from moisture trapped within the pacemaker at manufacture.

To confirm that the hermetically sealed units were saturated with moisture, gas analyses of these units were conducted after a method first described by Bergsten and McDowell[5] and refined by Thomas.[6] The apparatus, shown in figure 2, consists of a closed, thermally stable system with an enclosed package opener and a magnetic mass spectrometer to analyze the gas removed from the pacemaker case. The chamber which houses the sample is kept at 37°C to simulate operating conditions while the remainder of the apparatus in contact with the gas is main-

---

[3]We are grateful for the assistance given us by the following in the compilation and analysis of the data. Mr. Sid Yarrow, Senior Technical Officer, Clinical Physiology Department, Greenland Hospital, Auckland, N.Z.; Doug Baird, M.D., Royal Prince Alfred Hospital, Sydney, Australia; Biomedical Engineering Staff of St. Vincent's Hospital, Sydney, Australia; Mr. Tibor Nappolz and Mr. Mike Krockmal of Telectronics, Australia; Dr. Fred Gollob, Ph.D. of Gollob Analytical Service, Berkeley Heights, New Jersey.

[4]Personal communication with Tom O'Nan of Mallory Battery Company, Tarrytown, New York.

[5]Bergsten, W. E., and McDowell, J. F., The Internal Atmosphere of Hermetically Sealed Components, *14th Annual National Relay Conference*, Oklahoma State University, Stillwater, Oklahoma, April 1955.

[6]Thomas, R. W., Microcircuit Package Gas Analysis, *14th Annual Proceedings, Reliability Physics Symposium*, April 20-22, 1976, pp. 283-294.

Table 1A. Cumulative Survival Data for 107 Epoxy-Encapsulated, Model P7, Pacemakers.

TOTAL 107 PMKRS
AVG MOS 23.9966
PMKR MOS 2567.63

CUMULATIVE SURVIVAL CALCULATIONS, P7

(M) AGE MOS	(N) NR. SURVIVD	(A) INCMPLT LIFETME	(B) CURTLD. LIFETME	(D) FAILD UNITS	(T) TOTAL A+B+D	(X) EXPOSED Z=A+B X=N-Z/2	(F) FRACT FAILD F=D/X	(S) FRACT. SURVIV. S=1-F	(SI) CUMULTV SURVIV. SI=SI*S	
0 - 3	107	0	11	0	11	101.5	0.000	1.000	1.000	
3 - 6	96	0	2	0	2	95.0	0.000	1.000	1.000	
6 - 9	94	0	2	0	2	93.0	0.000	1.000	1.000	
9 - 12	92	0	5	0	5	89.5	0.000	1.000	1.000	
12 - 15	87	0	3	1	4	85.5	0.012	0.988	0.988	
15 - 18	83	0	5	0	5	80.5	0.000	1.000	0.988	
18 - 21	78	0	2	2	4	77.0	0.026	0.974	0.963	
21 - 24	74	0	5	0	5	71.5	0.000	1.000	0.963	
24 - 27	69	0	8	0	8	65.0	0.000	1.000	0.963	
27 - 30	61	0	20	2	22	51.0	0.039	0.961	0.925	
30 - 33	39	0	23	1	24	27.5	0.036	0.964	0.891	*
33 - 36	15	0	6	0	6	12.0	0.000	1.000	0.891	
36 - 39	9	0	2	0	2	8.0	0.000	1.000	0.891	
39 - 42	7	0	1	0	1	6.5	0.000	1.000	0.891	
42 - 45	6	0	3	0	3	4.5	0.000	1.000	0.891	
45 - 48	3	0	1	0	1	2.5	0.000	1.000	0.891	
48 - 51	2	0	1	1	2	1.5	0.667	0.333	0.297	**
TOTALS	0	0	100	7	107					

* 90% CUMULATIVE SURVIVAL AT BEGINNING OF QUARTER
** 50% CUMULATIVE SURVIVAL AT BEGINNING OF QUARTER

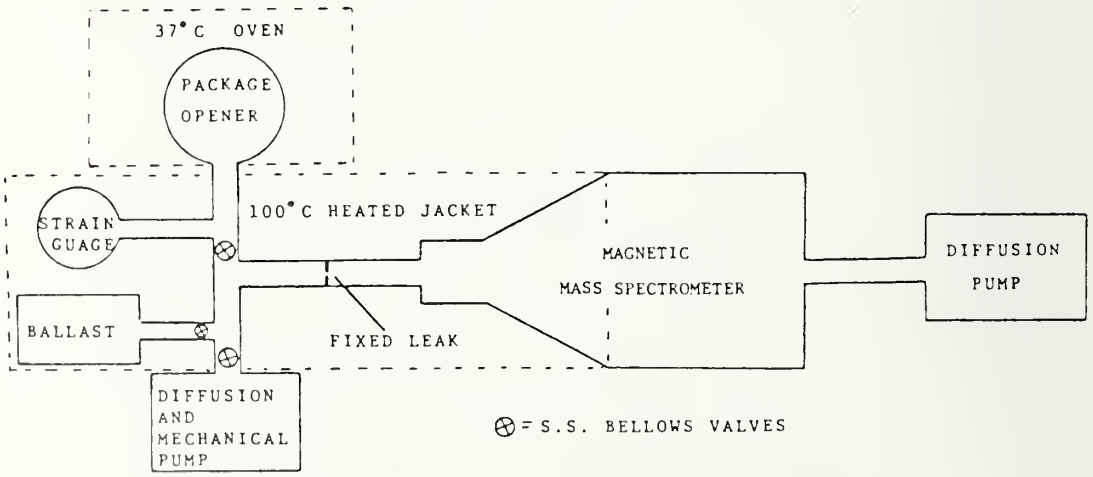

Figure 2. Schematic of mass spectrometer analysis system for pacemakers.

Table 1B. Cumulative Survival Data for 88 Hermetically Sealed, Model P9, Pacemakers.

TOTAL 88 PMKRS
AVG MOS 25.3890
PMKR MOS 2234.23

CUMULATIVE SURVIVAL CALCULATIONS, P9

(M) AGE FRACT. MOS SURVIVD	(N) NR. CUMULTV SURVIV. S=1-F	(A) INCMPLT LIFETME SI=SI*S	(B) CURTLD. LIFETME	(D) FAILD UNITS	(T) TOTAL A+B+D	(X) EXPOSED Z=A+B X=N-Z/2	(F) FRACT FAILD F=D/X	(S)	(SI)
0 - 3	88	0	5	0	5	85.5	0.000	1.000	1.000
3 - 6	83	0	2	1	3	82.0	0.012	0.988	0.988
6 - 9	80	0	3	0	3	78.5	0.000	1.000	0.988
9 - 12	77	0	2	0	2	76.0	0.000	1.000	0.988
12 - 15	75	0	2	0	2	74.0	0.000	1.000	0.988
15 - 18	73	0	4	0	4	71.0	0.000	1.000	0.988
18 - 21	69	0	10	0	10	64.0	0.000	1.000	0.988
21 - 24	59	0	6	1	7	56.0	0.018	0.982	0.970
24 - 27	52	0	4	1	5	50.0	0.020	0.980	0.951
27 - 30	47	0	12	1	13	41.0	0.024	0.976	0.928
30 - 33	34	0	8	0	8	30.0	0.000	1.000	0.928
33 - 36	26	0	10	0	10	21.0	0.000	1.000	0.928
36 - 39	16	0	10	0	10	11.0	0.000	1.000	0.928
39 - 42	6	0	2	0	2	5.0	0.000	1.000	0.928
42 - 45	4	0	0	0	0	4.0	0.000	1.000	0.928
45 - 48	4	0	2	0	2	3.0	0.000	1.000	0.928
48 - 51	2	0	1	0	1	1.5	0.000	1.000	0.928
51 - 54	1	0	0	0	0	1.0	0.000	1.000	0.928
54 - 57	1	0	1	0	1	0.5	0.000	1.000	0.928
TOTALS	0	0	84	4	88				

* 90% CUMULATIVE SURVIVAL AT BEGINNING OF QUARTER
** 50% CUMULATIVE SURVIVAL AT BEGINNING OF QUARTER

tained at 100°C to prevent condensation during sampling. The process of making gas analyses of pacemaker samples involves the following steps after the system is temperature-stabilized over a 24-h period. The system containing the pacemaker and the chamber that will contain the gas prior to analysis is evacuated for one hour with high-vacuum diffusion pumps. The system is tested for 1 min using a mass spectrometer to detect leaks. The pacemaker is then punctured by the package opener while being monitored by a strain gauge to determine effective puncture. About 30 s is allowed for the pressure of the punctured pacer to equilibrate with the chamber. The gas scan is then performed by the mass spectrometer over a period of about 10 min and the data recorded and calculated.

Test results of gas analyses of different pacemakers are as follows. To determine the effect of pacemaker temperatures on the moisture content measurements, tests were performed on a control series of model P9 pacemakers for three temperatures, 37, 55, and 70°C. The results are shown in table 2. It is not possible or advisable to heat pacemakers over 70°C to the temperature and time

needed to expel all moisture (i.e., 100°C, 48 h). So it is not clear what percentage of total moisture content is indeed measured, or what percentage of the total water content is bound, in vapor phase or in liquid phase. The results of gas analyses of model P9 pacemakers from the study are shown in table 3. Finally, the results of gas analyses of pacemakers from various manufacturers in use or offered for sale in 1977 are shown in table 4. It is apparent from these results that a large amount of moisture is present in pacemakers. In fact, no pacemaker measured by the method outlined was found to be less than 100 percent saturated with water vapor within its outer hermetic enclosure at 37°C.

In view of these findings, any demonstrated increase in reliability of today's pacemakers over their predecessors[7] may simply be due to the use of lithium batteries, better quality electronic components, and refined production and testing techniques, rather than hermetic sealing — as it is presently being performed by many manufacturers.

[7]Ferreira, L. A., The Performance of Over 12,000 Lithium Powered Pulse Generators, *Telectronics Pacemaker Reliability Report* (April 1977).

Table 2. Gas Analysis Results of Hermetically Sealed (Model P9) Pacemakers Held at Temperatures of 37°, 55°, and 70°C.

Model/Serial No. of Pulse Generator	P9/6484		P9/6480		P9/6453	
Gas Composition	Volume %	Volume cm^3	Volume %	Volume cm^3	Volume %	Volume cm^3
Nitrogen	0.66	1.9	1.11	3.14	1.12	0.15
Oxygen	0.13	0.38	0.10	0.28	0.002	0.027
Argon	39.4	11.39	48.0+	13.58	50.0+	6.85
Carbon dioxide	0.016	0.46	0.019	0.53	0.005	0.068
Hydrogen	12.5	3.61	3.6	1.2	34.6	4.74
Helium	-	-	-	-	-	-
Water	45.0+	13.01	46.2	13.07	13.9	1.9
Organics	1.8	0.52	0.043	0.12	0.18	0.2
Total Gas Mixture	100	28.9	100	28.3	100	13.7
Helium leak test	Not Done		Not Done		Not Done	
Test temperature	70°C		55°C		37°C	
Product age (months)	18		18		30	
History	No Load-Not Impl.		No Load-Not Impl.		No Load-Not Impl.	
Internal pressure (psi)[1]	10.6		10.4		5	

[1]One psi (pounds per square inch) $\approx$ 6.9×10^3 Pa.

Table 3. Gas Analysis Results of Hermetically Sealed (Model P9) Pacemakers Held at 37°C.

Model/Serial No. of Pulse Generator	P9/6114		P9/5778		P9/5743		P9/5787		P9/5721	
Gas Composition	Volume %	Volume cm^3	Volume %	Volume cm^3	Volume %	Volume cm^3	Volume %	Volume cm^3	Volume %	Volume cm^3
Nitrogen	2.6	7.8	0.85	2.93	1.11	1.47	0.71	2.47	1.76	2.6
Oxygen	-	-	-	-	-	-	-	-	-	-
Argon	16.5	49.5	7.3	25.2	24.2	32.2	9.6	33.4	21.8	32.3
Carbon dioxide	0.011	0.03	0.012	0.41	-	-	-	-	-	-
Hydrogen	51+	153+	59+	203.5	56+	74.5	79+	274.9	66+	97.7
Helium	-	-	-	-	-	-	-	-	-	-
Water	29	87	32.2	111.1	17.5	23.3	10.4	36.2	9.9	14.6
Organics	0.058	0.174	0.13	0.45	0.35	0.46	0.07	0.24	0.38	0.56
Total Gas Mixture	100	300	100	345	100	133	100	348	100	148
Helium leak test[1] ($atm \cdot cm^3/s$)	2×10^{-6}		1×10^{-6}		1×10^{-6}		1×10^{-6}		1×10^{-6}	
Test temperature	37°C		37°C		37°C		37°C		37°C	
Product age (months)	51		54		55		54		56	
History	Impl. 26 mos.		Impl. 23 mos.		Impl. 29 mos.		Impl. 28 mos.		Impl. 35 mos.	
Internal Pressure (psi)[2]	110		127		49		128		54	

[1]Test conditions: 50 psi; 6 h.

[2]One psi (pounds per square inch) $\sim$ 6.9×10^3 Pa.

Table 4. Gas Analysis Results of Hermetically Sealed Pacemakers from Various Manufacturers, in Use or Offered for Sale in 1977. Pacemakers were held at 37°C prior to puncture.

Pulse Generator	Product A		Product B		Product C		Product D		Product E	
Gas Composition	Volume %	Volume cm^3	Volume %	Volume cm^3	Volume %	Volume cm^3	Volume %	Volume cm^3	Volume %	Volume cm^3
Nitrogen	4.1	0.19	7.7	0.29	4.2	0.08	31.4	1.51	1.6	0.02
Oxygen	-	-	-	-	-	-	9.9	0.48	0.06	0.001
Argon	56	2.63	70	2.59	54	0.97	0.50	0.02	0.019	0.0003
Carbon dioxide	0.46	0.02	7.2	0.27	0.007	0.0001	0.12	0.006	0.012	0.0002
Hydrogen	0.16	0.007	0.33	0.012	30.2	0.54	0.16	0.008	4.1	0.074
Helium	3.7	0.17	3.9	0.14	-	-	0.06	0.003	0.02	0.0003
Water	35.1	1.65	10.1	0.37	10.9	0.2	57+	2.73	94	1.7
Organics	0.015	0.001	0.78	0.03	0.24	0.004	0.89	0.043	0.09	0.002
Total Gas Mixture	100	4.7	100	3.7	100	1.8	100	4.8	100	1.8
Helium leak test ($atm \cdot cm^3/s$)	5×10^{-7}		7×10^{-7}		?		?		2×10^{-4}	
Test temperature	37°C		37°C		37°C		37°C		37°C	
Product age (months)	24		24		24		18		24	
History	All units are presently being offered for sale by four different manufacturers.									
Internal pressure (psi)[2]	6.3		6.8		approx. 13		?		?	

[1]Test conditions: 50 psi; 6 h.

[2]One psi (pounds per square inch) $\sim$ 6.9×10^3 Pa.

What are some results of operating in a moist environment? The following is a brief description of examples of moisture-related pacemaker failure modes.

Dendritic growth on printed circuit boards or through a passive medium requires a potential difference, moisture, and one of the "gypsy" metals (silver, copper, etc), all conditions found in pacemakers. A contaminant such as chlorine can considerably accelerate this failure mode. Also, any number of chemicals commonly used in production leave behind a variety of residues which combine with moisture to form acids or ionized solutions, most of them detrimental to circuit reliability and stability. Such residues have led to electrical short circuits at terminal feed-throughs and in semiconductor devices. The problem of nonhermetic batteries operating in a high humidity environment is one the industry has lived with in the past and must still face in the future. At least one mercury and two lithium batteries in use in pacemakers today are not hermetically sealed. The lithium cells, in particular, will either suffer much reduced life expectancy or leak electrolyte with the natural ingress of moisture.

In conclusion, the following points are submitted regarding the matter of moisture and reliable cardiac pacemakers:

- Moisture inside all parts of a pacemaker should be below 6,000 ppm, the dew point of water at 37°C. The maximum ambient moisture content inside high reliability active components should be 2,000 ppm.
- The mass spectrometer method should be better defined and refined to obtain absolute, repeatable values of moisture content for routine analyses of production pacemakers and failed explants. At present, this method costs as much as 25 percent of the value of the pacemaker to perform. The profile provided, however, gives vital clues to the causes of failure.
- The use of temperature cycling of pacemakers as a routine production test for stressing mechanical bonds can have the detrimental effect of condensing available moisture on critical areas of the electronic circuitry.
- Claims by many manufacturers about the control of moisture levels in their pacemakers are, at best, highly theoretical and as yet unproven.
- Standards should be devised to define acceptable moisture levels in pacemakers.
- Techniques for moisture removal before hermetic sealing should be developed. The unit should be welded in a dry environment at the end of the drying procedure. This approach may not be successful for units filled with epoxy.
- The use of sensors to monitor moisture levels and the use of desicants to immobilize moisture should be considered.

- Moisture-related failures are by nature low-level chemical reactions. As such, most of them occur in a slow progressive manner and may be detected as a gradual change in performance, allowing timely pacemaker removal. With the routine use of telephone surveillance equipment and home-check devices, many potential failures may be detected in time. These methods of verifying pacemaker reliability performance should be mandatory for all pacemaker-dependent patients.
- Whatever the reason, moisture is the enemy of reliability and until it is immobilized, reduced, or removed, the dream of a reliable ten-year pacemaker may remain just that.

3.3.4 The Relationship Between Moisture, Reliability, and Leak Rate — A Status Report[1]

Robert E. Sulouff
Martin Marietta Aerospace
Orlando Division
P.O. Box 5837
Orlando, FL 32805
(305) 352-4261

This study is to evaluate the influence that water vapor has on the reliability of solid state devices. The correlation between helium leak rate and the failure rate for packages with unpassivated monolithic operational amplifiers (type 741) operating in a bias life test at 85°C and 85-percent relative humidity is being developed. The packages open to the environment have had a mean time to failure (MTF) of 1,480 hours. The packages with initial leak rates from the gross level to 10^{-8} atm·cm^3/s have had a failure rate of 1,675 hours MTF. Failure analysis has indicated that the helium leak rates have randomly changed several orders of magnitude over the life of the test. The external pins have indicated a susceptibility to stress corrosion failure and have been a primary failure mode.

The evaluation of the dew point technique has indicated that the accuracy and precision of the method is in question. Packages sealed with given amounts of water vapor could not be correlated with the dew point technique.

Studies of helium leak rate versus moisture leak rate have shown that 1.5×10^{-5} atm·cm^3 of helium leak rate corresponds to a water vapor leak rate of 1.6×10^{-8} cm^3, with a water vapor pressure difference of 8-mm mercury (10^3 Pa). The same helium leak rate of 1.5×10^{-5} atm·cm^3/s showed a water vapor leak rate of 2.6×10^{-7} cm^3/s with a pressure difference of 370-mm mercury (4.8×10^4 Pa) at 85°C and 85-percent relative humidity.

[1]This work is supported by the Defense Advanced Research Projects Agency (Order No. 2397, Program Code 8Y10) under NBS Contract No. 5-35880.

3.3.5 Experimental and Theoretical Analysis of the Rate of Water Vapor Penetration Into Non-Hermetic Enclosures

Aaron Der Marderosian and Vincent Gionet
Raytheon Company
Equipment Division
Sudbury, MA 01776
(617) 443-9521

A review of the literature dealing with packaged semiconductor devices reveals that a large percentage of the failures are associated with one type of corrosion mechanism or another. Moisture continues to play a large part in this mode of failure.

The sources of moisture in these packages have been described in various papers[1,2,3] and may be categorized as follows: (1) moisture that has been trapped inside the package due to poor bake-out procedures, (2) moisture that is generated internally from material decomposition and outgassing and from residues of the solder glass devitrification process, (3) moisture that permeates through polymer seals, and (4) moisture that penetrates the package through cracks and faulty seals. The last of these sources is addressed here by attempting to relate the rates of moisture ingress to the leak rates of packages, in the range of from 10^{-1} to 10^{-5} atm·cm^3/s.

To determine the rate of moisture penetration into a given enclosure, calibrated systems consisting of a glass tube narrowed at one end to a capillary, a TO-5 transistor package, and a moisture sensor were assembled as shown in figure 1. The air leak rates of a number of different sized capillaries were measured using the rate of pressure rise method. The method involves measuring the time it takes for the pressure in a known volume to increase by a certain amount. In this case, the time measurement was for pressure increases from 1 to 2 or from 1 to 10 torr,[5] depending on the magnitude of the leak rate. The leak rate was determined by dividing the product of the pressure rise and enclosure volume by the pressure rise time.

These capillary tubes were used to calibrate the remaining 65 capillary tubes by another and quicker method. This method[6] involves submerging the capillary end

---

[1]Thomas, R. W., Moisture Myths and Microcircuits, *Proc. 26th Electronic Components Conference*, San Francisco, California, April 26-28, 1976, pp. 272-276.

[2]Der Marderosian, A., Nichrome Resistor Investigation, *Raytheon Internal Report* IS:72:6 (January 26, 1972).

[3]Traeger, R. K., Non Hermeticity of Polymeric Lid Sealants, *IEEE Trans. Parts, Hybrids, and Packaging* PHP-13, 147-152 (1977).

[4]Leak rate is commonly given in units of atm·cm^3/s (10^{-1} Pa·m^3/s).

[5]1 torr = (1/760) atm $\simeq$ 133 Pa.

[6]Stinnet, D., Der Marderosian, A., and Nelson, P., Weight Test Method Detects Gross Leaks in Components, *Evaluation Engineering* 9, 12-16 (1970).

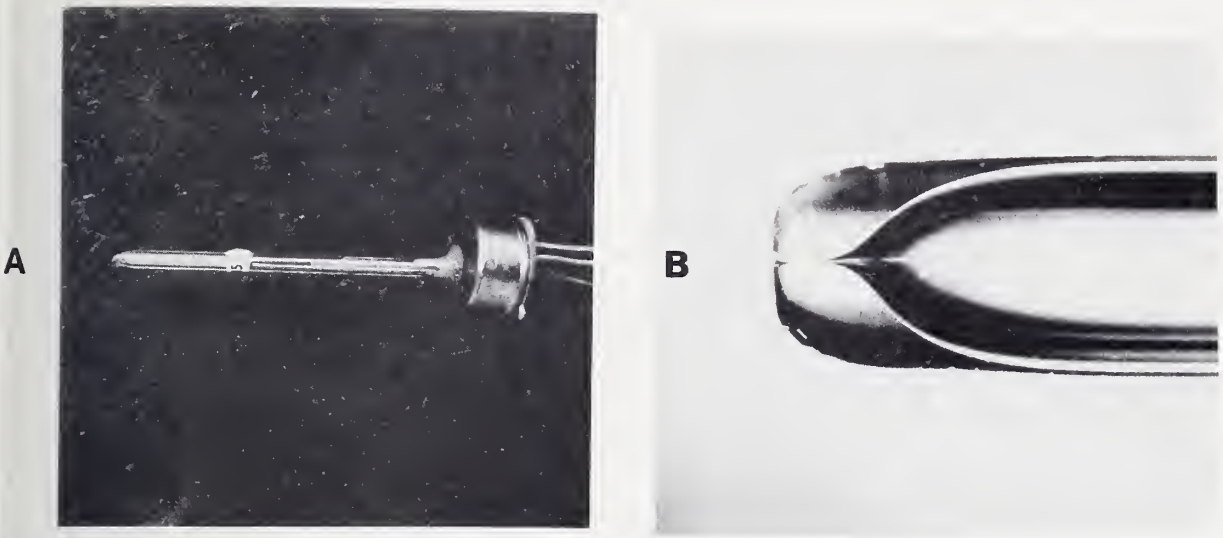

Figure 1. Calibrated system showing (A) completed assembly of calibrated gross leaker and TO-5 can and (B) end of capillary tube of calibrated gross leaker.

of the tube in FC-77 liquid, while the other end is connected to a nitrogen gas source. The gas pressure is slowly raised until bubbling is initiated. This was done for capillaries with leak rates from 10^{-1} to 10^{-5} atm·cm^3/s to establish a calibration curve of the differential pressure required to initiate bubbling versus air leak rate.

After the leak rates of the remaining capillaries were measured, each capillary tube was sealed to a cover of a TO-5 transistor package. A surface conductivity type moisture sensor, calibrated under known humidity conditions, was then attached to the base of each respective TO-5 package and finally sealed to the top of the TO-5 package. A drawing of the moisture sensor is shown in figure 2, while a typical calibration curve is shown in figure 3.

These parts were placed, capillary side down, through a test plate pre-drilled to accept the TO-5 cover. The parts were then wax-sealed at the edges, and the capillary was exposed to a constant humidity of 80-percent relative humidity (RH) generated from a saturated salt solution. The time constant of moisture ingress was measured, from which the moisture leak rate was calculated. The moisture versus the air leak rate for each of the surviving capillary tubes[7] is plotted in figure 4.

In an attempt to develop a method for calculating the moisture leak rate for a capillary from its air leak rate, the following was done. The diameter of the capillary for the range from capillary leak rates considered (10^{-0} to 10^{-5} atm·cm^3/s) was calculated using gas flow equations for viscous (10^{-0} to 3×10^{-3} atm·cm^3/s) and

[7]Many of the capillary tubes became plugged and were retired from the experiment.

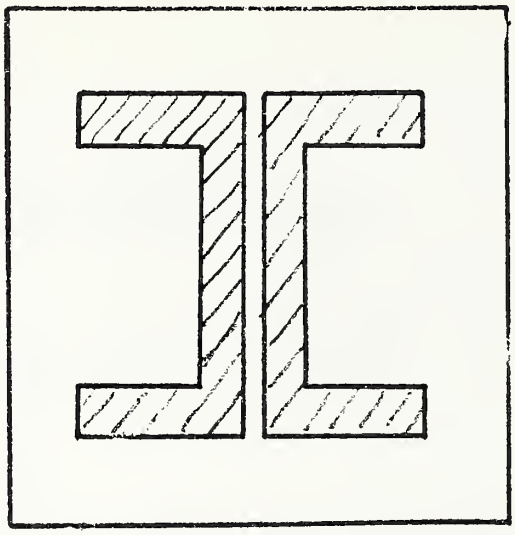

Figure 2. Sketch of surface conductivity-type moisture sensor consisting of a 1-μm thick aluminum metallization (shaded area) on a glass or aluminum substrate. The 1-mm high "C"-shaped metallization areas are separated by a distance of 0.05 mm.

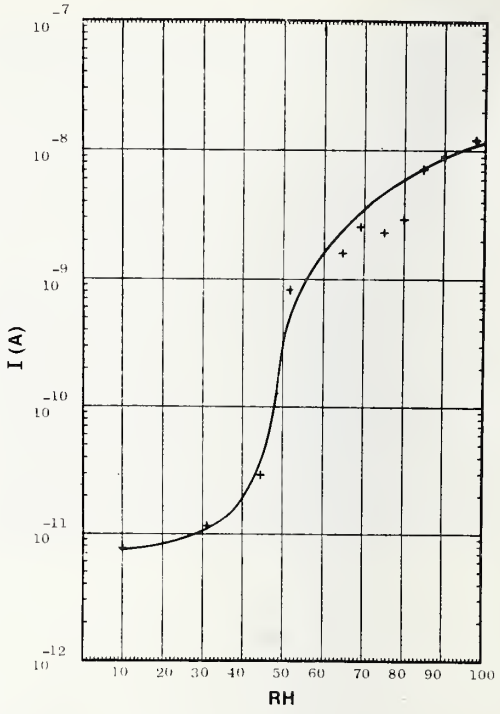

Figure 3. Calibration curve for surface conductivity-type moisture sensor where the surface leakage current, I, is plotted against relative humidity (RH) in percent for 22°C.

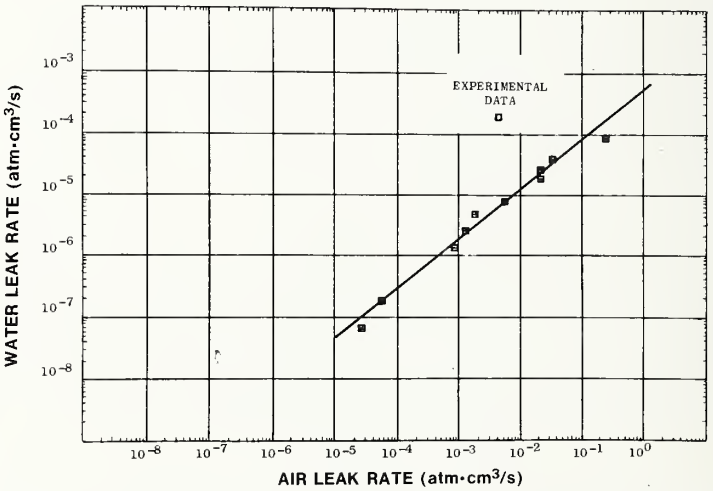

Figure 4. Water leak rate versus air leak rate for a capillary 0.6 mm long exposed to 80-percent relative humidity at 22.2°C.

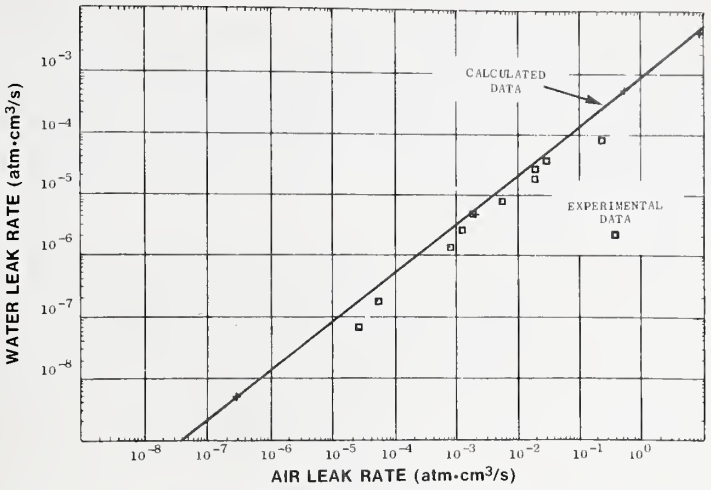

Figure 5. Water leak rates versus air leak rate of capillary as calculated assuming viscous and transition flows for air and molecular flow for water (straight line) with experimental points from figure 4.

for transitional (3×10^{-3} to 10^{-5} atm·cm^3/s) flow regimes. These flow regimes are expected to apply for air at these air leak rates and for the one atmosphere pressure difference used. With the "effective" capillary diameters, a water vapor leak rate was calculated using the molecular flow equation.[8] The calculated values of water vapor leak rate were compared and found to be in relatively good agreement with the measured water vapor leak rates, as may be seen in figure 5. Based on this agreement, molecular flow was again assumed for water vapor to calculate the rise in dew point of the TO-5 package versus time as a function of air leak rate, shown in figure 6.

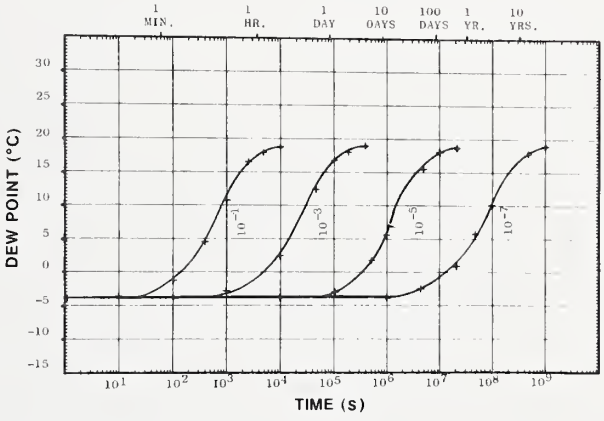

Figure 6. Change in dew point versus time as a function of air leak rate in ambient environment of 80-percent relative humidity at 22.2°C.

Based on the results of this test program, the following conclusions are made:

1. The moisture ingress rate of a leaky component can be calculated using conventional flow equations and, at least in the range studied, is from 2 to 3 orders of magnitude less than the standard air leak rate.

[8]See, for example, Dushman, S., *Scientific Foundations of Vacuum Techniques*, J. M. Lafferty, Ed., 2nd. ed., Chapters 1 and 2 (Wiley, New York, 1962).

2. The data suggest that for long-term reliability (especially in humid environments) military standard leak rate specifications[9] are far too lenient. For the TO-5 package with an internal volume of 0.17 cm^3, an air leak rate of 10^{-6} atm·cm^3/s is considered to be tolerable. The data presented here suggest that a time constant for moisture ingress is only 70 to 80 days and that only 20 to 30 days are needed for the dew point to exceed 0°C.

3. Although no experimental data were presented for packages with cracked or porous seals, one should be able to base reject criteria on the basis of leak rates for a cylindrical hole because this would tend to be the worst case situation. This would be very convenient, because in reality the exact physical shape of a leak is rarely known.

---

[9]Method 1014.2; MIL-STD-883A, Test Methods and Procedures for Microelectronics, November 15, 1974. Also, Method 1071.1, MIL-STD-750B, Test Methods for Semiconductor Devices, February 27, 1970.

3.3.6 Moisture Measurement Studies

Kenneth L. Perkins
Rockwell International Corporation
Electronic Devices Division
P.O. Box 4192
Anaheim, California 92803
(714) 632-3316

This report presents the results, to date, of two moisture measurement studies — one to evaluate the interlaboratory precision of mass spectrometric moisture measurements[1] and the other to monitor the internal moisture content of various packages[2] using aluminum oxide moisture sensors.[3]

The first study included designing and constructing standard packages, filling these packages with known concentrations of moisture, distributing these packages to five analytical laboratories for mass spectrometric moisture measurement, and comparing the results obtained.

The package used for this application is a 1-in. square (25 by 25 mm) gold-plated Kovar package blank (i.e., a package without electrical feed-throughs) sealed with a gold-plated Kovar lid containing two 1/8-in. (3-mm) OD gold-plated

---

[1]Performed under Army/MIRADCOM contract (No. DAAK40-76-C-117). This is a Manufacturing Method and Technology study on the screen testing of electronic components.

[2]Performed under a contract (No. NAS8-31992) with NASA/Marshall Space Flight Center. This contract is concerned with the investigation of low-cost, high-reliability sealing techniques for hybrid microcircuit packages.

[3]Panametrics Aquamax moisture sensors.

copper tubes located diagonally in two corners of the package. The setup for filling the standard packages is shown in figure 1. The packages are first purged with dry nitrogen from a laboratory supply. Then nitrogen with the desired moisture content is fed into the system from the moisture generator and the packages are allowed to equilibrate. The precise value of moisture content is measured using an optical dew point hygrometer. When equilibrium conditions are reached at the desired moisture content, the packages are sealed off (cold welded) with a crimping tool. Photographs of a package before and after pinch-off are shown in figure 2.

Standard packages were prepared with three different moisture concentrations (approximately 1000, 6000, and 10,000 ppm) at two fill temperatures (room temperature and +125°C) and sent to five different laboratories for moisture analysis. Each laboratory was sent a total of 18 packages consisting of three packages prepared under each of the six different conditions. The packages were prepared in batches of five, and one package from each batch was sent to each laboratory to ensure that the sets of packages analyzed by each of the laboratories were identical.

To date, results have been received from three laboratories. Results for the packages prepared at room temperature and at +125°C are given in tables 1 and 2, respectively. The results obtained by the three laboratories differ widely from each other and none of them agree with the fill values. These results are significant in that they are representative of the state-of-the-art capability of moisture measurement and attest to the need for improvement in the interlaboratory precision of mass spectrometric moisture measurements.

There also is another interesting observation to be made from these results. It was expected that the measured moisture contents would be higher for the packages filled at room temperature than for those filled at 125°C for the three different moisture contents. This was expected because more moisture would be absorbed on the walls of the packages at the lower temperature, and this moisture would be released at the higher temperature (100°C) at which the moisture measurements are made. However, this was not the case — the measured moisture contents of the packages filled at 125°C, in general, were at least as high or higher than those filled at room temperature.

The second study involved monitoring the internal moisture contents of a seam-sealed, gold-plated Kovar package and three adhesive-sealed ceramic packages using solid state moisture sensors located inside the packages while they were subjected to a 60°C/98-percent RH environment (equivalent to a moisture concentration of 190,000 ppm_V) for 15 days. The sensors used were calibrated at 60°C over a range of 200 to 10,000 ppm_V prior to sealing. After sealing, the packages were leak

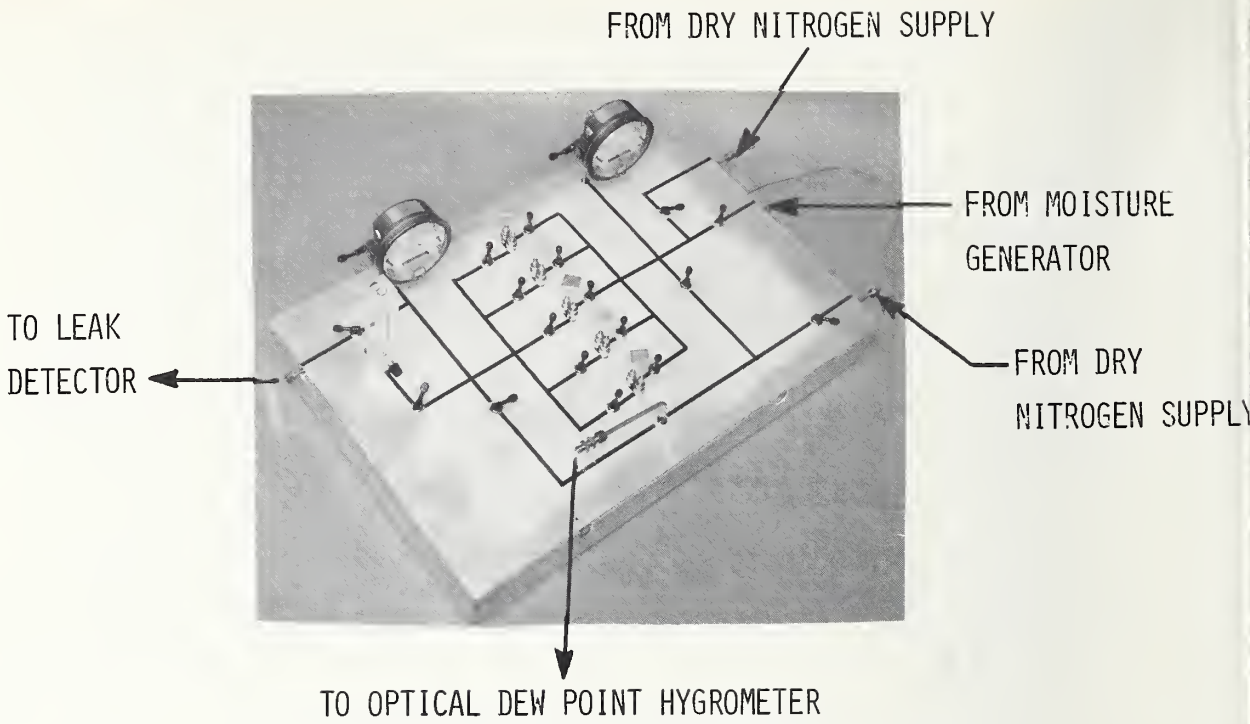

Figure 1. Setup for preparing standard packages.

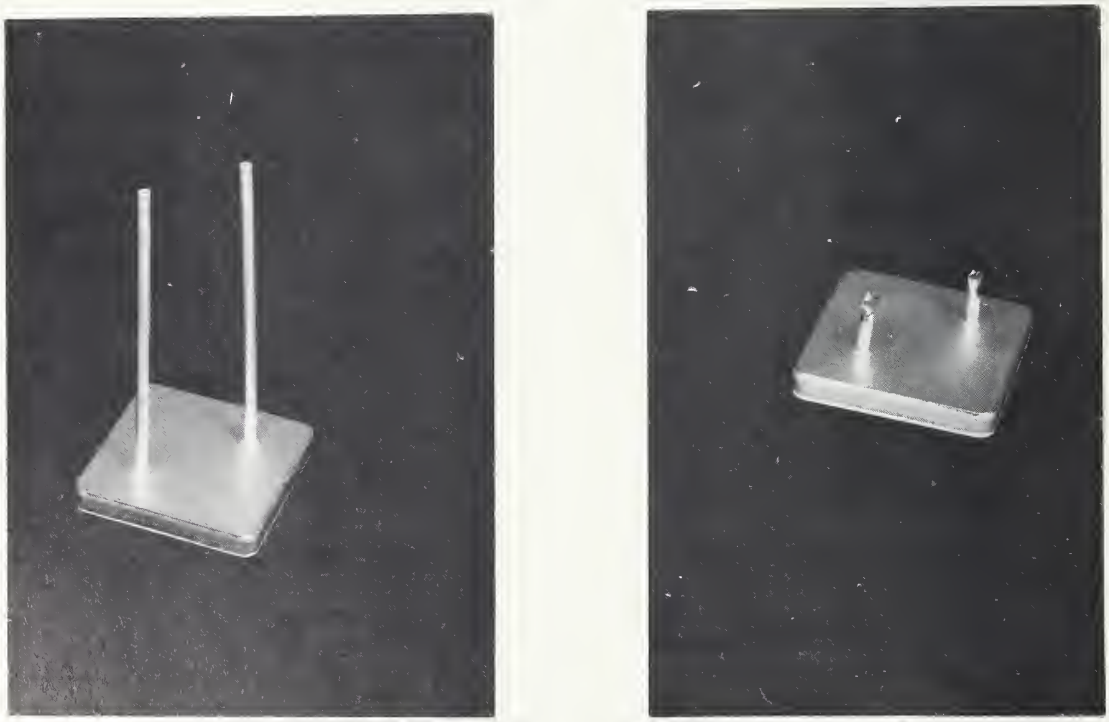

a. before pinch-off. b. after pinch-off.

Figure 2. Moisture standard package.

Table 1. Results to Date (Packages Filled at Room Temperature).

Initial Moisture Content (ppm_V)	Moisture Content Measured (ppm_V)		
	Lab 2	Lab 3	Lab 4
1,050	500	3,000	158
	900	2,700	60
	600	3,100	83
5,950	7,000	19,400	1,448
	9,800	20,400	1,525
	11,600	23,000	1,124
10,000	14,500	37,000	2,864
	17,600	-	3,095
	17,100	33,000	3,140

Table 2. Results to Date (Packages Filled at 125°C.

Initial Moisture Content (ppm_V)	Moisture Content Measured (ppm_V)		
	Lab 2	Lab 3	Lab 4
1,050	<500	11,000	186
	500	3,100	135
	500	3,100	88
5,950	13,100	24,000	1,458
	13,900	21,000	1,419
	15,600	20,500	1,540
10,000	14,000	42,000	2,967
	17,700	40,000	2,750
	17,800	34,000	2,730

tested.[4] The fluorocarbon gross leak test indicated that one of the adhesive-sealed packages had a gross leak. After the environmental stress test, the sensors were removed from the packages and recalibrated. These calibration curves were used to interpret the sensor data obtained during the test.

The results of the study are as follows:

(1) For the seam-sealed, gold-plated Kovar package, the dew point remained constant throughout the 15-day exposure at a value that was too low to be measured. It was certainly less than -40°C (corresponding to 130 ppm_V moisture) and probably around -55°C (corresponding to 20 ppm_V moisture). This indicates that seam-sealing can provide a good hermetic seal.

(2) For the gross-leak, adhesive-sealed ceramic package, the output of the moisture sensor increased rapidly and went off the scale in less than 24 hours in response to the rapid increase in the moisture content of the package — a result that was expected. However, the sensor was severely corroded by exposure to the high temperature, high humidity environment — a result that was not expected. Figure 3 is a photograph of the sensor that was removed from this adhesive-sealed ceramic package. As can be seen, this sensor is extensively corroded. This sensor failed in just a little over 24 hours after the stress test was begun. Figure 4 is a photograph of one of the other sensors and is typical of the appearance of the sensors that were removed from the seam-sealed, gold-plated Kovar package and the other adhesive-sealed packages.

[4]Method 1014.1, MIL-STD-883A, Test Methods and Procedures for Microelectronics (November 15, 1977).

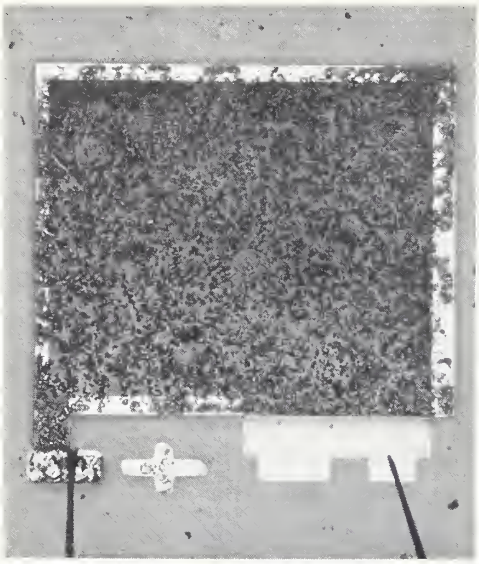

Figure 3. Appearance of Aquamax moisture sensor removed from adhesive-sealed ceramic package that was a C_1 gross leaker.

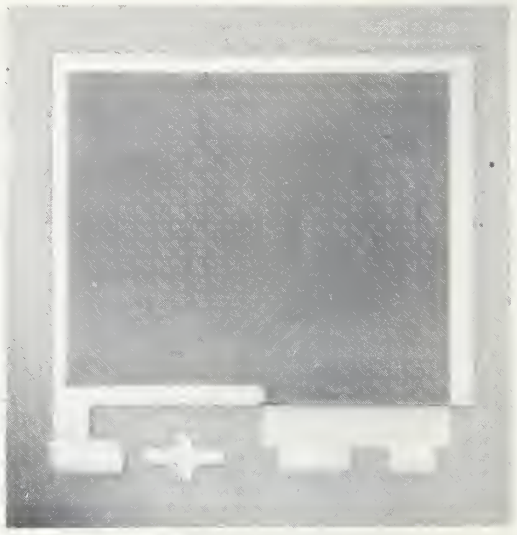

Figure 4. Appearance of Aquamax moisture sensors removed from seam-sealed gold-plated Kovar package and good adhesive-sealed ceramic packages.

(3) For the good adhesive-sealed ceramic packages, the moisture contents were initially at the same value as that of the seam-sealed, gold-plated Kovar package. Thereafter, the moisture contents increased very slowly for the first few days, and then more rapidly and linearly for the remainder of the 15-day exposure, as shown in figure 5. This indicates that the moisture was diffusing into the packages rather than leaking into them, and shows that adhesive-sealed ceramic packages are not hermetic. At the end of the 15-day exposure, one package contained 14,600 ppm_v moisture and the other 19,000 ppm_v. From the linear portion of the curves, the moisture permeation rates were calculated to be 1,230 ppm_v/day for one package and 1,400 ppm_v/day for the other. Also, direct scaling from the curves showed that the time

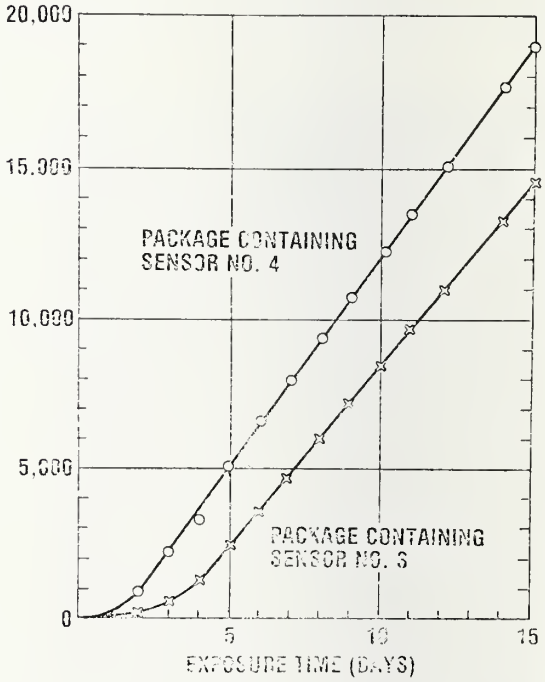

Figure 5. Results for good adhesive-sealed ceramic packages.

required for the moisture content to reach 6,000 ppm_v was 5-1/2 days for one package and eight days for the other. Calculations indicated that the permeability for the particular adhesive used was 1.3 to 4.4 $\times 10^{-13}$ g $(H_2O)/cm \cdot s \cdot Torr$ and the time to half ambient (i.e., the time required for the moisture content of the packages to reach a value equal to half that of the external environment is 90 to 100 days.

3.3.7 Humidity Calibration Facilities at NBS

Saburo Hasegawa
Center for Mechanical Engineering
and Process Technology
Thermal Processes Division
National Bureau of Standards
Washington, DC 20234
(301) 921-2794

The National Bureau of Standards (NBS) is responsible for maintaining the national standards for humidity and for disseminating such standards throughout the scientific and technological communities. As part of its program to accomplish this, it provides a service to government agencies and to the public for the calibration of humidity-measuring instruments. Humidity calibration ranges and accuracies of the NBS facility are listed in table 1.

Calibration is ususlly performed by subjecting the test instrument to atmospheres of known humidity produced by the NBS two-pressure humidity generator. If the highest accuracy is required, the test instrument is compared with the NBS standard hygrometer, an apparatus that is based on the gravimetric method of moisture measurement and possesses the highest order of accuracy in the NBS hierarchy of humidity-measuring instruments.

The NBS standard (gravimetric) hygrometer yields a direct measure of water-vapor content in units of mass of water vapor per unit mass of associated dry gas. In meteorology, this quantity is usually called the mixing ratio; in several of the engineering disciplines, it is referred to as the humidity ratio; and in the chemical field, it is often expressed as parts per million by weight (ppm). In theory, the gravimetric method has great inherent precision and accuracy. In practice, great care must be exercised in making a determination and careful attention must be given to a multitude of details.

The gravimetric hygrometer consists of a drying train for removing the water vapor from a moist gas and a gas-volume measuring system for measuring the volume of the dry gas associated with the water vapor. The calibration is performed in the following way. Test gas of constant humidity from the NBS two-pressure humidity generator is allowed to flow simultaneously through the NBS standard hygrometer and the instrument under calibration. At the termination of a run, the mass of water vapor removed by the drying train, which consists of three demount-

Table 1. National Bureau of Standards Humidity Calibration Ranges and Accuracies.

Standard	Humidity Parameter	Range	Accuracy*
Standard (gravimetric) hygrometer	Mixing ratio r (g water vapor per kg dry air)	$0.19 \leq r \leq 20$	0.13% of value
Two-pressure humidity	Mixing ratio, r_w (g water vapor per kg dry air)	$0.0005 \leq r_w < 0.0015$	3.0% of value
		$0.0015 \leq r_w < 0.005$	1.5% of value
		$0.005 \leq r_w < 0.1$	1.0% of value
		$0.1 \leq r_w < 0.3$	0.5% of value
		$0.3 \leq r_w < 515$	0.3% of value
	Volume ratio, V (ppm_v)	$1 \leq V < 3$	3.0% of value
		$3 \leq V < 10$	1.5% of value
		$10 \leq V < 170$	1.0% of value
		$170 \leq V < 500$	0.5% of value
		$500 \leq V < 820{,}000$	0.3% of value
	Dew-point temperature, T_d(°C)	$-80 \leq T_d < -70$	0.2°C
		$-70 \leq T_d < -35$	0.1°C
		$-35 \leq T_d < +80$	0.04°C
	Relative humidity, RH (%) at test chamber temperature T_c (°C) of:		
	$-60 \leq T_c < -40$	$3 \leq RH \leq 98$	1.5%
	$-40 \leq T_c < -20$	$3 \leq RH \leq 98$	0.8%
	$-20 \leq T_c < 0$	$3 \leq RH \leq 98$	0.4%
	$0 \leq T_c < +80$	$3 \leq RH \leq 98$	0.2%
Low frost-point humidity generator	Dew-point temperature, T_d(°C)	$-100 \leq T_d < -30$	0.05°C

* The estimated bounds to systematic error plus three times the standard deviation.

able glass absorption U-tubes filled with anhydrous-magnesium perchlorate and phosphorus pentoxide, is determined by precision weighing. The mass of the dry gas is obtained by multiplying the measured dry gas volume by the appropriate gas density. The ratio of the masses is the desired quantity.

The gravimetric hygrometer provides an average value of the moisture content of a test gas for the duration of a run. The test gas is sampled at flow rates of 2 L/min or less for periods of time long enough to ensure that the mass of water collected by the drying train is sufficient to permit weighing with high accuracy (about 0.6 to 1.0 g of water being required). Thus, as the humidity decreases, the duration of a run increases. The following practical considerations limit the humidity range over which the hygrometer is used: the highest measurable value is determined by the ambient room temperature. Because the latter is controlled nominally at 25°C and to prevent condensation in the lines, the dew-point temperature of the test gas must be kept below 25°C. The highest practical measurable humidity is limited therefore to a mixing ratio of about 20 g of water vapor for 1 kg of dry air. The lowest measurable value is governed largely by the sampling time required to accumulate sufficient water, which in turn is related to operator endurance and equipment reliability. Mixing ratios as low as 0.15 g/kg (-35°C frost point) have been measured without any degradation in accuracy, but this is seldom done since it involves continuously sampling for about 30 h. The maximum duration of a run has been set at 10 to 12 h as a reasonable limit. This permits mixing ratio measurements as low as 0.4 g/kg (-25°C frost point).

With the gravimetric hygrometer serving as the primary standard, two precision humidity generators constitute the principal facilities for calibrating transfer and secondary standards and for testing and evaluating hygrometers and sensors. One of these generators operates on the two-pressure principle. A stream of gas at an elevated pressure is saturated with respect to the liquid or solid phase of water and then expanded to achieve a lower pressure. Measurements of the pressure and temperature of the saturated gas stream, before and after expansion into the test chamber, yield the data necessary to compute the water vapor content of the gas stream at the lower pressure. By selecting and maintaining appropriate temperatures and pressures, it is possible to generate any desired level of humidity in the gas stream. The two-pressure humidity generator produces a continuous stream of gas which can flow at any specified rate up to 0.005 m^3/s through a test chamber in which the relative humidity can be varied from 3 to 98 percent, the temperature from -60°C to 80°C, and the absolute pressure from 5 to 200 kPa (0.05 to 2 atm).

The second precision humidity generator is called a low frost point humidity generator. This generator operates on the principle of saturating the gas at some predetermined temperature and since there is no significant pressure drop in the system, the gas temperature at the exit end of the saturator is, therefore, the

same or very close to the saturation temperature, that is, it is the value of the frost point of the gas stream. The generator produces frost points from -30°C to -100°C at ambient pressures from 0.5 to 200 kPa (0.005 to 2 atm). The generator test gas can be fed to a test chamber with independent temperature control between 25°C and -100°C.

Acceptance of an instrument for calibration depends upon the type of hygrometer and the nature of the user's requirements. Requests for calibration should be accompanied by technical information on the type of instrument, manufacturer, operating range(s), and number of test points required. Calibrations can be furnished in terms of most humidity parameters, including dew-point temperature, mixing ratio, and relative humidity.

Calibrations with the NBS two-pressure generator are performed in either of two ways. With one method, the instrument, or its sensor, is placed inside a test chamber and is subjected to a known humidity, or set of humidity points, at any desired controlled temperature in the range of from -60°C to +80°C. Instruments must be remote-indicating or recording because there is no provision for observing a dial or other indicator within the test chamber. The electric hygrometer is a typical example of an instrument calibrated in this fashion. With method two, the calibration is performed with the instrument located in the laboratory under ambient conditions, i.e., at atmospheric pressure and 25°C, and with a continuous flow of the test gas of known humidity is fed to it at any desired flow rate up to 200 L/min. The upper humidity of the test gas is limited to a dew point of 25°C; otherwise, condensation may occur. The lowest dew point that can be generated is -80°C.

During the early part of 1978, a facility for making humidity response time tests will be completed. The facility is being designed to introduce a step-function change in humidity in a period of approximately 0.1 s.

3.4 Session IV Testing and Reliability

3.4.1 Electrostatic Damage to Semiconductors[1]

Roy C. Walker
Reliability Analysis Center
IIT Research Institute
RADC/RBRAC
Griffiss AFB, NY 13441
(315) 330-4151

The cardiac pacemaker industry should be concerned with electrostatic discharges (ESD) and their damaging effect to certain electronic parts. What happens during an ESD can be described as what happens when a capacitor is charged to some potential and then discharged through a resistor.

In the past, evaluation and qualification tests of electron devices have not addressed a device's susceptibility to ESD. This is because evaluation and qualification are directed toward reliability and functional characterization. When a device is damaged by ESD, it is technically not the fault of the device; it can be said that failure was externally induced. But today, as MOS technology and small geometry devices have become prevalent, ESD susceptibility must be established to determine the controls and protection techniques needed to avoid unnecessary production waste and even field reliability problems as a result of ESD-induced latent failure mechanisms or system transients.

From the survey experience of the Reliability Analysis Center (RAC), it has become apparent that under certain circumstances it would be convenient to classify ESD-sensitive devices into three groups, as shown in table 1. *This grouping should be considered a generalization and the reader is cautioned that ESD sensitivity within a device classification or technology can vary widely.* When in doubt, individual part types should be tested for sensitivity. For example, in some cases metallization crossovers with very thin (<0.3 μm) oxide should be more appropriately classified as "highly ESD sensitive" rather than simple "sensitive."

ESD-type overstresses can induce latent failure mechanisms in both MOS structures and bipolar junctions which are not necessarily detectable with typical electrical tests. One MOS structure mechanism involves a current-limited gate dielectric breakdown that leaves no apparent damage. Yet, the voltage at which subsequent breakdown can occur is reduced to as low as one-third the original breakdown value, making it susceptible to failure some time after an initial voltage transient in applications where voltage excursions are encountered.

Another latent MOS overstress failure mechanism is possible due to designs involving metallization paths, connecting the input to the gate, that are separate from metallization paths to the input protection circuit. In these instances,

[1]This work was sponsored by the U.S. Air Force under contract #F30602-77-C-0167.

Table 1. ESD Sensitivity Grouping

ESD Classification	Device Description	Sensitivity Type
Highly sensitive	MOS without input protection OP AMPS with MOS capacitors SAW devices	Voltage threshold to dielectric breakdown
Sensitive	MOS with input protection JFETs with low leakage or greater than 100-V breakdown, or both Small-geometry *pn* junctions (especially emitter-base) Metallization crossovers over low resistance (active) regions (i.e., V_{CC} over n^+ isolated diffusions) Linear ICs with low leakage inputs or high input impedance Fine metal bipolar Dielectric isolated bipolar (small geometry) Microwave diodes High-speed ECL Semiconductors operating at frequencies greater than 1 GHz Film resistors	Voltage threshold and energy to secondary breakdown or to dielectric breakdown (also dv/dt for protected MOS)
Marginally Sensitive	Low and intermediate power semiconductors TTL, DTL, RTL Semiconductors operating at frequencies greater than 100 mHz	Voltage threshold and energy to secondary breakdown

the metallization to the protection circuit can be open while leaving the gate connected to the input pin. A subsequent minor excursion above the dielectric breakdown of the gate can produce a failure at some later time when another voltage excursion occurs.

Another latent failure mechanism can operate in any *p-n* junction where the damage threshold is marginally transgressed. The effect would be to round off the knee of the breakdown curve or increase the leakage slightly without causing a functional failure. In these cases, the damage threshold and sometimes the reverse breakdown voltage is lowered such that another pulse, for example, 80 percent of the original damage threshold, will now cause further degradation and perhaps a functional failure.

In MOS structures, the overstress can produce a dielectric breakdown of a self-healing nature when the current is not limited. When this occurs, the device may retest good but contain a hole in the gate oxide where the breakdown occurred. It is theorized that holes from which metallization has been marginally vaporized have the potential for behaving like a pinhole or a marginally programmed fusible-link PROM which can react in time to temperature or voltage, or both, to produce a

short circuit. It is of concern that, when this occurs, the failure analyst would probably have no way of identifying the mechanism as latent. Several instances with potential for this mechanism have been reported for bipolar integrated circuits where V_{CC} metallization and low resistance diffusion crossovers separated by thin oxide form an MOS structure with little or no current limitation. Another instance has involved a mask error on some CMOS devices which inadvertently left the gate protection circuit disconnected.

To avoid subjecting sensitive devices to ESD, the precautionary measures program in a manufacturing plant should be a four-step approach. For some, only the first three steps will be needed. The steps are as follows:

1. Eliminate all sources of static electricity.
2. Institute grounding philosophy, the ultimate goal of which is never to have the operator separated from ground by more than 10 MΩ.
3. Store devices in conductive packaging materials. The ultimate is to have all leads shunted together.
4. When steps 1 through 3 are not enough or grounding is not possible, use ionized air precipitators with optimum levels of relative humidity.

To avoid unnecessary ESD sensitivity, the following design rules are suggested:

1. Include use of large-area diodes and diodes of both polarities and add series resistors and distributed network effects in MOS input protection circuitry improvement techniques.
2. Avoid cross-unders beneath stripes connected to external pins. Also, recognize that the oxide over the n^+ (emitter) diffusion is likely to have a low dielectric breakdown and to etch faster than other oxides. Thus, the location of the cross-under should be carefully chosen, the thickness of the grown oxide carefully controlled, and buffer etches prior to metal deposition closely monitored. Deep n-type diffusions should be used for cross-unders instead of the emitter diffusion if a deep n-type diffusion is used in the process.
3. Lay out all MOS device input protection circuits so that ESD damage to them will cause the protected circuit to be inoperative (fail-safe).
4. Maintain 70 μm or greater between the edge of the metallization contact and the junction on bipolar devices.
5. Fabricate linear integrated circuit capacitors in parallel with a p-n junction with a breakdown voltage lower than those of the capacitors.
6. Avoid designs for bipolar devices that permit a high transient energy density to exist in a p-n junction depletion region under an ESD. Use series resistance to limit ESD current or parallel elements to divert current from critical elements. Keep critical junctions out of reverse breakdown by adding clamp diodes between the vulnerable lead and one or

more power supply leads. If a junction cannot be kept out of reverse breakdown, increase its area to reduce the initial transit energy density.

7. Protect transistors by increasing the emitter perimeter adjacent to the base contact, which helps by proportionately lowering transient energy density in the critical emitter sidewall. Enlarging the emitter diffusion area also helps in some pulse configurations.
8. Use a "phantom emitter" transistor to improve ESD resistance as an alternative to using clamping diodes, which consume chip area and may cause unwanted parasitic effects. This transistor incorporates a second emitter diffusion, shorted to the base contact, which creates a deliberate separation of the base contact from the normal emitter diffusion to add additional extrinsic base resistance ballasting without interfering with normal transistor operation. The second emitter provides a lower breakdown path $V_{BR(CEO)}$ between the buried collector and the base contact.
9. Avoid pin layouts which put the critical ESD paths on corner pins which are prone to ESD.

To avoid ESD damage, the following system design precautions are offered:

1. To avoid latchup in CMOS circuits, limit input current to 10 mA. For the CD4049 and CD4050 circuits, however, limit output current to 5 mA when the output is higher than V_{DD} or lower than V_{SS}. One way to do this is to isolate each output from its cable line with a 200-Ω resistor and clamp the line to V_{DD} and V_{SS} with two 1N4148 high-speed switching diodes. In the case of long input cables with the possibility of noise pickup, use filter networks.
2. To obtain additional protection for MOS devices, add external series resistors at device inputs. For CMOS circuits, use 10 kΩ for gate inputs and 1 kΩ for transmission gate inputs.
3. To protect sensitive inputs on bipolar devices, use an R-C network consisting of a relatively large valued resistor and a capacitor of at least 100 pF, if system performance allows its use. However, if circuit performance dictates against this use, two parallel diodes (clamping to a half volt in either polarity) can be used to shunt the input to ground. This provides minimum disturbance to the input characteristics.
4. To protect sensitive devices on circuit board or module layouts that bring leads directly to the outside world, use series resistance, shunts, clamps, or other protection means. For any electronic assembly that is going to be handled, examine assembly design to avoid unnecessary exposure of ESC-sensitive parts during such handling.
5. Design any system which has a keyboard, a control panel, manual controls, or a key lock to permit any operator discharge to go directly to chassis ground.

6. Identify ESD-sensitive parts in the system design process and minimize their use if possible.

3.4.2 Procuring High Reliability Hybrid Circuits for Use in Cardiac Pacemakers

Warren A. Gerz
Cordis Corporation
P.O. Box 370428
Miami, FL 33127
(305) 578-2000

Earlier pacemaker circuit designs using discrete components do not meet the present design goals for circuit density, power consumption, weight, size, stability, increased functional complexity, and the high reliability performance needed for long term patient care. Present design goals can be met by hybrid circuits. Custom circuits are usually necessary, however, to satisfy the special requirements imposed by cardiac pacemaker circuits and by the special environment and power source limitations of pacemakers.

Procuring and qualifying custom hybrids for pacemaker application requires total understanding of patient needs and the elements which are required to reliably produce and test hybrid circuits. The events which are required to assure high reliability from design inception to including the hybrid as part of a finished product meeting patient needs are indicated in figure 1. A number of these events will be discussed below.

Some very basic considerations for the design of a high reliability hybrid circuit are as follows:

Circuit design simplicity should be maintained while considering low current-drain performance stability over the intended usage period, and inclusion of redundancy when possible to prevent critical failure modes which may affect patient safety.

Components selected should be established high reliability performance types, where possible, with ready availability. Unique device characteristics should be fully defined to assure that requirements are met even if special sorting is required. Components should also be selected with an understanding of the attachment process to be used in the hybrid circuit.

Materials selected should not impair circuit performance or reliability objectives. Epoxies should have low mobility characteristics, good strength, low temperature curing ability, minimal or no conductivity change over a broad temperature range, low absorption characteristics to minimize moisture entrapment, and chemical constituents whose effluents will not degrade circuit performance. Thick film materials should be compatible with substrate and component attachment methods. Conductive material should have good ad-

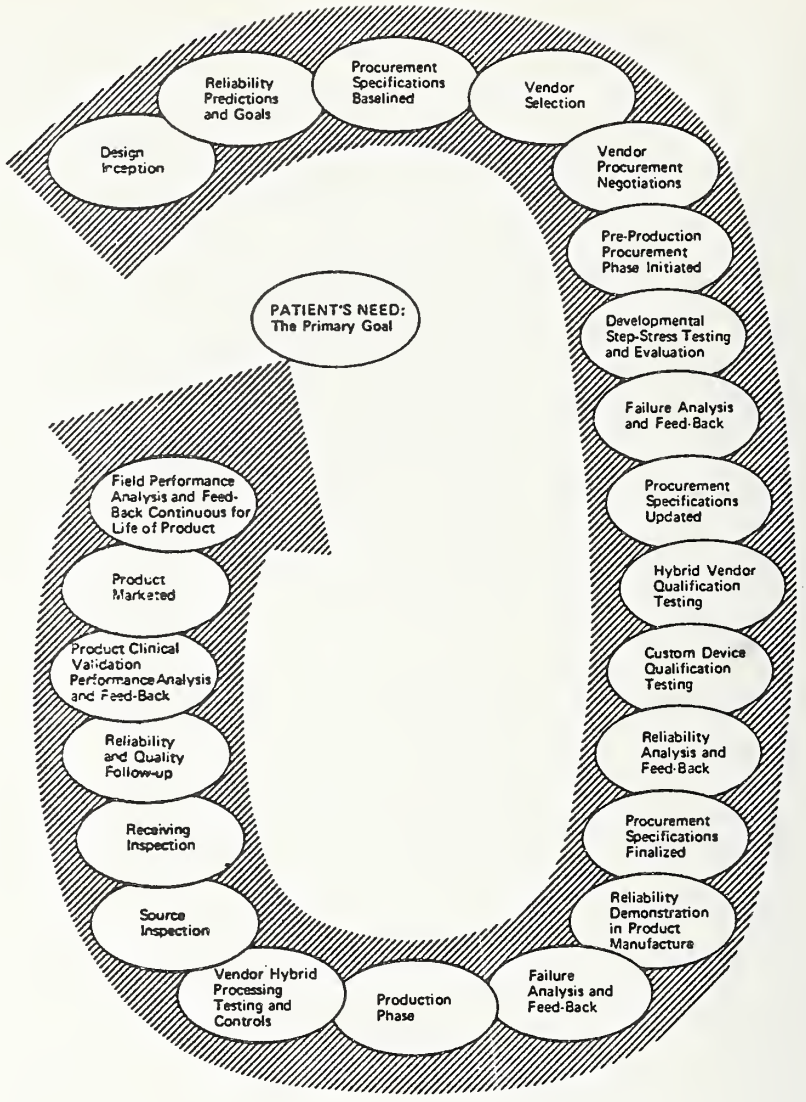

Figure 1. Events to provide high reliability procured hybrid circuits to meet patient needs.

hesive and wire bonding properties. Resistor inks, in addition, should have stable temperature characteristics and be insensitive to hydrogen.

Packages selected should be weldable, have glass-to-metal hermetic seals, and have good surface and plating finishes compatible with wire bonding integrity. The package should sustain its hermetic qualities throughout processing, testing, and end application.

Processes utilized during fabrication should be closely keyed to the elements to be assembled. Wire bonding, component attachment curing, cleaning, sealing, and testing should not exceed the temperature and mechanical limitations of the components or materials selected.

The next step is to obtain developmental sample hybrids from a potential vendor. The same criteria apply to vendors as to the hybrid circuit design technology. The vendor to supply high reliability hybrid circuits should be one who has had experience in volume production of high reliability hybrid circuits. Special consideration should be given to vendors who have successfully supplied the pacemaker company with similar high reliability circuits in the past. If not, the materials, processes, and components must be jointly developed by the pacemaker company and the vendor so that, in the end, the vendor technology will match the pacemaker design requirements.

The following are basic factors to be considered when selecting a hybrid circuit vendor:

1. Process technology compatible with design objectives.
2. Wafer fabrication capability (preferred).
3. Test capability.
4. Data analysis and trend analysis capability.
5. Strong quality assurance organization.
6. Process control techniques, high reliability compatible.
7. Past high reliability experience.
8. Fabrication area in controlled environment (clean room preferred).
9. Failure analysis capability.
10. Procurement procedure and documentation control, including subsupplier change control.
11. Raw material and component receiving inspection ability.
12. Test equipment accuracy and measurement repeatability.
13. Traceability method.
14. Captive or dedicated line manufacturing practice (no multiple product line process, i.e., commercial devices intermingled with reliability components would be unacceptable).
15. Qualified technical staff.
16. Operator and inspector training program.

To assess all of these factors, a plant survey is essential. A good survey team will include members from purchasing, quality assurance, engineering, and reliability departments.

Once the supplier's capability is verified, basic negotiations can proceed to define to the supplier the absolute requirements of the program. The traditional vehicle for communicating these definitions is the procurement specification. With the design requirements and assembly approach established, a procurement specification can be finalized for vendor concurrence prior to manufacture. The specification should detail the mechanical and electrical function requirements, special processing tests and methods, quality assurance requirements, and the overall high reliability qualification requirements. Full and frank communication between the

intended supplier and the cardiac pacemaker manufacturer is essential for a successful procurement program. The relationship between the supplier and the pacemaker manufacturer will become a team effort and requires mutual dedication to succeed.

A clear understanding of subsupplier control requirements is of particular importance. The minimum requirements for procuring hybrid-circuit components should be:

1. For active components such as integrated circuit chips, transistors, etc.,
   a. Device glassivation,
   b. 100-percent wafer electrical sorting,
   c. 100-percent wafer metallization SEM analysis to MIL-STD-883,[1] Method 2018,
   d. 100-percent visual die inspection to MIL-STD-883, Method 2010 ("B" level, minimum),
   e. Wafer sampling acceptance testing through a burn-in scheme,
   f. Verification of bondability for each wafer lot,
   g. Proper wafer lot traceability to diffusion and evaporation runs,
   h. Control of process and assembly changes, and
   g. Second sources.
2. For passive components such as capacitors,
   a. 100-percent electrical testing,
   b. 100-percent burn-in testing,
   c. Construction analysis via microsectioning,
   d. Lot traceability to materials and processes,
   e. Control of process and assembly changes, and
   f. Second sources.
3. For thick film materials such as resistive inks, conductors, and dielectrics,
   a. Assurance of lot-to-lot consistency of material composition,
   b. Assurance of lot-to-lot consistency of resistor ink bulk resistivity, and
   c. Assurance of lot-to-lot consistency of as-fired conditions for adhesion, bondability, resistance range, and temperature coefficients.

When developmental hybrid circuits are received, the first tests will be functional, and adjustments will normally be required to optimize the circuit for its intended function. When the functional aspects of the circuit have been ironed out, step-stress testing begins. The data obtained from step-stress testing are used to determine qualification testing requirements and to uncover weaknesses in the hybrid design or construction.

---

[1]Method 2010, MIL-STD-883B, Test Methods and Procedures for Microelectronics (August 31, 1978).

Step-stress testing is conducted by applying incrementally increasing levels of stress until the majority of test samples fail and the test results are repeatable. Typical stress tests are elevated temperature, elevated voltage, acceleration, mechanical shock, and thermal shock. Performance of the stressed units is compared to a control group operated under conditions simulating the normal use environment. As units fail under stress testing, they are analyzed and their failure modes are assessed. Acceleration factors derived from stress testing are used to formulate qualification and acceptance test criteria to assure proper in-process screening is established to sustain design integrity.

Once step-stress testing is satisfactorily completed, the qualification test program for hybrids would include full electrical tests and performance characterization under stress conditions indicated in table 1.

The results of the qualification should be thoroughly evaluated and analyzed against the original design and reliability goals to determine successful qualification of the vendor and hybrid design interrelationship. If the vendor's qualification is successful, then the vendor is considered ready to produce for implantable cardiac pacemakers.

To routinely assure repeatable results and adequate control over the vendor's production, once qualification is complete, appropriate accelerated screening tests must be performed on a lot-by-lot basis. Typical acceptance screening tests for hybrid circuits are indicated in table 2.

Upon completion of initial environmental screening, the hybrid should receive a pre-burn-in electrical test followed by repeated series of biased burn-in and electrical tests as indicated in figure 2. Burn-in testing for a minimum of 240 h is used to improve the hybrid circuit population by removing infant mortality failures before they can be used in pacemakers. Each lot of hybrid circuits is subjected to a series of 120-h periods of biased burn-in at 125°C, followed each time by full electrical testing at room temperature. A successful passage of a circuit lot is characterized by a decreasing rate of electrical test failures with subsequent 120-h burn-in test cycles until no failure is recorded, and by an initial number of failures which does not exceed a predetermined percentage of allowed defective circuits. A PDA (Percent Defective Allowed) should be specified for each of these key electrical tests in order to detect process variations and stimulate corrective actions by highlighting excessive fallout. If the initial number of failures does exceed this value, acceptance of the lot is dependent on the results of failure analyses. A lot that exhibits an increasing failure rate is rejected. Failure analyses of circuits in this lot will determine impact on subsequent lots from the vendor. See figure 3 for a graphic illustration of this burn-in performance procedure.

It should be obvious from this overview of the procurement process that high reliability in hybrid circuits for cardiac pacemakers is neither cheap nor quick.

Table 1. Qualification Tests for Hybrid Circuits.

Test Nomenclature	Test Methods and Conditions	A.F.*
Subgroup 1		
Baseline electrical	Appropriate electrical test with variables recorded	0
Hi-temp storage	MIL-STD-883, TM 1008, Cond B for 1000 h, 150°C	
Temp Cycling	MIL-STD-883, TM 1010, Cond B 60 cycles	
Fine leak	MIL-STD 883, TM 1014, Cond A	
Gross leak	MIL-STD-883, TM 1014, Cond C	
Post electrical (repeat baseline test)	Electrical with computation of variables	
External visual	MIL-STD-883, TM 2009	
Subgroup 2		
Baseline electrical	Appropriate electrical test with variables recorded	0
Shock	MIL-STD-883, TM 2002, Cond C	
Vibration	MIL-STD-883, TM 2007, Cond A	
Acceleration	MIL-STD-883, TM 2001, Cond C	
Post electrical (repeat baseline test)	Electrical with computation of variables	
External visual	MIL-STD-883, TM 2009	
Subgroup 3		0
Solderability	MIL-STD-883, TM 2003	
Lead integrity	MIL-STD-883, TM 2004, Cond B 1	
Fine leak	MIL-STD-883, TM 1014, Cond A	
Gross leak	MIL-STD-883, TM 1014, Cond C, step 1	
Marking permanency	MIL-STD-202E, TM 215	
Subgroup 4		0
Electrical	Baseline electrical by variables	
Accelerated life test	1,000 to 3000 h, 125°C at rated voltage	
Electrical	Post life electrical - variables and limits analyzed	
External visual	MIL-STD-883, TM 2009	
Destructive wire-bond analysis	MIL-STD-883, TM 2011	

*Allowable failures.

Table 2. Acceptance Tests for Hybrid Circuits.

Test Nomenclature	Test Methods and Conditions	Sample Size
Wire Bond Destructive	MIL-STD-883, TM 2011, Cond D	Representative Samples
Int. Visual	MIL-STD-883, TM 2010 - Cond B	100%
Baseline Electrical	Electrical specs requirements	100%
Thermal Shock	MIL-STD-883, TM 1011, Cond A, 15 cycles	100%
Temperature Cycling	MIL-STD-883, TM 1010, Cond B, 15 cycles	100%
Acceleration	MIL-STD-883, TM 2010, Cond B	100%
Fine Leak	MIL-STD-883, TM 1014, Cond A	100%
Gross Leak	MIL-STD-883, TM 1014, Cond C, step 1	100%
Loose Particle Detec.	Dunegan^{R} Method, 11 $\pm$ 3 G peak acceleration 50 $\pm$ 10 Hz for 10 $^{+5}_{-0}$ s, amp 0.09 $\rightarrow$ 0.01 in.	100%
Pre Burn-in Electrical	Electrical specs requirements	100%
Burn-in to Zero Failures	125°C, rated voltage 240 h minimum	100%
Post Burn-in Electrical	Electrical spec limits and variable criteria	100%
Solderability	MIL-STD-883, TM 2003, except aging and 10X magnification requirements	Sample/ lot
Fine Leak	Same as above	100%
Gross Leak	Same as above	100%
External Visual	MIL-STD-883, TM 2009	100%
Final Electrical	Electrical limits	100%
Sealing Environment	Desired gas analysis limits	Sample/ Seal batch

The effort is essential, however, to help avoid the trauma of surgical re-entry to replace a defective pacemaker, or even worse an illness or injury resulting from pacemaker malfunction. While the pacemaker manufacturer can never eliminate all random failures, especially as pacers become more intricate, a considerable number of potential failures can be screened out before they are implanted in patients by applying fundamental high reliability procedures and continuous surveillance.

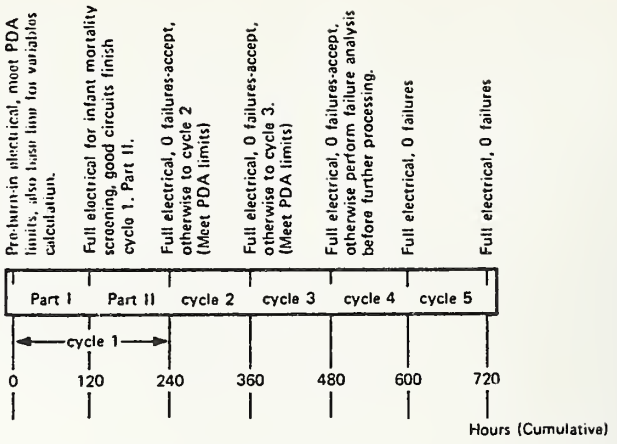

Figure 2. Burn-in to zero failures plan. Each 120-h burn-in segment is conducted at 125°C; electrical tests are performed at room temperature.

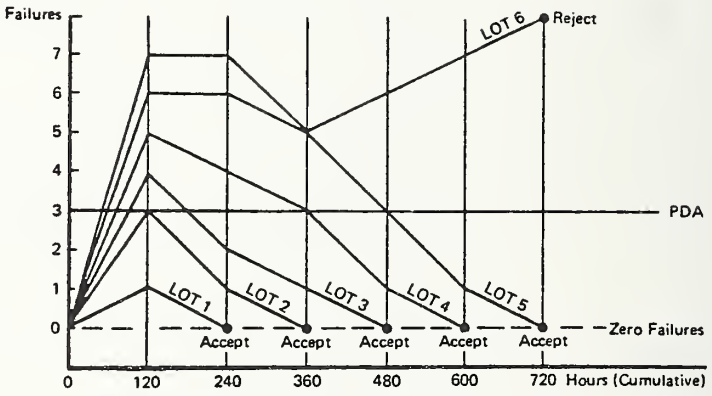

Figure 3. Illustration of burn-in performance procedure. Lots 1 through 5 illustrate decreasing failures rate pattern. Where PDA is exceeded (lots 3 to 5), acceptance is dependent on results of failure analysis. Lot 6 illustrates an increasing failure rate pattern that requires lot rejection. Failure analysis will determine potential impact on subsequent lots.

3.4.3 Reliability Trends for Semiconductor Components for Cardiac Pacemakers

Dr. Francesco Blanco
SGS-ATES SpA
Via C. Olivetti, 2
20041 Agrate Brianza (Mi) Italy
(039) 650441

We manufacture semiconductors and produce components within the following two large device families for use in pacemakers: (1) special products in ceramic or plastic packages and (2) metal-can transistors and diodes. SGS-ATES' officially certified Hi-Rel Line has, in the period from 1968 to 1977, produced the following cumulative quantities for European pacemaker manufacturers: 361,000

special products, 605,000 transistors, and 315,000 diodes.

Up to now, because no recognized quality standard has existed for devices used in this sector, our products have been manufactured as follows: Discrete families have been manufactured according to specifications similar to JAN-TXV but with increased screening time. And special products have been manufactured according to an extended version of the SGS-ATES SURE Program. This comprises military-standard-based specifications developed in consultation with the customer.

As an example of the good results obtained through the use of these test procedures, the following data have been observed on pacemakers manufactured by Vitatron Med using SGS-ATES Special Products:

Pacemakers observed	32,500 units
Special Products (S.P.) used	140,300 pieces
Maximum lifetime of observed pacemakers	42 months
Total observed operation time	2×10^9 pieces × hours
Total S.P. failed	16 pieces
Percentage of S.P. failed	0.01 percent
Equivalent failure rate of single transistor	8×10^{-9} h^{-1}

The advent of lithium-iodine batteries has caused pacemaker manufacturers to search for components having much longer life than those used in first-generation pacemakers and to make efforts towards miniaturization by using hybrid circuits built with integrated circuits rather than with discrete components.

The requirements for longer life of the electronics have brought to light the following requirements which must be met. A set of qualification procedures must be developed to give reliability for an average component life of ten years. The basic principle is that the components must have a built-in reliability which is ensured by production technology and methods rather than by having reliability screened-in after manufacture. These procedures shall be valid both for procured components as well as for the assembly and test methods of the total system. A set of procurement specifications must also be developed that can anticipate and certify finished product quality and reliability for all components. This is particularly critical in the case of semiconductor dice for hybrid circuits, when these circuits are not manufactured directly by the semiconductor manufacturer.

A short-term solution proposed for improving reliability of the electronics is as follows. Pacemaker hybrid circuits shall be designed in such a way that the active components can be grouped in reliable hermetic packages. The design and production of such a customer special assembly (in a multichip ceramic flat type package) shall be performed by a semiconductor device manufacturer. This is the only way to guarantee the required reliability through the application of the correct established manufacturing and screening specifications.

A proposed long-term solution is to define a system of qualification and quality conformance tests for high reliability devices. The system shall be suitable for the increased complexity of integrated circuits and their production technologies. We propose to adopt a system similar to that already existing for space-application devices. Unlike those of other industrial sectors, the requirements of space and biomedical sectors are very similar. For example, the certitude of zero failure is required on very small production quantities. This means that, as well as maintaining a low overall failure rate, no individual batches must be allowed to pass through with a high percentage of failures. For this reason, a thorough knowledge is required of the production processes as well as the product specifications. Furthermore, the low applied stressing and the high derating of the devices result in failure mechanisms which are uncommon and therefore little known to those experienced in high volume standard products.

The C/MOS family evaluation and qualification program for space provides an example with which the long-term proposal can be explained. The three phases of the program are outlined below. Phase 1 involves an evaluation and certification of the production line and of the production processes. Phase 2 involves an evaluation of the product at its physical operation limits. This is performed by means of accelerated tests capable of detecting possible failure mechanisms affecting the ultimate reliability of the products. These tests allow the identification of the activation energies for such failures and the introduction of corrective actions on the product when needed. Phase 3 involves a qualification of the product, based on a matrix of conventional tests, to confirm the results of the above two phases on large samples of actual production.

The continuing conformity of the product to the quality requirements outlines is assured by "freezing" the production identification document as well as by a periodical verification of qualification on a lot-by-lot basis.

3.4.4 Recent Advances in Automated Testing of Pacemakers

Harold R. Meyering[1]
Motorola, Inc.
Mail Drop 1023
8201 East McDowell Road
Scottsdale, AZ 85257
(602) 949-4467

The purpose of this paper is to share some of the time- and money-saving techniques developed during the course of designing and building an automatic test system for pacemakers.

Recent advances in the development of microprocessor-based control systems have opened new opportunities for the use of automated test systems which were not

[1]Work performed while employed by Custom Devices, Inc., Phoenix, AZ.

economical previously. Some of the most significant advances have been made in the areas of interface architecture and development of high level programming languages. The development of new interface structures such as described in a recent standard[2] has greatly simplified the problems of hardware interfacing. In addition, this new interface system has reduced cost and improved the reliability of interface networks. The development of new software operating systems with interactive editing capability has greatly reduced the amount of time and effort which is now required to develop the sophisticated software required in an automatic test system. These two developments coupled with the cost reductions in small computer systems have put the automatic test system easily within the reach of even the smallest manufacturing company and have now made it practical to perform 100-percent testing at every major production step. With the increased test capabilities which these systems now afford, it is possible to assure the detection and correction of manufacturing problems before they are perpetuated in the assembly process. This will assure that the products are not only highly reliable but also economical.

Consider first the typical system measurement and stimulus capabilities required for pacemaker testing. Table 1 presents a list of typical parameters required and their associated ranges and resolutions. The values for these parameters do not push the state-of-the-art in testing equipment. Virtually all of the electronic testing can be done with simple inexpensive measurement circuits or modules. In general, sophisticated and expensive general purpose test equipment is not required in most pacemaker test systems.

[2]IEEE Standard 488, Standard Digital Interface for Programmable Instrumentation 1975.

Table 1. Typical Measurement and Stimulus Parameters for Pacemaker Testing.

	Approx. Range of Values	Resolution
Refractory	250 ms to 400 ms	1 ms
Pulse interval	800 ms to 2000 ms	1 ms
Pulse width	500 μs to 600 μs	1 μs
Limit interval	250 ms to 1000 ms	1 ms
Pulse amplitude	2 V to 6 V	0.01 V
Current drain	5 μA to 40 μA	0.1 μA
DC supply voltage	1 V to 3 V	0.01 V
Simulated Heartbeat		
Amplitude	±1.2 mV to 100 mV	0.1 mV
Pulse width	20 ms to 50 ms	1 ms
Period	200 ms to 600 ms	1 ms
Function	cosine squared	

Next, consider the most difficult measurement problems encountered to demonstrate that the use of simple test circuits is indeed feasible and appropriate. This is assuming that the test system is to be dedicated and not intended for general purpose testing.

One of the most difficult problems which had to be overcome in the manufacturing process was that of automating the functional laser trim procedure. Among some of the problems were noise effects caused by the laser trimmer itself, noise due to light-sensitive dice in the hybrid circuit, and parameter drift due to the variation in the temperature at which the part was trimmed. Most of these problems were alleviated by designing a special trimming jig such as the one shown in figure 1.

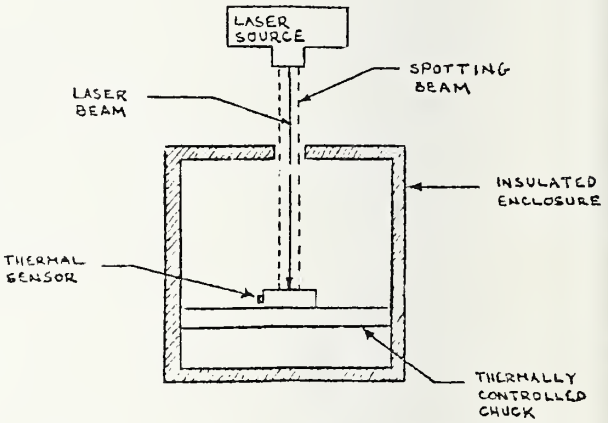

Figure 1. Special laser trimming jig.

Almost all external light was eliminated except for the spotting beam. The spotting beam was controlled by a foot switch and was shut off after the laser beam was aligned. The automatic test system shut off the laser beam when the unit was within tolerance. The special function keys on an HP9825 calculator were programmed so that the operator could call for any one of the various parameter test setups by pressing one key. The only problems encountered with this system were with the regulation of the trim temperature and the electrical interference caused during one trim which actually would cause the hybrid to perform erratically. To cure the temperature problem, a method is being developed in which the actual temperature of the unit under test is sensed, and the parameter tolerance limit is calculated by the calculator for that specific thermal condition. This method is viable because the parameter drift due to temperature is well-defined over a narrow band centered about 37°C. The only method of attack on the problem due to erratic electrical behavior is to use the trim-and-try method where the beam is actually shut off while the measurement is being made. It is possible that this one particular problem could be completely eliminated by a design change in the hybrid layout.

Some problems were also encountered when the hybrid circuits included electrolytic capacitors. The problem in this situation was the result of performing a thermal cycling test on the part which caused the capacitor to be elevated above the Curie temperature of the dielectric. This problem was alleviated by waiting for the part to return to its normal condition or to trim the part by calculating the tolerance based on the Curie temperature.

The last major problem encountered was the waiting time before parts could be tested after being powered. This time, of several seconds, was a large part

of the total test time on the system. This problem was overcome by applying power to the units before they were ready to be tested. This reduced the overall test time considerably and improved the throughput.

In view of the previous statements regarding the use of inexpensive circuit modules, the casual observer might theorize that these modules coupled with an inexpensive microprocessor chip set might be the most economical system. However, nothing could be further from the truth due to the tremendous hidden costs in software development. Probably the most common pitfall in system design is to underestimate the cost of software development. Although a microprocessor-based system is enticing due to low hardware cost, it can be a disaster unless you have expert software programmers to develop a good operating system.

It has been shown in a study[3] that for medium-sized systems one of the most economical approaches is the utilization of a programmable calculator-based system such as the Tektronix 4051 or the Hewlett Packard 9825. The elements of different control systems are shown in table 2. In the study, these three systems were analyzed in a cost trade-off study. The results of the study are shown in figure 2 which is a graph of cost versus number of systems produced for these types of systems.

[3]Benson, R., Implementation and Cost Trade-Off of a Modular Automatic Test Set, A Motorola In-Plant Technology Study written for Motorola Government Electronics Division, Scottsdale, AZ, August 1976.

Table 2. Three Possible Configurations for an Automated Test System.

1. Minicomputer System
   - HP2105 computer with 32 bytes of memory
   - HP2644 crt/cartridge data station
   - HP6940 multiprogrammer
   - HP RTE-M operating system with BASIC language
   - HPIB hardware interface
2. Calculator System
   - HP9825 calculator with 23k bytes of memory, I/O ROM, string variables ROM, and HPIB interface
   - HP6940 multiprogrammer
   - HPL Hewlett Packard high level programming language
3. Microprocessor System
   - M6800 microprocessor with 16k bytes of memory
   - Dicom 176 cassette tape system
   - TTY terminal
   - Practical automation printer
   - Two general purpose I/O boards
   - High level programming language
   - IEEE 488 interface bus

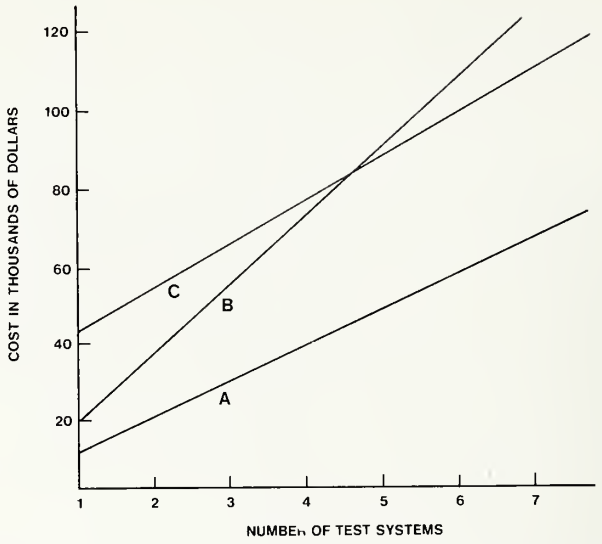

Figure 2. Cost versus number of systems for three types of controllers: (A) HP9825A, (B) HP2105, and (C) M6800.

The great power of these calculator systems is due to the fact that they have resident extended BASIC compilers with on-line interactive editing capabilities. In addition, these systems have an input/output (I/O) structure which is based on the IEEE 488 1975 standard. Because these systems require few or no peripherals for system operation and they have simplified I/O with high level programming language, the overall cost of system software and hardware development is significantly reduced. Both the Tektronix and Hewlett-Packard systems have a basic price of approximately $6,000. However, competition is quickly bringing the price down, and at least one manufacturer is now producing a system with power which is almost equivalent to the Tektronix 4051 with a price under $1,000. What all of this means is that it is now possible to have an extremely powerful automatic test system for cardiac pacemakers at a cost under $10,000.

As a general guideline for the development of an economical test system, it is a wise choice to utilize a system with a well-developed BASIC software package and avoid assembly language programming. If any cost cutting is to be performed, it should be in the area of peripheral equipment and not on the processor/controller. Care should be taken to avoid costly general purpose test equipment; use inexpensive dedicated modules.

To assist in the explanation of the design of the automatic testing system developed, a block diagram of the system is provided in figure 3. It must be pointed out that the system was designed to serve as a general purpose hybrid integrated circuit test system and was not dedicated solely to the testing of pacemakers. As a result, the system has a number of features and capabilities

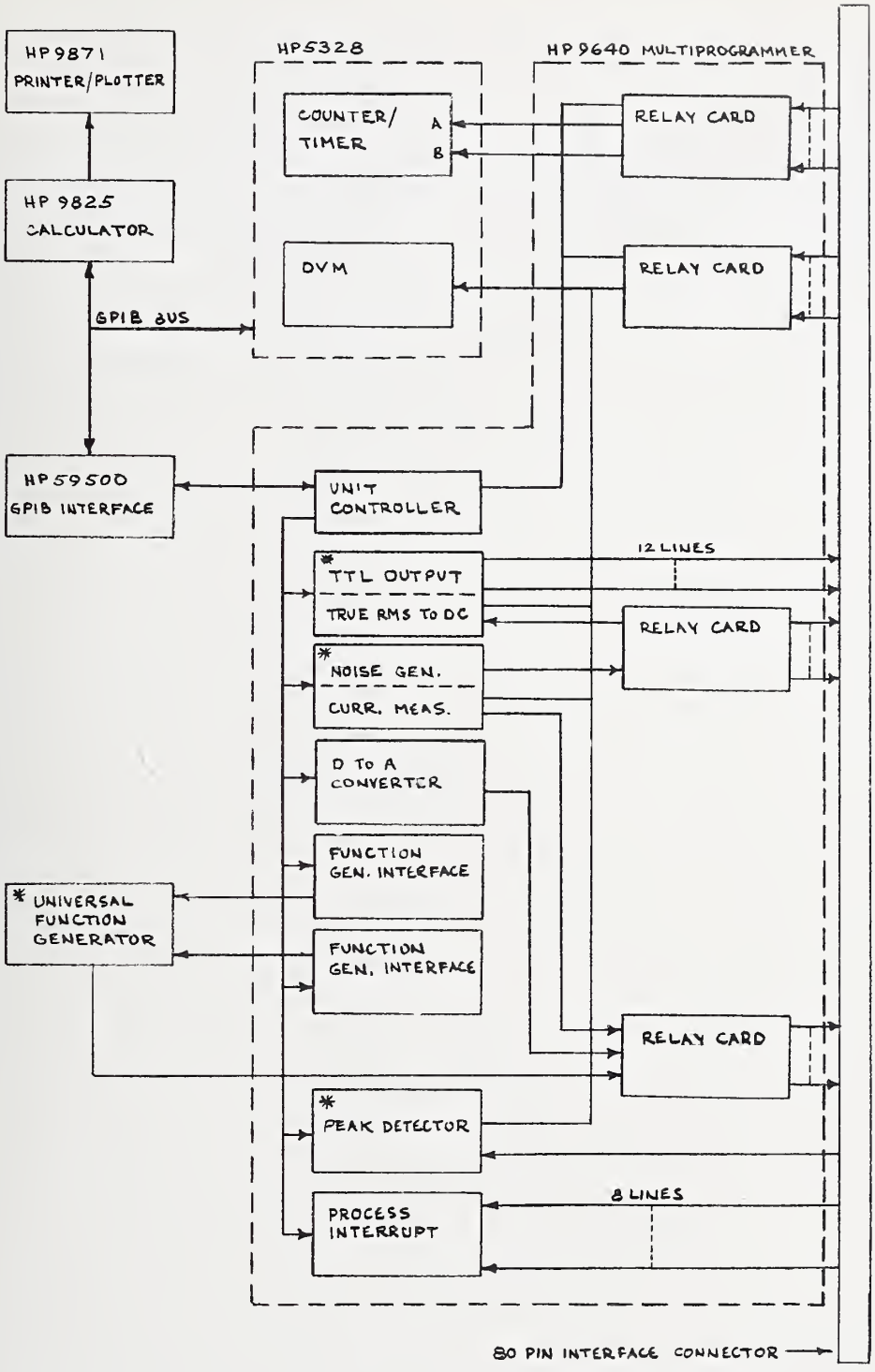

Figure 3. Block diagram of the automated test system.

which are not really required for the testing of pacemakers and which could be eliminated for a reduction in the overall system cost.

There are only two interface cables to the calculator. One is a 16-bit parallel interface to the HP9871 printer/plotter, and the other is an interface specified in IEEE Standard 488. The calculator, which controls the HP9640 multiprogrammer, is controlled through an HP59500 interface adapter.

The counter/timer/DVM combination receives its inputs from two relay cards which consist of 12 spst relays which have been used to multiplex the inputs. The relay cards are one of the standard interface cards for the multiprogrammer. The HP5328 has more power than is actually required for pacemaker testing and is one place where hardware costs could be reduced.

The HP9640 multiprogrammer has been set up to provide all of the special purpose test modules as well as a relay matrix interface. Each unit denoted by an asterisk was custom built or purchased as a module and placed on one of the standard multiprogrammer breadboard cards. The TTL output card provides 12 programmable outputs which can be used for control functions in an external test fixture. The true RMS-to-dc converter is a module which was purchased and can measure ac voltages from 10 mV to 7 V. Its output is monitored by the system DVM for data readout. The noise generator and current measuring circuit were custom designs for the particular pacemakers which are tested on this system. The digital-to-analog (D to A) converter is another standard multiprogrammer module which is programmable from -10.240 V to +10.235 V. It is used as a power source for pacemakers under test. Two standard TTL output cards are used to program the universal function generator. The universal function generator was designed and developed by the author for less than $200. It has the power to generate virtually any function and also has programmable period, duty cycle, output voltage, and offset voltage. In this system, it is used to generate all of the various square waves, square pulses, and haversine pulses used in pacemaker testing. The peak detector was a custom design although there are a number of good low-cost modules available commercially. The process interrupt card is another standard multiprogrammer module which provides the system with true interrupt capability and, thus, allows the system to operate in a time-sharing mode.

A flowchart of the basic software system is shown in figure 4. The software system was designed to be interactive with the operator and, thus, it guides him through the test sequence with a series of questions which the operator must answer before the program proceeds. The program takes advantage of the HP9825 self-starting feature and, thus, the operator only has to place the program tape in the calculator and turn on the power. The program automatically initializes and begins to prompt the operator.

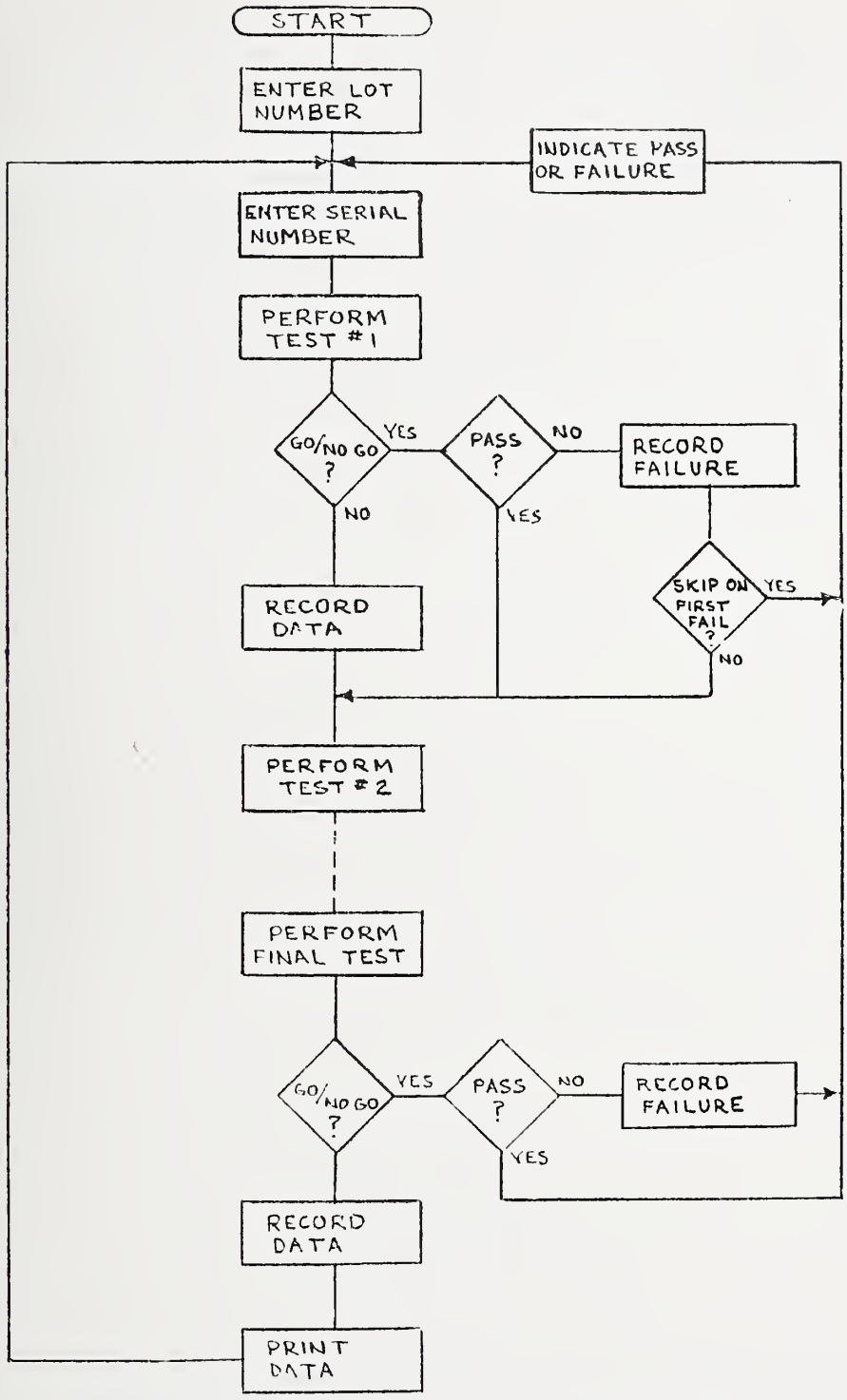

Figure 4. Software flowchart of automated test system.

The software system was designed to be able to operate in a go/no-go environment for high speed testing at the early stages of the hybrid assembly and also in a complete data recording mode by serial number for testing in the final stages of the assembly process.

The complete software system resides in approximately 6,000 words of memory and took about one man-month to develop. The entire test program performs 18 specific tests in about 40 s. In the go/no-go mode of operation, the system displays the test number of any test which failed and, if the test was completed successfully, it prints out a pass indication. The software also performs testing of the test system itself as a background operation and prints out error messages if any faults are detected.

For engineers who are planning to build an automated test system, the following list of guidelines is offered, based on experience gained from the system just described.

Guidelines for the System Designer:

1. Do not overdesign the system with greater accuracy and resolution than is actually required.
2. Do not try to develop your own software operating system; use BASIC.
3. Design the system with IEEE 488 bus capability.
4. Purchase a control system with built-in software operating system and interactive editor.
5. Do not build a modular test system based on a microprocessor chip set unless you are making many systems; it can be an economic disaster.
6. Whenever you can substitute a specific circuit or module to replace a general purpose unit, do it.
7. Do not skimp on documentation.

3.4.5 An Actuarial Analysis of Lead and Pacemaker Failure

Phillip Hurzeler,[1] Richard Whitman,[2] and
Seymour Furman
Montefiore Hospital and Medical Center
111 East 210th Street
Bronx, NY 10467
(212) 920-5429

In order to assess the useful life of pacemaker endocardial electrode leads, a retrospective study was undertaken at the Montefiore Hospital and Hospital Medical Center, in which the electrode lead service lifetimes were calculated

---

[1]Now with Cardiac Datacorp, Inc., 1280 Blue Hills Avenue, Bloomfield, CT 06002 (telephone: (203) 242-0761).
[2]Now with Electro-Catheter Company, 2100 Felver Court, Rahway, NJ 07065 (telephone: (201) 382-5600).

and displayed according to an actuarial method.[3] Leads whose service lifetimes were terminated due to wire fracture or breach of insulation were classed as "failures" and leads still in service or whose service lifetimes were terminated for any other reason (e.g., infection, myocardial perforation, displacement, or unexplained exit block) were classed as "lost to follow-up." (A more descriptive classification would have been "removed from risk.") Only electrode leads transvenously applied to the right ventricle were included. All lead wires were made of helical Elgiloy coils.

Summary actuarial tables are shown for manufacturers A, B, and C in table 1. The retrospective finding of no failures for manufacturer B and only one for manufacturer C is consistent with subjective clinical recollection at our institution. However, note the greater exposure to risk for manufacturer A. Thirty-eight units were exposed for ten years, while a similar number of manufacturer B's units were exposed for less than six years and C's units were exposed only some four years. Plus or minus 1.96 standard errors about the cumulative percentage are equivalent to 95-percent confidence limits under the assumption that the data are normally distributed. In the present context, this assumption does not seem justified, and these confidence limits probably have little meaning.

To estimate the reliability of pacemakers implanted at the Montefiore Hospital and Medical Center, a computerized analysis system of their longevity was started in 1974 with data back to 1965. The present data base includes approximately 2500 pacemakers from 85 different models manufactured by 13 different companies. A failure, defined from the clinician's (or patient's) viewpoint, includes either battery exhaustion or electronic malfunction. The actuarial statistics were performed according to the AAMI proposed standard[4] except that the 95-percent confidence limits were calculated using the classical normal theory method.[5] Rapid technological developments suggest that comparisons should be made among different power sources, different types of circuitry, different output settings, and different manufacturers. To assure statistical significance, only broad comparisons are included in this report.

By comparing the longevity of all units employing mercury-zinc batteries with all those containing lithium-iodine batteries, the extended survival expected for the latter units is shown in figure 1.

In the comparison between discrete component and hybrid circuitry shown in figure 2, the expected superiority of the hybrid circuitry models is believed to

---

[3]Anderson, R. P., Bonchack, L. I., Greenhemeier, G. L., Lambert, L. E., and Starr, K., The Analysis and Presentation of Surgical Results by Actuarial Methods, *J. Surg. Res.* 16, 224-230 (1974).

[4]AAMI Pacemaker Standard, RDA Contract No. 223-74-5083 (August 1975).

[5]Cutler, S. J., and Ederer, F., Maximum Utilization in the Life Table Method in Analyzing Survival, *Chronic Diseases* 8, 699 (1958).

Table 1. Actuarial Tables for Pacemaker Leads from Manufacturers A, B, and C.

13:22EDT 10/10/77

Manufacturer A

Intervals in Years (1)	Operational Beginning of Interval (2)	Failed During Interval (3)	Lost To Follow-Up (4)	Effective # Exposed to Risk (5)	Proportion Failing (6)	Proportion Operational (7)	Operational at Start of Interval: Cumulative Percentage (8)	1.96SE Confidence Limits: Lower (9)	Upper (10)
0- 1	543	8	88	499.0	0.0160	0.9840	100.00	100.00	100.00
1- 2	447	3	77	408.5	0.0073	0.9927	98.40	97.29	99.50
2- 3	367	7	64	335.0	0.0209	0.9791	97.67	96.31	99.04
3- 4	296	5	48	272.0	0.0184	0.9816	95.63	93.63	97.64
4- 5	243	3	60	213.0	0.0141	0.9859	93.88	91.38	96.37
5- 6	180	3	42	159.0	0.0189	0.9811	92.55	89.68	95.42
6- 7	135	2	38	116.0	0.0172	0.9828	90.81	87.38	94.24
7- 8	95	2	34	78.0	0.0256	0.9744	89.24	85.24	93.24
8- 9	59	0	21	48.5	0.0000	1.0000	86.95	81.96	91.95
9- 10	38	0	22	27.0	0.0000	1.0000	86.95	81.96	91.95
10- 11	16	0	15	8.5	0.0000	1.0000	86.95	81.96	91.95
11- 12	1	0	1	0.5	0.0000	1.0000	86.95	81.96	91.95
		33	510						

13:28EDT 10/10/77

Manufacturer B

Intervals in Years (1)	Operational Beginning of Interval (2)	Failed During Interval (3)	Lost To Follow-Up (4)	Effective # Exposed to Risk (5)	Proportion Failing (6)	Proportion Operational (7)	Operational at Start of Interval: Cumulative Percentage (8)	1.96SE Confidence Limits: Lower (9)	Upper (10)
0- 1	315	0	77	276.5	0.0000	1.0000	100.00	100.00	100.00
1- 2	238	0	72	202.0	0.0000	1.0000	100.00	100.00	100.00
2- 3	166	0	64	134.0	0.0000	1.0000	100.00	100.00	100.00
3- 4	102	0	53	75.5	0.0000	1.0000	100.00	100.00	100.00
4- 5	49	0	24	37.0	0.0000	1.0000	100.00	100.00	100.00
5- 6	25	0	10	20.0	0.0000	1.0000	100.00	100.00	100.00
6- 7	15	0	4	13.0	0.0000	1.0000	100.00	100.00	100.00
7- 8	11	0	9	6.5	0.0000	1.0000	100.00	100.00	100.00
8- 9	2	0	2	1.0	0.0000	1.0000	100.00	100.00	100.00
		0	315						

16:32EDT 10/10/77

Manufacturer C

Intervals in Years (1)	Operational Beginning of Interval (2)	Failed During Interval (3)	Lost To Follow-Up (4)	Effective # Exposed to Risk (5)	Proportion Failing (6)	Proportion Operational (7)	Operational at Start of Interval: Cumulative Percentage (8)	1.96SE Confidence Limits: Lower (9)	Upper (10)
0- 1	110	1	51	84.5	0.0118	0.9882	100.00	100.00	100.00
1- 2	58	0	17	49.5	0.0000	1.0000	98.82	96.51	100.00
2- 3	41	0	7	37.5	0.0000	1.0000	98.82	96.51	100.00
3- 4	34	0	9	29.5	0.0000	1.0000	98.82	96.51	100.00
4- 5	25	0	11	19.5	0.0000	1.0000	98.82	96.51	100.00
5- 6	14	0	11	8.5	0.0000	1.0000	98.82	96.51	100.00
6- 7	3	0	3	1.5	0.0000	1.0000	98.82	96.51	100.00
		1	109						

have been masked out by secondary changes to correct initial deficiencies that resulted in early failures. The remaining difference does not become significant until the thirty-third month and then only slightly.

To reduce further battery drain, a special low output (225 ± 25 μs pulse period) series of pacemakers were implanted with 6907 leads having a surface area of 11 mm^2. When compared to conventional units (with pulse width of approximately 900 μs), the low output series showed prolonged survival beginning at 36 months after implant, as shown in figure 3.

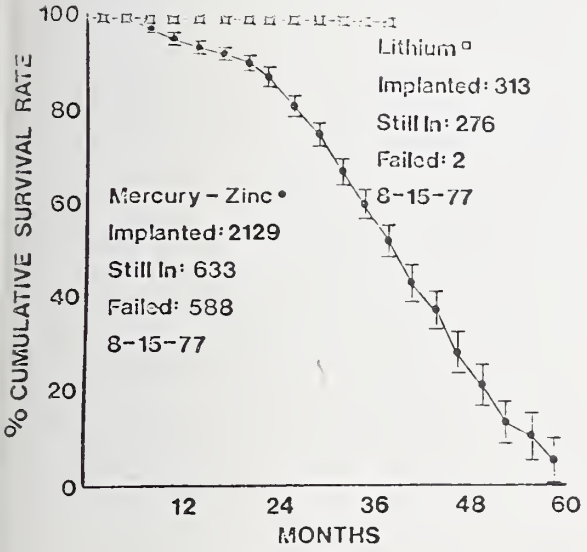

Figure 1. Longevity comparison of pacemakers using mercury-zinc batteries with those using lithium batteries.

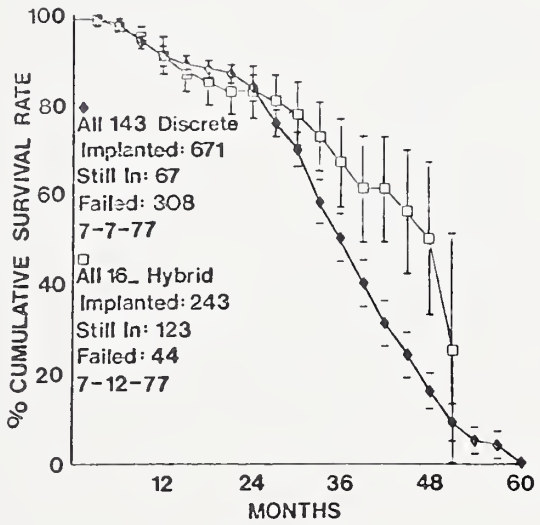

Figure 2. Longevity comparison of pacemakers using discrete components with those using hybrid circuitry.

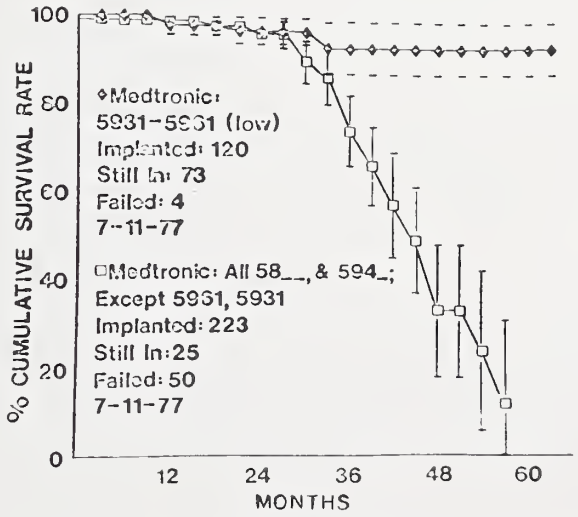

Figure 3. Longevity comparison of pacemakers using a specially short pulse width with those using a conventional pulse width.

The remaining data, shown in figures 4 through 7, illustrate survival curves for all implanted pulse makers from four separate manufacturers. While keeping in mind that manufacturer #1 (fig. 4) includes more older units than do the others, a comparison between them at 24, 36, and 45 months would rank the manufacturers (according to prolonged survival of all units implanted at Montefiore Hospital) as: manufacturer 2, 4, 3, and 1.

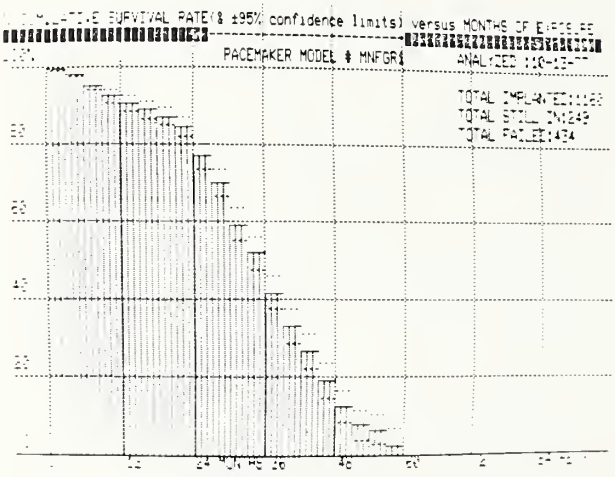

Figure 4. Survival curves of pulse generators by manufacturer 1.

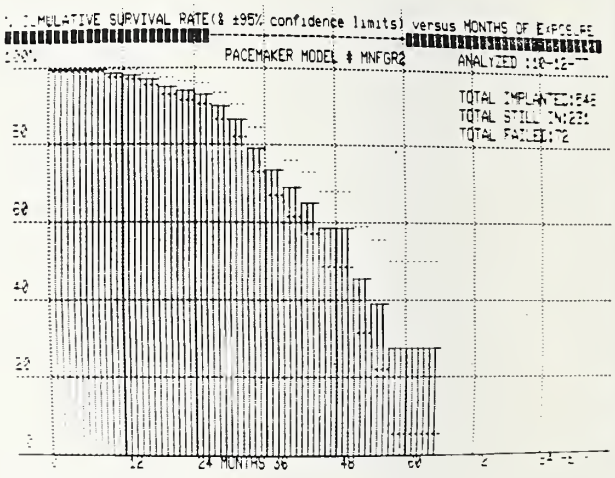

Figure 5. Survival curves of pulse generators by manufacturer 2.

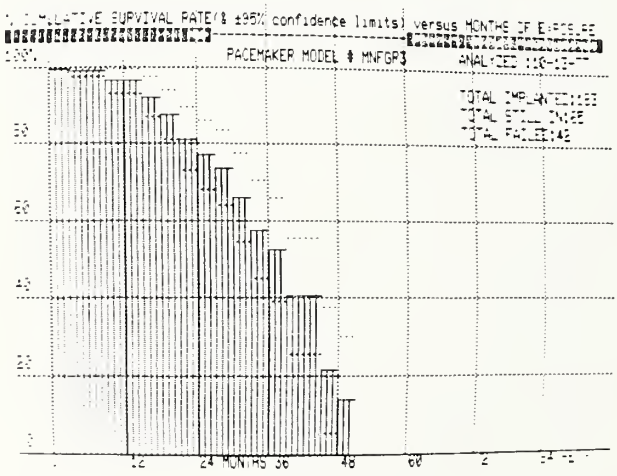

Figure 6. Survival curves of pulse generators by manufacturer 3.

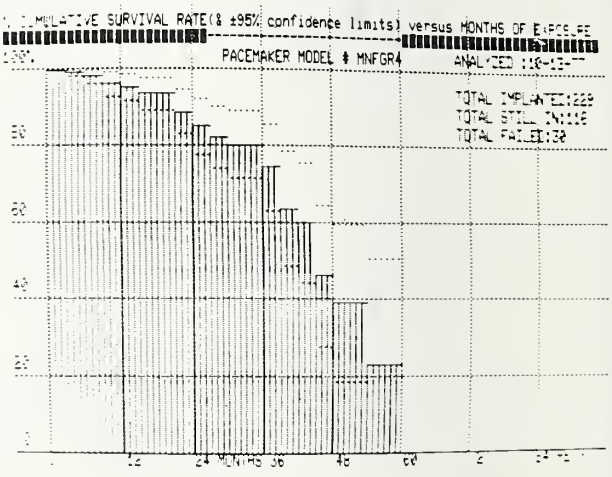

Figure 7. Survival curves of pulse generators by manufacturer 4.

3.5 Session V Materials and Processes

3.5.1 Factors to Consider in the Selection of a Welding Process for the Welding of Cardiac Pacemaker Enclosures

E. R. Bangs
IIT Research Institute
10 West 35th Street
Chicago, IL 60616
(312) 567-4191

The ability to produce a reliable welded hermetic seal for a cardiac pacemaker enclosure requires a comprehensive analysis in the selection of the welding process, design of the weld joint, and anticipated welding metallurgy. Two major factors in selecting a welding process are the base material thickness and the weld joint design. In addition to designing the weld joint for compatibility with the welding process, one must consider the corrosion resistance, mechanical properties, and inspectability of the completed weld.

The majority of enclosure thicknesses fall within a range of from 0.002 to 0.025 in. (0.005 to 0.6 mm), which from a welding engineering viewpoint categorizes the pacer enclosure weldment as a sheet metal component. Welding engineering problems inherent to the sheet metal assembly are poor fit of parts and weld-joint distortion. The weld is ordinarily made without the use of weld-joint filler metal. Therefore, the essential criteria of the welding process selected should be its ability to cope with parts that fit marginally and its capability for producing welds with a steep temperature profile.

There are four welding processes that may be considered for application: the plasma arc, gas tungsten arc, laser, and electron beam processes. Three of the four processes — plasma, laser, and electron beam — may be classified as high energy sources due to the high temperature created by these sources at the work surface. The prime technical advantages that characterize the high energy process are the production of fusion zones with high depth-to-width ratios, a minimum distortion, and high welding speeds. The application of fine focal point processes to electrical feed-throughs and other small attachments that require a weld face width dimension of less than 0.020 in. (0.5 mm) are ideal applications for laser and electron beam processes. The prime disadvantage of the high energy, fine focal point heat source is the need for close part fit tolerances. Poorly fitted parts that exceed those tolerances shown in table 1 may expect to produce weld-joint defects.

The gas tungsten arc welding process is a lower energy process compared to the other three. Its major disadvantages in the enclosure application are its tendency to produce wide fusion zones and enlarged heat-affected zones and its relatively slow travel speed. The application of properly designed fixturing will reduce fusion zone width and heat-affected zone growth. Advantages include its ability to produce acceptable welds in marginally fitting parts and its abil-

Table 1. Suggested Weld Joint Design Dimensional Guidelines

Weld Joint Design	Welding Processes					
	Electron Beam, Laser, and Plasma		Gas Tungsten Arc		Gas Tungsten Arc (pulsed current)	
Thickness of thinner member	2 to 8 mils (0.05 to 0.2 mm)	8 to 25 mils (0.2 to 0.64 mm)	2 to 8 mils (0.05 to 0.2 mm)	8 to 25 mils (0.2 to 0.64 mm)	2 to 8 mils (0.05 to 0.2 mm)	8 to 25 mils (0.2 to 0.64 mm)
Edge Weld[a] Dimension A	0	10	0	25	0	35
Edge Weld[a] Dimension B	20	25	100	50	150	50
Square Grooved Butt Weld[a] Dimension A	0	10	0	10	10	25
Square Grooved Butt Weld[a] Dimension B	10	15	15	20	20	30

[a]Dimensional tolerance in percent of thinner member.

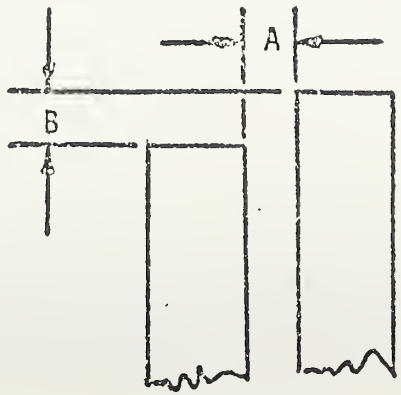

EDGE WELD

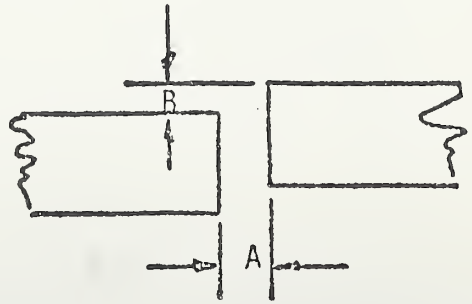

SQUARE-GROOVED BUTT WELD

ity to produce a smooth root area reinforcement in square-grooved, butt-joint designs.

Most weld-joint designs used in pacemaker enclosures are either edge welds or square-grooved butt joints. The edge weld has advantages over the square-grooved butt in that it is easier to produce due to to its ease in fixturing, and it can tolerate larger variations in edge length without degrading weld quality. Another advantage over the square-grooved design is the greater separation of the heat-affected zone from components contained in the enclosure. Disadvantages of the edge weld design are the inherent crack present in the root area of the fusion zone, the insufficient fundamental engineering stress criteria for the stress analysis required to factor in the influence of the stress riser, and the inability to inspect the internal quality of the weld with nondestructive techniques.

The material thickness and the position in which the edge weld is to be welded will have a strong bearing in the selection of the welding process. In most electron beam or laser systems, the beam is perpendicular to the joint during welding. When the combined thickness of the two members to be edge-welded is less than 0.01 in. (0.25 mm), beam and focal point alignment become difficult and weld-joint defects can result. In this case, the use of the gas tungsten arc process is frequently more suitable when used with carefully designed fixturing.

The square-grooved joint design, although more difficult to produce, has the better mechanical properties of the two joint designs with its full root penetration and crack-free cross section. It is inspectable using ultrasonic techniques and meets the design requirements of all welding codes. Disadvantages to be dealt with include the protection of components inside the enclosure and the need to fit the abutting edges in accordance with the general tolerance guidelines shown in table 1.

The square-grooved, butt-joint design can be welded with any of the processes mentioned; however, if full penetration is to be obtained without the use of backing strips or similar devices, the gas tungsten arc process is recommended because it will provide a more uniform root reinforcement and eliminate the internal damage that can be caused by beam penetration into the enclosure.

The welding fixture used in the positioning of the enclosure, regardless of process, must fulfill the following functions if optimum weld quality is to be obtained. It must: (1) provide for the sizing of the assembly in the area of the weld joint; (2) control part movement during the welding process; and (3) provide heat suppression in the area of the weld joint (water-cooled, copper-chrome alloy fixtures have worked effectively in these applications). Welding fixture design features should also provide easy installation and removal of the weldment. In addition, it should be compatible with on-line sensing and inspection techniques.

After the welding process has been selected, the definition of the base material quality and the preweld cleaning techniques is critical. The present American Society for Testing and Materials (ASTM) specifications for surgical quality stainless steel do not really meet the microstructural cleanliness levels that are mandatory for the optimum pitting and crevice corrosion resistance required for this industry. Modified chemical compositions for the 316-L alloy have been formulated at IITRI and will be proposed to the responsible ASTM committee.

Prior to welding titanium-base materials, the surfaces to be welded should be chemically pickled within 8 h of welding to minimize lack-of-fusion defects and contaminant gas absorption. The cleaning procedures suitable for the stainless steels include chemical vapor degreasing or pickling with no restriction on time at which welding should be performed.

As a result of analyses performed over the past four years at IITRI, the following has been concluded:

1. A large portion of the edge welds presently in use contain regions in the weld joint that do not contain a fusion zone throat dimension equivalent to the minimum wall thickness.
2. Present leak test and visual inspection procedures cannot reliably measure internal quality of the final edge weld.
3. The full penetration butt joint design is recommended over the edge weld design due to its improved properties, full fusion zone penetration, reproducibility, and inspectability.
4. The pulsed current gas tungsten arc process is preferred to the high energy processes because:
   a. there is better control of fusion zone penetration in both joint designs,
   b. weld joint quality is not largely influenced by marginal part fit, and
   c. it has the ability to produce welds with relatively unskilled labor.
5. Additional welded joint corrosion testing should be performed to determine the corrosion resistance limitations of titanium enclosures.
6. An industry-wide welding code should be established for cardiac pacemaker weld joints. The code should classify the weld joints in order of criticality, define the qualification and inspection requirements, and establish defect acceptance standards.

3.5.2 High Energy Beam Welding As An Aid To More Reliable Pacemakers

Steven A. Llewellyn
Energy Beam Systems
EBTEC Corporation
120 Shoemaker Lane
Agawam, MA 01001
(413) 786-0393

Electron beam welding has been used since the late 1950's. It was developed originally in the nuclear industry and was then used in the aerospace industry. The demands of these industries for high integrity welds have shaped the equipment of today into the stable and repeatable units now made available to customers throughout the world. Laser welding equipment is now being introduced into the industrial environment. The similarity of power densities of the two processes indicates that lasers will be able to replace electron beam welding in some cases.

The advantages of using either one of these high energy density processes to produce hermetic packages are as follows: they involve low heat input, allow deep penetration welds without excessive lateral heating, produce little distortion, and allow relatively high welding speeds.

In deciding to use either one of the two processes, the following selection criteria are offered. For seam welds, if they are to be the final sealing weld and a vacuum inside the container is of no concern or is an advantage (for example, for welding titanium), electron beam welding can offer lower capital and running costs compared to laser welding. If the weld is a subassembly, either process can produce high integrity welds with the electron beam being economically superior if the seam weld is longer than about 1-1/4 in. (3.8 cm). For spot welding on short seams, the laser is preferred, providing the much lower cost resistance or capacitor discharge welding techniques are not viable for some reason.

The two processes are compared further in table 1 based on experience at the EBTEC Corporation with CO_2 and YAG laser welding and high- and low-voltage electron beam welding.

The following paragraphs address a number of reliability problems with these processes and should be considered if a selection between the two is to be made.

Contamination of the joint by dirt or potting compound or by oxygen or hydrogen (for welding titanium) presents more of a problem for the laser than for the electron beam welding process.

Because of the ways electrons behave in the molten pool, a combination of speed and material surface tension can give the welds of the pool an instability that can lead to "spiking." In full penetration welds, this is not a problem.

In order to produce a full penetration weld, it is necessary for some electrons or photons (depending on the process used) to penetrate the joint. Such

Table 1. Comparison of Electron Beam and Laser Welding Processes

Feature	Electron Beam		Laser	
	Low Voltage (3 kW)	High Voltage (6 kW)	YAG (400 W)	CO_2 (225 W)
Welding Speed — in./min (cm/min)	60 to 200 (150 to 500)	60 to 200 (150 to 500)	20 to 60 (50 to 150)	10 to 30 (25 to 75)
Maximum Weld Penetration — in.(mm)	0.05 (1.3)	1.5 (3.8)	0.06 (1.5)	0.025 (0.6)
Capital Cost	$60k to 80k	$180k to 250k	$40k to 70k	$30k to 45k
Operating Cost	low	low	high	moderate
Complexity	high	high	high	high
Contamination Tolerance	good	good	poor	poor

penetration can damage sensitive components inside the pacemaker package, cut wires, and break down insulation. This problem is most serious with high-voltage electron beams because of their high kinetic energy and long depth of focus.

A standard approach to avoid the particle penetration problem has been to use a backing strip. This can produce a secondary problem with either welding process because part of the material of the backing can be vaporized and be deposited subsequently on sensitive elements inside the pacemaker housing.

The fact that these high energy density processes produce narrow welds can lead to joint alignment problems which impose restrictions on the preparation of the parts to be welded. The contours now being considered by the pacemaker industry for practical, aesthetic, or other reasons cannot always be welded without placing significant demands on sophisticated contour-following work stations.

In summary, both laser and electron beam welding can produce, under the correct conditions, high reliability welds on the joints and materials being used or considered for cardiac pacemaker components. The ability of electron beam and laser systems to produce welds can give the designer the opportunity to build smaller, lighter, and more reliable welded packages in materials which are difficult to weld conventionally. The manufacturer can utilize these processes to produce pacemaker subassemblies more quickly and more reliably with reduced reject rates, and, in the case of the laser welder, to make final assembly welds in any environment required.

3.5.3 Measurement of Surface Contamination Using a Contact Angle Goniometer

Byron Gilman
Medtronic, Inc.
3055 Old Highway Eight
Minneapolis, MN 55418
(612) 574-3050

In the manufacturing of an implantable pulse generator, wettability of a surface is important in several operations: in soldering, both surfaces to be joined must be wetted by the solder in order to obtain a strong connection; in welding, clean wettable mating surfaces are needed to avoid oxidation and bubbles; and in adhesive bonding or encapsulation, the surfaces to be bonded or encapsulated must be wetted by the adhesive in order to obtain a good adhesive bond. This paper will discuss wettability and surface contamination primarily in the context of adhesive bonding and encapsulation. However, the concepts of surface contamination are equally important and applicable to soldering and welding.

In many pulse generators or parts thereof, adhesion of an epoxy encapsulant to an interconnecting wire or other surface is crucial to insuring the reliability of the device. A necessary but not sufficient condition for obtaining good adhesion to a substrate is that the epoxy must wet the surface. That is, the contact angle, θ (formed by the solid surface and a line tangent to the drop of liquid at the point of intersection), must be 0 deg. The contact angle has been shown[1,2] to be dependent only on the surface tension of the liquid and the outermost molecular layer of the solid surface.

This layer is so thin it cannot be analyzed by conventional techniques. However, a general classification of the surface can be assigned based on data obtained with a contact angle goniometer. By measuring the contact angles of a series of liquids with a wide range of surface tensions, a "critical surface tension," γ_c, for the surface can be determined. A graph of cosine θ versus surface tension produces a straight line as shown in figure 1.

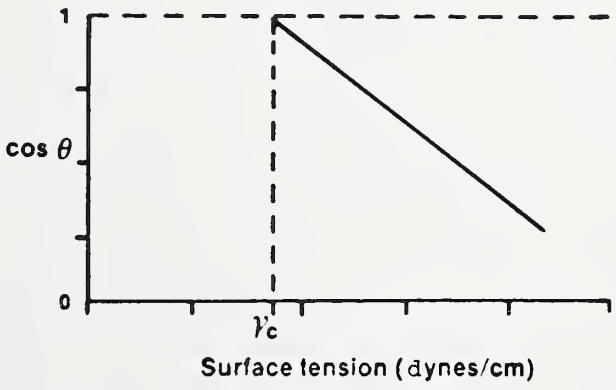

Figure 1. Schematic of the relationship between the cosine of the contact angle, θ, on the surface tension of different liquids applied to a flat solid surface.

The surface tension at which this line intercepts cosine θ = 1 is defined

[1]Shaffain, E. G., and Zisman, W. A., Constitutive Relations in the Wetting of Low-Energy Surfaces and the Theory of the Refraction Method of Preparing Monolayers, *J. Phys. Chem.* 64, 519-524 (1960).
[2]Zisman, W. A., Relation of Equilibrium Contact Angle to Liquid and Solid Constitution, *Adv. in Chem.* 43, 1-51 (ACS, Washington, D.C., 1964).

as γ_c, "the critical surface tension of wetting." The critical surface tension of a surface is a constant depending only on the constitution and packing of the outermost molecular layer of the surface. By comparing the γ_c of an unknown surface to those of known surfaces reported in the literature, the nature of the surface can be determined. The physical significance of the critical surface tension is that liquids having surface tension lower than γ_c will wet the surface.

Thus, the conclusion that high energy surfaces should be easily adhered to is true, except that such surfaces are quickly converted to low energy surfaces by the adsorption of water vapor or organic contaminants from the air. Herein lies a major problem in obtaining good adhesive bonds. Since it is impossible to prevent the adsorption of such contaminants, processes and adhesives must be designed in such a way as to insure that γ_c of the surface is higher than the liquid surface tension of the adhesive at the time of encapsulation.

Values of the critical surface tension of wetting are available for a variety of common surfaces in the literature. A few selected values are shown in table 1.

The contact angle goniometer can be used in conjunction with known literature values of γ_c of a surface, and comparing it to the liquid surface tension of the adhesive, one can determine if the adhesive will wet the surface to be bonded. Secondly, γ_c can be compared to the known value of a substrate in order to confirm cleanliness or to indicate the presence of a contaminant. Further information regarding the identity of the contaminant can then be obtained by comparing the observed γ_c to literature values for various surfaces.

Experiments utilizing these principles were performed using platinum as a substrate primarily for ease of cleaning. The results are summarized in table 2.

Experiment 1 showed that flame-cleaned platinum has a γ_c comparable to that reported in the literature for glasses and metals at 1-percent relative humidity. In addition, this control showed that our handling and measuring procedure did not introduce any extraneous contaminants.

Experiment 2 showed that the solvent cleaning process did not introduce any residue, and, further, if we now intend to use an epoxy adhesive with a liquid surface tension of 40 dyn/cm, it will wet the surface.

Experiment 3 revealed that after storage in polyethylene bags for seven days (care was taken to insure that the polyethylene did not touch the platinum) the γ_c had dropped to 34 dyn/cm. Comparing this to table 1, we see that this is very close to the value of γ_c for polyethylene (31 dyn/cm) indicating that the platinum was now covered with a thin layer of polyethylene.

Experiment 4 revealed that samples stored in a silicone rubber curing chamber had a γ_c of 22.8 dyn/cm. In comparing this to known values of γ_c, we concluded that this surface was covered with silicone rubber.

Table 1. Critical Surface Tension of Selected Solid Surfaces.

	γ_c (dyn/cm)[a]
Polytetrafluoroethylene (Teflon)	18.5
Polydimethyl siloxane (silicone)	22
Polyethylene	31
Polystyrene	33
Polymethyl methacrylate	39
Polyvinyl chloride (PVC)	39
Polyethylene terephthalate (Polyester)	43
Metals and Glasses (at 1-percent relative humidity)	42 to 46

[a] 1 dyne = 10^{-5} newton.

Table 2. Observed Critical Surface Tensions on a Platinum Substrate.

Experiment No.	Treatment of Substrate	γ_c (dyn/cm)[a]
1	Flame cleaned (control)	42.5
2	Solvent cleaning process	44
3	Stored in polyethylene bags	34
4	Stored in silicone curing chamber	22.8
5	Solvent cleaning after silicone chamber	19.5

[a] 1 dyne = 10^{-5} newton.

In experiment 5, the γ_c of samples from the silicone curing chamber was measured after a solvent cleaning to evaluate the effectiveness of the cleaning. The observed γ_c of 19.5 dyn/cm indicated that the silicone was not removed and further that oriented solvent molecules may have been trapped at the surface, further lowering γ_c.

In summary, our work has shown that the contact angle goniometer is a quick and simple tool to evaluate organic contamination, and it can be used to monitor or design processes and procedures in order to insure good adhesion.

3.5.4 Susceptibility to Corrosion of Various Implant Metals Used for Pacemaker Encapsulations

M. Schaldach and R. Thull
Zentralinstitut für Biomedizinische Technik
der Universität Erlangen-Nürnberg
Turnstrasse 5, D-8520 Erlangen
Germany

The requirements for a service life of 10 or more years for pacemakers place great demands not only on the power source and electronics, but also on the metallic encapsulation as well. Not only must the metal be resistant to corrosion, but it must be body-compatible and easy to work and weld. On the basis of these

criteria, three available encapsulation materials were investigated and classified, namely, stainless steel (AISI 316 L), pure titanium, and the multiphase alloy MP35N on a cobalt base.

Homogeneous corrosion of these metals can be neglected in comparison to localized corrosion that can occur in the body environment. A number of localized corrosion phenomena can occur in the body environment: pitting corrosion, caused by the attack of chlorine ions; crevice corrosion, as a result of chlorine ions in the presence of an oxygen gradient; and fretting corrosion, caused by the rubbing of scar tissue against the oxide surface of the encapsulation material.

The forming of metals into a pacemaker housing and the subsequent annealing and welding steps can significantly affect the corrosion resistance of the encapsulation material.[1] Forming the metal changes the grain size and increases the grain boundary density.[2-4] The thermal stressing on either side of a welding seam can lead to the precipitation of impurities at the grain boundaries and, consequently, greater risk to corrosive attack.

A regeneration of the original grain structure can be accomplished by an annealing process after forming. The heat treatment must be conducted so that (1) any inert gas or impurities in the furnace do not change the state of the alloy (a vacuum furnace is needed for the materials under consideration), (2) the duration of the heat treatment is long enough to homogenize the material but short enough to prevent significant grain enlargement, and (3) the period of cooling is rapid enough to avoid precipitations at grain boundaries.[5]

In contrast to the annealing procedure, the welding step to make a hermetic seal is a poorly controlled process. Nevertheless, by selecting the most suitable welding technique and by adjusting welding parameters, a relatively optimal welding process can be obtained. Electron beam welding is recommended over plasma or laser beam welding because of the smaller heating zone formed and the reduced problem with precipitates.

---

[1]While stainless steel has to be subjected to heat treatment after the forming process to achieve an adequate resistance to corrosion, titanium and the cobalt-based alloy both are much less susceptible to corrosion attack. Nevertheless, annealing is desirable to improve the welding properties of these metals.

[2]Dull, D. L., and Raymond, L., Thermal and Mechanical Effects on the Corrosion Behavior of Ti-6Al-4V Alloy, *J. Electrochem. Soc.* 120, 1632-1637 (1973).

[3]Mazza, B., Pedefem, P., Sinigaglia, D., Cigada, A., Lazzari, L., Re, G., and Wengler, D., Relationship Between the Electrochemical and Corrosion Behavior and the Structure of Stainless Steels Subjected in Cold Plastic Deformation, *J. Electrochem. Soc.* 123, 1157-1163 (1976).

[4]Rentler, R. M., and Green, N. D., Corrosion of Surface Defects in Fine Wires, *J. Biomed. Mater. Res.* 9, 597-610 (1975).

[5]Tennese, W. W., and Cahoon, J. R., "Sensitization" Still a Problem in the Intergranular Corrosion of Stainless Steel Surgical Implants, *Biomat., Med. Dev., Art. Org.* 1, 635-645 (1973).

Consider now several examples of corrosion. To demonstrate the corrosive attack on structural inhomogeneities, figure 1 shows a part of an unannealed welded stainless steel housing which had been exposed to 12 h of a 10-percent solution of ferric chloride, at a temperature of 37°C. The corrosion, if not triggered by, is at least promoted by the chlorine ions in the electrolyte.[6-10] The primary corrosive attach occurred in the strongly distorted regions of the metal structure[3,11] but not in the welding seam where a comparatively homogeneous structure exists due to melting by the electron beam. Conducting the same test after an anneal treatment did not lead to any surface corrosion. Only after extending the test time to 15 h at the higher temperature of 60°C did intercrystalline destruction occur at regions of high grain density, as is illustrated in figure 2.

Compared to stainless steel, the cobalt-based multiphase alloy MP35N is more resistant to corrosion.[12-17] To illustrate this, consider figure 3 where the surroundings of the weld seam of a pacemaker housing are shown before (A) and after (B) a 12-h exposure to a 10-percent solution of ferric chloride at a temperature of 37°C. Although the surface was abraded after an anneal treatment, there are no signs of any attack. Patches of silicone rubber were applied to cleaned sur-

---

[6]Beck, T. R., Pitting of Titanium, I. Titanium-Foil Experiments, *J. Electrochem. Soc.* 120, 1310-1316 (1973).

[7]Beck, T. R., Pitting of Titanium, II. One-Dimensional Pit Experiments, *J. Electrochem. Soc.* 120, 1317-1324 (1973).

[8]Beck, T. R., Electrochemistry of Freshly Generated Titanium Surfaces - 1. Separated-Rotating-Disk Experiments, *Electrochemica Acta* 13, 807-814 (1973).

[9]Beck, T. R., A Review: Pitting Attack of Titanium Alloys Localized Corrosion, *NACE* 3, 644 (1974).

[10]Galvele, J. R., Transport Processes and the Mechanism of Pitting of Metals, *J. Electrochem. Soc.* 123, 464-474 (1976).

[11]Seys, A. A., van Haute, A. A., and Brabers, M. J., On the Initiation Process of the Pitting Corrosion on Austenitic Stainless Steel in Chloride Solution, *Werkstoffe und Korrosion* 25, 663-376 (1974).

[12]Devine, T. M., and Wulff, J., Cast vs. Wrought Cobalt-Chromium Surgical Implant Alloys, *J. Biomed. Mater. Res.* 9, 151-167 (1975).

[13]Devine, T. M., and Wulff, J., The Comparative Crevice Corrosion Resistance of Co-Cr Base Surgical Implant Alloys, *J. Electrochem. Soc.* 123, 1433-1437 (1976).

[14]Kuhne, D., Die Gewebeverträglichkeit Verschiedener Metallischer Implantatwerkstoffe in Pulverform, Inaugural Dissertation - Johann Wolfgang Goethe, Universität Frankfurt/Main (1975).

[15]Lemons, J. E., Niemann, K. M. W., and Weiss, A. B., Biocompatibility Studies on Surgical-Grade Titanium-, Cobalt-, and Iron-Base Alloys, *J. Biomed. Mater. Res. Symp.* 7, 549-553 (1976).

[16]Society of Automative Engineers, Inc., Aerospace Material Specification AMS 5758A-Alloy Bars, High Strength, Corrosion Resistant 35 NI-35 Co-20 Cr-10 Mo Solution Heat Treated (1972).

[17]Younkin, C. N., Multiphase MP35N Alloy for Medical Implants, *J. Biomed. Mater. Res. Symp.* 5, 219-226 (1974).

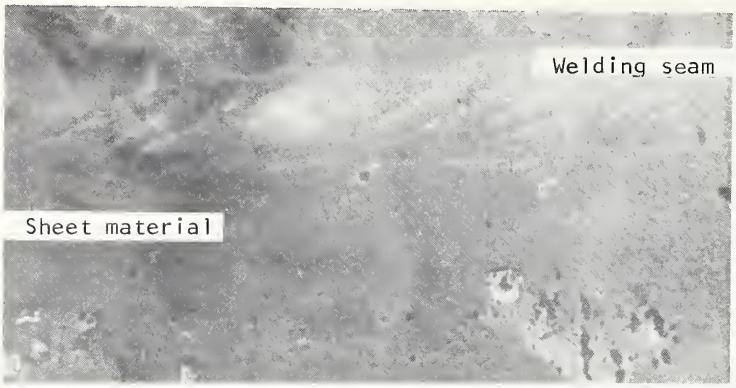

Figure 1. Part of an unannealed welded stainless steel housing after a 12-h exposure to a 10-percent solution of ferric chloride at a temperature of 37°C.

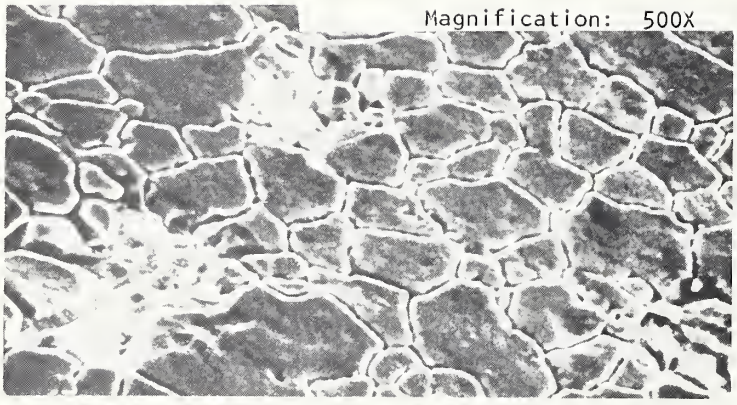

Figure 2. Part of an annealed stainless steel housing after a 15-h exposure to a 10-percent solution of ferric chloride at a temperature of 60°C.

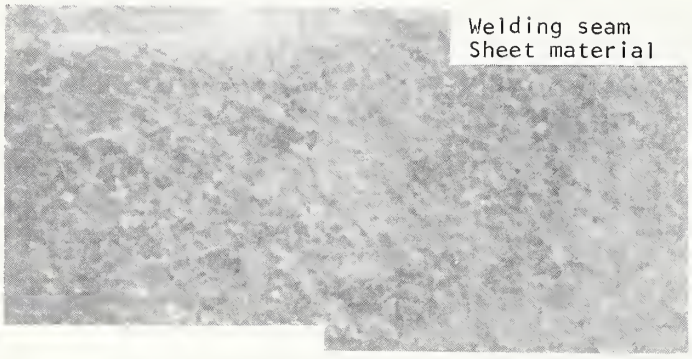

(A) Before exposure.

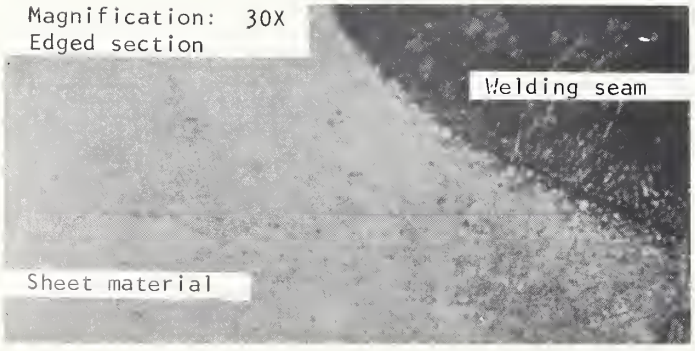

(B) After 12-h exposure.

Figure 3. Surfaces of the cobalt-based multiphase alloy MP35N: (A) before and (B) after a 12-h exposure to a 10-percent solution of ferric chloride at a temperature of 37°C.

faces of housings made of MP35N and titanium, as shown in figure 4A. At the boundary of these patches, the metal is susceptible to crevice corrosion. After 15 h in a 10-percent solution of ferric chloride at 60°C, neither housing revealed any significant changes to the surface, as seen in figures 4B and 4C.

The interaction between scar tissue and the pacemaker housing material leads to a local destruction of the protective oxide layer and fretting corrosion.[18-19]

---

[18]Rätzer-Scheibe, H. J., and Buhl, H., Die Bedeutung des Wassers für die Bildung einer Passivschicht auf der Titanlegierung Ti6Al4V, in Neutralen Elektrolyten, *Werkstoffe und Korrosion* 26, 2-5 (1975).

[19]Rätzer-Scheibe, H. J., and Buhl, H., Das Potentialabhangige Repassivierungsverhalten der Titanlegierung Ti6Al4V, in Neutralen Elektrolyten, *Werkstoffe und Korrosion* 27, 1-5 (1976).

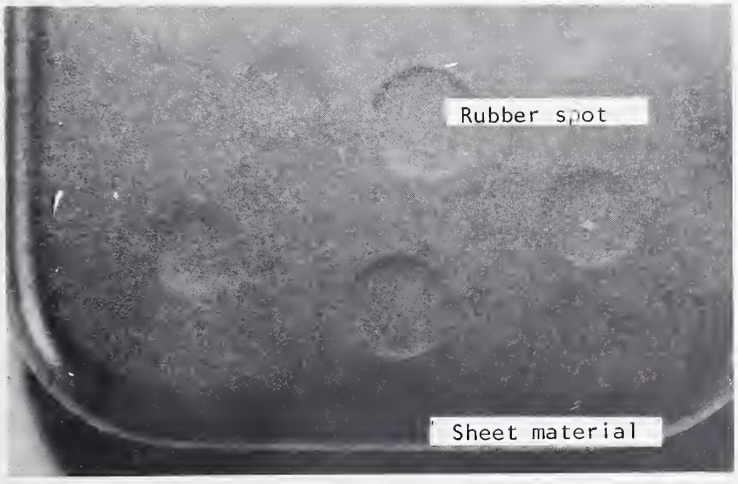

A.

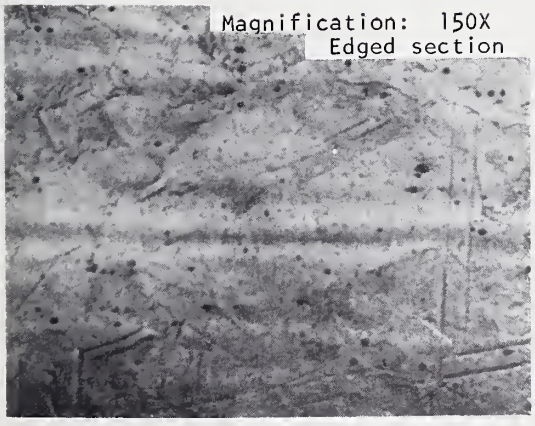

B.

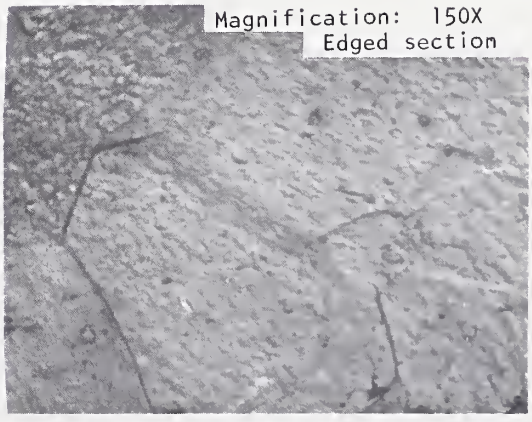

C.

Figure 4. Patches of silicone rubber applied to cleaned surface of a pacemaker housing prior to corrosion test (A), and surfaces of housings made of (B) the MP35N alloy, and (C) titanium after a 20-h exposure to a 10-percent solution of ferric chloride at a temperature of 60°C.

The state of the surface of the implanted metal in contact with tissue can be described by the mixed potential which develops between the implant and a reference cathode which is measurable *in vitro* or *in vivo* experiments.[14,20,21]

To achieve a realistic simulation of corrosion conditions, a test for fretting corrosion was carried out for various metals in an animal experiment. A telemetric system which transmits the mixed potentials measured was implanted into an animal. This was done to avoid complications of infection when connections through the skin are used. Using a reference electrode of silver/silver-chloride, mixed potentials for pure titanium, two titanium alloys, a cobalt-based alloy, and stainless steel (316 L) were measured once daily. The mixed potentials of all samples revealed marked changes with time, as shown in figure 5. In contrast to the mixed potentials of the cobalt and steel alloys, which settled to a stable value after 4 to 6 weeks, those for titanium and its alloys[22] showed significant changes up to the end of the 26-week test. The latter result can be explained only by a fretting corrosion behavior for such materials and agrees with clinical observations of tissue reactions with titanium implants. The behavior for the steel and cobalt alloy also correlates with clinical observation. The tissue initially moves in relation to the implant and enters into a reciprocal mechanical effect with the surface.[20,23] Following the formation of the scar tissue proper, a shrinking occurs which tightens the contact between tissue and metal surface and, thereafter, permits only limited relative movement.

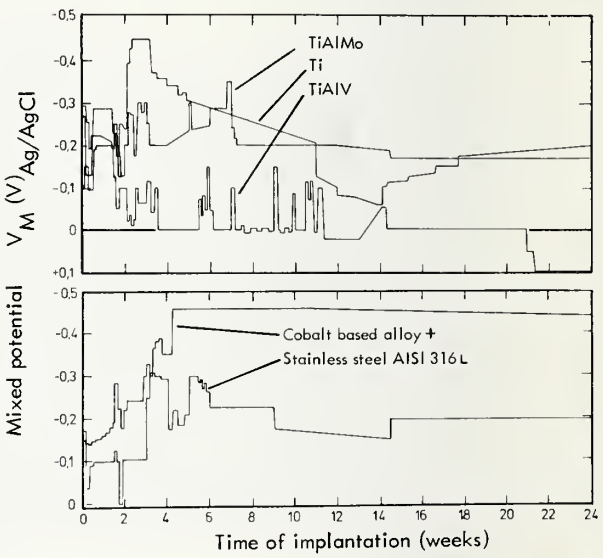

Figure 5. Mixed potentials between a silver/silver-chloride electrode and different metals as a function of implant time. The cobalt-based alloy is the cast alloy made by Sulzer Brothers AG, Switzerland. The conductivity of the oxide is similar to that of MP35N.

Regarding the relative merits of materials for pacemaker housing, the following comments are offered. At the present time, the use of stainless steel (MP35N) for long-lived pacemaker housings is more justifiable than the use of titanium. This is

---

[20]Meachem, G., and Williams, D. F., Changes in Nonosseous Tissue, *J. Biomed. Mater. Res.* 7, 555-572 (1973).

[21]Thull, R., The Long-Term Stability of Metallic Materials for Use in Joint Endoprosthesis, *Medical Progress Technology* 5,103-112 (1977).

[22]Williams, D. F., and Meachem, G., A Combined Metallurgical and Histological Study of Tissue-Prosthesis Interactions in Orthopedic Patients, *J. Biomed. Mater. Res. Symp.* 5, 1-9 (1974).

[23]The changes for TiAlMo are comparable with those of stainless steel.

based on the relative lack of clinical experience in long-term implants, the results of animal experiments, and the greater danger of contamination during any abrasion of the softer titanium. Nevertheless, it should be noted that stainless steel is susceptible to crevice corrosion and pitting which mitigates against its use in procedures with a service life of more than 10 years.

3.5.5 Conformal Coatings for Pacemaker Applications

Arnold Thornton
Cardiac Pacemakers, Inc.
4100 North Hamline Avenue
P.O. Box 3079
St. Paul, MN 55165
(612) 631-3000

In common with current industry practice, CPI uses epoxy for encapsulating its electronic components. Epoxy has generally excellent resistance to moisture vapor permeation[1] and is easily cast into complex shapes. Disadvantages, however, include a 10-g weight penalty, high exothermic temperature during curing (∿150°C), and shrinkage during cure which can damage components. In addition, curing is time-consuming, epoxy delivery equipment requires constant maintenance, and the difficulty in removing the cured epoxy makes failure analysis a problem.

The concept of a conformal coating with moisture barrier properties equivalent to epoxy is very attractive since most of these difficulties would be avoided. Moreover, a simplification in manufacturing procedure would be possible. This report describes the evaluation of several materials for suitability as conformal coatings and concludes that Parylene C is a satisfactory choice.

The most important function of conformal coatings for printed circuits and electronic assemblies is that they act as moisture and gas barriers to prevent corrosion and breakdown of electrical insulation. Water absorption is of interest because of its effects on corrosion and degradation of the coating through dimensional changes, for example. It should be noted, however, that all present coatings absorb water and are permeable to moisture and other gases to a greater or lesser degree and cannot provide hermetic seals that welded metal packages can.

What are the coating alternatives to complete epoxy potting? Hysol epoxy is unsuitable for dip coating as its viscosity is too low and its surface tension is

---

[1]Epoxy encapsulation has been the subject of several studies.[2-4] The most detailed of these, by Debney,[4] shows that leakage through a 0.125-in. (0.32-cm) thick epoxy layer (immersed in distilled water) can take place in 18 to 456 days, depending on the type of epoxy.

[2]Mackey, R. S., Plastics and Other Materials, Biomedical Telemetry (John Wiley and Sons, New York, 1968), chapter 4.

[3]Wickham, G, G., and Cartmill, T. B., *Med. J. Australia* 2, 138-139 (1971).

[4]Debney, D. J., Cardiac Pacemaker Encapculation Investigation, *Biomedical Engineering* 6, 458-472 (1971).

too high to cover sharp points and edges. The same is true for Dow conformal coating QR4-3117, but to a lesser extent. The combination of silastic, silicone fluid, and spermaceti wax can also be ruled out, the silicone fluid being primarily responsible for the adverse performance. Moreover, the polyurethanes show excessive degradation or distortion in saline solutions.

Two experiments were used to evaluate a number of coating materials. In the first experiment, the following materials were used to fully encapsulate 15-MΩ resistors with a minimum coating thickness of 50 mils (1.3 mm): Hysol epoxy, silastic RTV 382, Paraplast tissue embedding medium (basically paraffin wax), Elvax 8003J and 8003K, and polyurethane F48-50MS and F78-50MS. After 220 days of complete immersion in a saline bath,[5] none of the resistors showed any change in resistance. The polyurethane coatings, however, showed considerable dimensional distortion, presumably from the temperature effects and from moisture absorption.

In the second experiment, resistors (>10 MΩ) were coated with materials listed in table 1 and immersed in a saline bath. The resistances of these resistors were measured daily. A resistor coating was judged to have failed when the value of the resistor had fallen to approximately 75 percent of its original value. "Successes" are coated resistors which are presently maintaining more than 75 percent of the original value. The results are summarized in table 1.

[5]11 g NaCl per liter, maintained at 37°C.

Table 1. Coated Resistors, Tank Tests.

Material	Samples (number)	Successes (percent)	Lifetimes of successes (days)	Lifetimes of failures (days)
Silastic 382RTV	4	100	213, 203, 203, 170	-
Silastic + 15% beeswax	2	100	197, 197	-
Wax/Elvax 85/15 (melt)	6	100	114, 114, 114, 114, 114, 114	-
Elvax 8003J (melt)	9	67	213, 183, 183, 183, 183, 183	3, 6, 5
Elvax 8003K (melt)	9	44	213, 196, 196, 196	14, 14, 60, 73
Parylene C	10	30	213, 203, 203	10, 10, 10, 20, 20, 65, 37
Beeswax (melt)	3	33	114	30, 64
F300 Saran (Soln)	11	18	204, 204	1 to 8
F310 Saran (Soln)	9	22	206, 206	1 to 10
Kel-F/800 (Soln)	23	9	170, 170	1 to 25
Dow QR4-3117	3	0	-	10, 10, 10
Polyurethane	5	0	-	3 to 50

These experiments showed that there are several polymers which can inherently provide good long-term moisture barriers, but that there are difficulties in obtaining good surface coverage when applying relatively low viscosity conformal coatings as is indicated in the results shown in table 1. Two factors ought to influence the results in table 1: the inherent permeability of the polymer and its thickness or covering power. The results do not seem to be explainable on this basis, however.

The results in table 1 would seem to indicate that Silastic RTV 382 (with or without beeswax) is the ideal conformal coating because no failures occurred. Although widely used for its excellent biocompatibility, silastic is universally condemned as a moisture barrier. It appears likely, however, that failures of materials other than Silastic arose primarily from the difficulty of applying a uniform, completely intact coating to the resistors rather than from an inherent permeability problem of the polymer itself. In the case of the Saran resins F300 and F310, the long-term successes (∿200 days) were all triple-coated with maximum viscosity solutions (20-percent resin, 80-percent MEK), while the failures had fewer coats or were 10-percent solutions. The Kel-F/800 resin behaves similarly; the short-term failures were single-coated, 10-percent solutions in THF. When triple-coated from a 30-percent solution, Kel-F/800 can deliver good performance. The solution-based coatings, Kel-F/800 and Saran, are best prepared by making a dilute solution (∿10 percent by weight), followed by slow solvent evaporation to the desired concentration (30 percent and 20 percent, respectively). If allowed to concentrate more than this, solvent bubbles can be trapped in the increasingly viscous solution. The paraffin wax/Elvax 260 blends show a high percentage of successes and are the easiest materials to apply. Elvax 8003J is to be preferred because of its high Elvax content (30 percent versus 15 percent), its consequent higher viscosity and covering, and its superior barrier properties.[6] These materials have a melting point of about 70°C, which is close to the maximum acceptable temperature for pacemaker handling.

Parylene C has the unusual property of providing a uniform thickness coating (generally 0.001 in.) even over points and edges, a consequence of the vapor deposition method of application. Results with this polymer should indicate the true permeability characteristics rather than any mechanical artifacts. According to published values of moisture permeability,[7,8] Parylene C should perform poorly; yet three samples were successes to more than 200 days. Since the Parylene film and application process are very consistent, in what way did these three samples

---

[6]DuPont Technical Bulletin: Elvax 200 Series Vinyl Resins.

[7]Licari, J. J., Plastic Coating for Electronics, p. 310 (McGraw-Hill, New York, 1970).

[8]Boretos, J. W., Concise Guide to Biomedical Polymers (C. C. Thomas, Springfield, Illinois, 1973).

differ from the rest? Similarly, Silastic should also fail early due to its high permeability, but table 1 shows 100-percent success for Silastic.

The common factor linking these two apparently inconsistent results is the surface adhesion strength between the polymer and the substrate. Silastics can have excellent adhesion even after repeated humidity testing and in the presence of surface contaminants, while Parylene, with a very low coefficient of friction,[9] has poor adhesion under these conditions. The resistivity of polymer films is normally in the range of 10^{12} to 10^{15} Ω·cm, and this is not changed by a factor of more than about 10 after moisture absorption. Hence, there are only two possible mechanisms for electrical leakage of coated MΩ-valued resistors. Either the permeating moisture overcomes the surface adhesion of a large section of the polymer film and moisture collects with ionic contamination (pre-existing or carried through the film)[10] or ionic corrosion products to provide the electrical leakage path, or the film separates at several very small areas because of poor adhesion and moisture builds up to cause a degradation of the film and create an electrical path.[11]

In order to test the adhesion hypothesis, several working Minilith pacemakers were assembled according to production specifications, except as indicated in table 2. All pacemakers were monitored by measuring pulse width, height, and rate, before and after coating at 37°C and 100-percent relative humidity, and finally at various times after immersion in 400-Ω·cm saline solution. These results are best summarized by looking at variations in rate, the most sensitive variable of the three. After 16 months, the standard deviation of the repetition period for the Parylene-coated pacemakers (Nos. 2, 3, and 4) were 4.0, 4.6, and 3.2 percent of the mean, while for the control pacemaker (No. 1) potted in Hysol epoxy, it was 3.3 percent of the mean. Pacemakers 5, 6, and 7 coated with the other materials failed due to corrosion after 6 weeks of immersion in the saline solution.[12] At 20 months, units 1, 2, 3, and 4 all failed due to corrosion at the output connections from the hybrid.

These results indicate that with adequate adhesion promotion,[13] Parylene C provides moisture barrier protection comparable to epoxy potting. In this application, other conformal coatings are unable to perform as well due to poor coverage of edges, points, and corners. A thick Silastic coating would probably be acceptable, but the weight savings and process improvements would be minimal. Parylene

---

[9]Parylene: product literature from Union Carbide.

[10]Wickham, G. G., and Cartmill, T. B., *Med. J. of Australia* (July 17, 1971). (No other information available.)

[11]Roger Olson, Novatran Corp., private communication.

[12]A normal production unit without encapsulated terminals would have failed in less than 30 days if subjected to the conditons of the test.

[13]There are surface treatments which will permit excellent adhesion to almost any surface.[12,14]

[14]Lee, Cupples, Neville, Culp, and Schubert, Artificial Heart Programme Conference, Chapter 65, p. 777 (1968).

Table 2. Protection Procedures for Seven Pacemakers to Test Adhesion Hypothesis.

Pacemaker	Protection Procedure
1 (control)	Lead connections to terminals individually potted in Hysol using a Silastic ring mold; standard Hysol first epoxy pour used on pacemaker contents in can which is left unsealed.
2,3,4	No external can used; 0.7-mil (17-μm) thick coating of Parylene applied after rigorous degreasing and deionizing procedure; teflon-coated lead wires replaced by magnet wire and porous tape on printed circuit board replaced by Silastic (to avoid contamination by soluble components during cleaning).
5	No external can used; coated with an 85-percent wax, 15-percent Elvax formulation blended in-house and melt-dipped at 70°C.
6	No external can used; two-stage coating process used where sharp edges are hand-coated with Silastic 382RTV followed by a melt dip into wax/Elvax as for pacemaker number 5.
7	No external can used; two dip coats of a commercially available silicon-based printed circuit board conformal coating.

C appears to be the material of choice. The application process is consistent, quantifiable, and well-suited to the requirements of pacemaker technology. Quality testing of the adhesion level can be accomplished by saline tank testing of samples for signs of separation or corrosion.

4. Reports of Group Encounters

4.1 Introduction

The following edited reports were prepared by scribes who accompanied the speaker groups as they met with four workshop groups to answer questions and enter into discussions. These reports are meant to summarize the questions and comments that developed in these group encounters. The scribes presented their reports at the end of the workshop so that all participants could share in the results of discussions in which they might not have been able to participate.

4.2 Encounters with Holmes, Hansen, Untereker, and Prosen

Topic: Microcalorimetric Measurements

Bert R. Staples
Chemical Thermodynamics Division
Center for Thermodynamics and
Molecular Science
National Bureau of Standards
Washington, D.C. 20234
(301) 921-3632

Is microcalorimetry applicable for other than just batteries, that is, can the entire pacemaker unit be tested? NBS now has a calorimeter to accept the entire pacemaker. Testing of component parts, however, seems to be the better approach because in testing the entire pacemaker more processes and circuitry are involved, making the interpretation of results very complex.

Can microcalorimetry be used as a 100-percent screening test to assure quality control? Probably not, for a number of reasons. While the method is extremely good as a nondestructive test, the slow equilibration for the batteries, particularly the larger batteries (with high heat capacity), requires long times to attain thermal equilibrium. Thus, only about 4 to 15 individual measurements per day are possible. The time to perform a measurement also depends somewhat on the time constant of the calorimeter which includes contributions from the electronic amplification and measurement system. Most calorimeters have a time constant that ranges from 15 to 60 min. It can be reduced, but that requires some loss in sensitivity or the use of computer prediction extrapolation methods, or both.

There was general agreement that microcalorimetry is not suited for screen testing, but it is suited for testing samples of different production lots. In this way, it can be used as a tool to study different construction and design characteristics and the effect of changes in fabrication processes. Also, microcalorimetric information coupled with electrical test information can resolve the condition of doubtful batteries. This is possible because for new batteries a large heat output is frequently observed if a high electrical impedance is measured.

Who makes the best microcalorimeter for battery measurements? There have been microcalorimeters built for various uses since about 1913. As interest in the application of this method to batteries has increased, commercial sources have developed. Many of the calorimeters have similar characteristics. The main differences are whether they have single or twin cells and the extent of the temperature ranges (5 to 60 or -10 to 70°C). Hart described his calorimeter which has a capability for measuring 1 μW and time constant about 1/2 h for small batteries and about 1 to 2 h for large batteries. Holmes' calorimeter, which is similar to NBS', has a thermal tray for input/output and thus pre-equilibrium is available for 6 to 12 batteries.

4.3 Encounters with Schneider and Gerrard

Topic: Battery Longevity Prediction

Donald B. Novotny
Electron Devices Division
Center for Electronics and
Electrical Engineering
National Bureau of Standards
Washington, D.C. 20234
(301) 921-3621

During the encounter sessions, the speakers realized that both of their results were in essential agreement. The area of disagreement is in how sharp the knee is on the voltage versus time plots of lithium-iodine cells.

There is a sincere interest in knowing how to predict reliably the end of cell life. Schneider explained that under certain specified current-drain level conditions, which the pacemakers can be designed for, definition of the knee of the curve by measuring a 15- to 40-kΩ rise in cell impedance should give a minimum of 5 months' warning prior to cell exhaustion.

It was also stressed that the cell is part of a circuit and the characteristics of this circuit should be incorporated in determining the life of the cell. For example, the knee is sensitive to the pulse energy — the time integral of the current-voltage product. If a pacemaker is designed to provide a constant energy pulse, the pulse duration must be increased as cell voltage drops and cell impedance increases. Under these conditions, the cell appears to expire much sooner and abruptly than under constant pulse width or constant external impedance conditions.

An interest in the kinetics of cell life was also expressed. The cell essentially derives its energy by the simultaneous oxidation of lithium and reduction of iodine. This process increases the thickness of the lithium-iodine electrolyte between the electrodes. After the process has proceeded to some extent, iodine is depleted from the poly-2-vinylpyridine complex. When this depletion reaches a certain point, the resistivity of the cell increases dramatically and the useful

cell energy is depleted. The depletion of this layer is irreversible to some extent. The degree of irreversibility depends on drain rates.

The modeling of the logarithm of the cell voltage drop as a function of the state of discharge of the battery, Q, shows a family of curves for different drain rates and is essentially in agreement with the kinetic models of discharge. The plot of logarithm voltage drop versus Q shows a characteristic up-swing indicating the termination of useful cell life. This model also implies that cell life estimates determined by initially high cell drains followed by periodic typical pacemaker drains may be optimistic. The reason is that the degree of irreversibility of a process occurring in the cell is history-dependent. The cell is more apt to completely recover from the effects of a large initial drain than from those effects caused by a continual low-level drain.

4.4 Encounters with Kraus, Epstein, Lehmann, and Garrett

Topics: Battery Characterization and Quality Control

Robert N. Goldberg
Chemical Thermodynamics Division
Center for Thermodynamics and
Molecular Science
National Bureau of Standards
Washington, D.C. 20234
(301) 921-2752

Regarding the use of neutron radiography, Garrett said that the technique cannot at present be used to detect the end-of-life of batteries. Side-view examinations have been attempted, but they were not successful; three-dimensional techniques may be attempted in the future. The proposal of exposing patients to neutrons in order to check the status of their pacemakers may not be practical. Neutron radiographs can be obtained commercially for approximately $50 per exposure. Facilities to make neutron radiographs cost about $120,000 or more, and they must be licensed. The effect of the neutron irradiation on the chemistry in the pacemaker is in all probability insignificant.

Regarding the lithium thionyl chloride battery, a question was asked about the so-called unforgiving design of the battery in that the quality of the chemicals must be very high, the design geometries are limited, and the sulfur dioxide evolved must be dealt with. In response, Epstein said that the quality of the reagents must be very high, but this is also true for the lithium-iodine battery. The problem of sulfur dioxide has been dealt with. Furthermore, the present design geometry "works" — of 60,000 batteries manufactured to date, not one has failed. In response to another question, he said that one possible way to detect one bad cell in the 200 in a lithium thionyl chloride cell is to use impedance measurements. To date, no one has been able to do this, however.

Regarding the life characteristics of lithium-iodine batteries, Kraus responded to questions saying that the maximum and average level of corrosion of stainless steel observed in her studies were 0.0018 in./yr (46 μm/yr) and 0.0001 in./yr (25 μm/yr), respectively. Moisture content appears to be the most significant variable affecting the type of corrosion. It was not necesssary to use 316 stainless steel because the 304 stainless steel used was sufficiently resistant to corrosion. Immersion life tests were linearly extrapolated from four months of data to get corrosion rates per year. The cathode current collector was measured for one year. It would be better to have more data to establish confidence in a linear extrapolation and work to obtain that data is underway.

Regarding the SAFT lithium battery, Lehmann in response to questions said that traceability of incoming raw materials is maintained insofar as it is possible. Also, tests are conducted on all incoming raw materials.

Other questions resulted in the following points. There is no center of information that collects reliability information on pacemakers. Each manufacturer maintains such information of its own products and FDA works with a few hospitals to collect such information which it makes available. A national pacemaker registry might be useful.

The lithium-iodine battery is reliable because of its low and uniform self-discharge rate. One can expect differences in the failure modes for different types of batteries. Battery failure occurs when either the raw material is nearly depleted or when an open circuit occurs.

4.5 Encounters with Thomas, Wilary, Ferreira, Sulouff, Der Marderosian, Perkins, and Hasegawa

Topic: Moisture and Reliability

Stanley Ruthberg
Electron Devices Division
Center for Electronics and
Electrical Engineering
National Bureau of Standards
Washington, D.C. 20234
(301) 921-3621

A question was raised about the relative value of using the mass spectrometer for gas analysis and for the measurement of moisture alone. If one is only interested in moisture, other more cost-effective measurement procedures are probably satisfactory. But it was pointed out that gas analysis is particularly useful for analyzing new devices to "fingerprint" the interior environment. Furthermore, one must be concerned about other gaseous contaminants such as oxygen, hydrogen, and fluorocarbons. For example, Freon TF plus moisture will form hydrochloric acid.

There was also concern expressed about ionic contaminants in a moist environment and the dendritic growths that can result. If one can achieve clean surfaces,

there is no problem with the presence of moisture, said one speaker. Another pointed out that there is some question about what is a clean surface. Reference was made to work done which showed that even a few atoms of chlorine interacting with moisture can cause aluminum corrosion. Another pointed out that even without ionic contamination one would have problems. The examples of silver and gold migration in a moist environment were cited.

The question about using desiccants in packages to absorb moisture was asked repeatedly. Some manufacturers use desiccants routinely. RADC says that desiccants must retain the absorbed water at a temperature of 100°C. Doubt was expressed if the available desiccants can meet that performance level. To make effective use of a desiccant, it must be dry initially and the amount of moisture that will need to be absorbed must be known.

Can one expect to have a reliable circuit if the water content in the package interior is less than 5000 ppm_v? RADC is starting two programs to make that determination. Moisture-induced parameter shifts have been observed in MOS circuits with a moisture content between 1000 and 5000 ppm_v. No changes have been observed for moisture contents less than 500 ppm_v. A participant pointed out that assuring an initial low water content is not insurance against moisture that will penetrate or evolve in the package during the life of the product.

Pertinent to bake-out procedures, a question was asked if there are any circuits that can be exposed to temperatures as high as 150°C. The response was yes. In particular, hybrid circuits with tantalum capacitors were mentioned. A lithium-iodine battery manufacturer volunteered that they have exposed about 750 batteries to 100°C for about a year.

Sulouff was asked if he was able to correlate helium detector leak rate measurements with hole size in their experiments. He said he could not because of the irregular passageways of their microholes.

4.6 Encounters with Bangs and Llewellyn

Topic: Welding of Pacemaker Enclosures

Stanley Ruthberg
Electron Devices Division
Center for Electronics and
Electrical Engineering
National Bureau of Standards
Washington, D.C. 20234
(301) 921-3621

Most of the questions asked pertained to a comparison of the laser and electron beam techniques. Regarding the advantages of each, the speakers said that there is little difference technically. They are both fusion welds, and the surface tension of the melt affects the nature of the weld. The quality of the weld depends on how the materials are prepared and fit together.

For final assembly welds, there is little difference in cost and capability between the two systems. There are differences in sensitivity to misalignment, however. Which method to use can be dependent on the joint design and the ability to control alignment. If a good fit of parts for welding is not feasible, then the electron beam is easier to use. If an edge weld is required, there is no difference in using either method. If full penetration welds are contemplated, however, the use of a laser beam is probably not advisable on a production basis.

An electron beam gives a greater depth-to-width weld than a laser beam. Use of a laser allows the weld to be made under controlled gas environments, while the use of an electron beam requires that welding be done in a vacuum. Laser beam welding could be done in a vacuum, but there would be no obvious advantage to do so.

During welding in a controlled atmosphere, there is no problem associated with thermal expansion of the gas near the end of the weld. In using an electron beam, however, there have been problems with contamination near the end of the weld, especially when there are plastic materials inside the container which evolve gas.

There are not enough data about the laser technique to say if it is more stable or more reproducible than the electron beam technique. The electron beam is stable to about one percent.

The optical properties of the parts to be welded are generally sufficiently uniform to provide uniform welds. There are hazards to the operator, however, due to reflections of the laser light. Damage to the retina is possible, so goggles or other safety barriers should be used. It was pointed out that goggles are not adequate protection for a 15-kW laser.

There was considerable interest in ways to test for weld integrity. The speakers related that with electron beam welding it is not practical to test with a helium leak detector method immediately after the weld because of the need to pressurize with the tracer gas. It is possible, however, to test immediately after laser welding because the tracer gas can be used as the gas environment during welding. This allows for the detection of tracer gas trapped inside the container as it leaks through any defect in the weld. The use of ultrasonics to test weld quality nondestructively is not really suitable for the small welds used in pacemakers. Also, there is a danger of damaging the electronics with the ultrasonic energy that might be transmitted inside the pacemaker case. One participant proposed the use of time-lapsed photography as a quality control tool, which was met with interest by the speakers. Sparks caused by material contamination have been seen during welding; such sparks could possibly be detected by this means. The speakers added that there is no significant difference in the integrity of the welds produced by the laser and by electron beam techniques.

A number of other questions were asked. How can crack formation be avoided? The reply was that appropriate joint design is important to avoiding cracks. Also, the weld contour needs to be monitored during the welding process. The biggest problem in making a good weld is the variability of the composition of the materials being used.

Is there any processing after the weld has been made to reduce the possibility of corrosion? Neither of the speakers knew of any.

If full penetration in both the electron and laser welds for pacemakers is not made, should there be a different code for pacemaker welds than for other types? The response was that it could be done. Pacemaker welds are made to achieve a hermetic seal rather than to provide structural strength.

Why is resistance spot welding not used? Problems would be expected in obtaining repeatable welds along the flange that would have to be used for this technique.

Some participants expressed having difficulty in buying 316 stainless steel in small lots. The speakers said that there are a number of suppliers such as Carpenter, Orbach, and others that will provide this material in small lots.

4.7 Encounters with Gilman, Schaldach, and Thornton

Topics: Contamination, Corrosion, and Conformal Coatings

James M. Cassell
Polymer Science and Standards Division
Center for Materials Science
National Bureau of Standards
Washington, D.C. 20234
(301) 921-3336

Does fretting corrosion occur clinically with pacemakers? One gentleman with clinical experience said he and his colleagues have never observed it nor have they been aware that such corrosion has been documented by anyone else. Therefore, is it logical to design or select metals for pacemaker application with an eye to this phenomenon? The strongest clinical evidence that was offered came from the orthopedic area; it was observed that the corrosion of metallic implants in animals when the implant was not rigidly fixed in place was different from the corrosion observed when it was. The question remains whether one can transfer orthopedic-related data to pacemakers.

The question of *in vivo* versus *in vitro* testing was discussed. The specific example noted was a corrosion test employing a 10-percent ferric chloride solution. The answer seems to be that until you have something better, such accelerated test conditons are useful in that they allow comparison with materials which have been demonstrated clinically to be acceptable over

long years of experience. Valid accelerated corrosion tests are needed for metals in order to establish standards.

The importance of the influence of contaminants on a metal's performance in a corrosive environment and the need to eliminate or minimize such contaminants was stressed repeatedly. This is particularly important when the welding aspects of metals required for pacemakers is considered.

Because Parylene C[1] is vapor phase deposited and its effectiveness against moisture requires sufficiently thick coatings over the entire area to which it is applied, the question of quality-control testing was raised. Because the failure mode with most polymeric conformal coatings was judged to be a lack of adequate adhesion to the substrate, a method of applying Parylene C was discussed. It involves a vapor degreasing step with a chlorinated organic solvent, washing with an industrial aqueous cleanser, rinsing with deionized water, drying with clean air, and applying a coupling agent, silane, without any chlorine.

There is no metal ideally suitable for pacemaker application, and we must use what is available. The cobalt-nickel-based alloy, MP35N, combines good working and excellent welding properties with good resistance to corrosion and appears to offer an alternative to the use of titanium. It was noted that the cobalt-chromium molybdenum alloy would be a candidate metal except that it is not obtainable in sheet form.

During fabrication, the excellent properties of a metal can deteriorate and every effort is required to guard against this. Properly annealed metals are a must.

The question of the relation between contact angle measurement and extent of surface coverage by a contaminant was raised. In the partial coverage of a high energy surface by a contaminant, the critical surface tension of that surface, δ_c, gradually decreases with increasing percent coverage until complete coverage yields a value of δ_c equal to that of the contaminant.

The cost of goniometer contact angle measuring equipment was judged to be in the $3,000 to $3,500 range.

---

[1]The chemical nature of Parylene C was defined as a monochlorinated xylene with the chlorine substituted in one of the alkyl positions.

4.8 Encounters with Walker and Meyering

Topics: Electrostatic Discharge Damage and Pacemaker Testing

Thomas F. Leedy
Electron Devices Division
Center for Electronics and
Electrical Engineering
National Bureau of Standards
Washington, D.C. 20234
(301) 921-3621

There are no good general studies on latent or "self-healing" failures, only failure analyses of "suspected lots." The susceptibility to degradation is highly dependent on device technology and often there are surprises. For example, an LPTTL inverter (54L04) showed problems that would not have been expected except after an examination of the circuitry arrangement. Also, internal capacitors in 740 operational amplifiers were zapped even though they were not directly connected to a package terminal.

The avoidance of electrostatic-induced damage requires care in various areas. Careful handling and the use of adequate precautions are important. For example, wrist straps have dramatically improved yields in linear integrated circuits. Checks should be made to assure that antistatic protective measures such as using conductive packaging are effective. Problems have been reported with packing materials which had insufficient conductivity. Additionally, the circuit design should be examined to assure that input/output pins are protected in a fail-safe manner. Some evidence exists that electrostatic-induced failures may be caused by solvent sprays and sandblasting techniques such as commonly used for cleaning and resistor adjustment, respectively.

For guidance in the area of protection from electrostatic degradation, refer to the MIL-M-38510 slash sheets where applicable and also to a future monograph on this subject from the Reliability Analysis Center.

Commercial automatic testing machines are very expensive ($100,000) and not really suited for testing pacemakers. The testing system described by Meyering is a calculator-based machine using a commercially available processor and a custom function generator designed especially for pacemaker applications.

The calculator system was felt to be the best compromise between system speed, flexibility, and language capability. The calculator has the advantage of having prepackaged mathematical routines, eliminating software writing for these functions.

The automated testing system cost was estimated to be about $30,000, of which the pacemaker part represents about $10,000. Time to develop the soft-

ware was about 1 man-month for a relatively experienced programmer in BASIC. There was a feeling that BASIC would be the language for such testing applications.

Microprocessors were felt, at this time, to be too limited in their input/output capability for use in such a complete testing system. However, at least one microcalculator is available for about $700 that may provide a breakthrough for low-cost data logging and testing operations.

With this calculator-based system, the program file can be run but not printed out or modified, and so be secure.

The computer system is commercially available and sets of the documentation of the specialized function generator are available for the price of reproduction costs.

4.9 Encounters with Gerz, Blanco, Hurzeler, and Whitman

Topics: High Reliability Assurance of Semiconductor Components and Lead and Pacemaker Failures

George G. Harman
Electron Devices Division
Center for Electronics and
Electrical Engineering
National Bureau of Standards
Washington, D.C. 20234
(301) 921-3621

Many questions were put to Gerz on communications with vendors with an emphasis on hybrid and chip procurement. Problems of getting vendors to report every significant processing change were cited by the members of the groups. Gerz said that it was possible, with effort, to develop the good communications necessary to obtain satisfactory results. He also distinguished between captive lines and dedicated lines and said that the former is preferred.

Questions on burn-in tests were asked. Gerz maintained that one cannot use a burn-in test without including the burn-in-to-zero-failure criterion he described in his paper.

In responding to the many questions on screen tests and reliability, Blanco emphasized that reliability must be built into the semiconductor device rather than to expect to achieve it by taking products from a normal production line and using selected screen tests. The production line must have proper technical procedures, controls, and processes, as well as proper attitudes of the personnel and management. He felt that one could build the entire electronics for a pacemaker on one chip, but it may be impractical economically.

There was considerable interest in the modes of lead and pacemaker failure. That leads are seldom recovered frustrates that interest. Data from pacemakers

are being studied and analyzed to help delineate various types of failure. Patient-induced death due to pacemaker failure is to be determined; the present death rate is very low.

Much interest was expressed in a slide that showed that pacemakers with hybrid circuits lived longer than those with discrete components. In general, newer models, whether they use hybrid or discrete electronic components, live longer than older models. It is too early to consider the results presented for pulse generators as definitive, however. Detailed interpretation of the data is difficult because the pacemakers in the data base include many changes in design and components.

A mini-symposium was held by one discussion group on the legal liability of suppliers and subcontractors to the pacemaker industry. One participant related that their annual insurance premium had increased from $4,000 to $23,000 in the last two years.

Acknowledgment

I would like to express my deep appreciation for the cooperation and patience of the speakers in the preparation of this report.

This report would not have been completed were it not for the dedicated efforts of Elaine C. Cohen and E. Jane Walters. Mrs. Cohen was responsible for performing the maze of tasks involved in collecting the component parts of this report to make it complete. Mrs. Walters took the final text and figures and created, unassisted, the camera-ready copy of the report. It has been a pleasure and my good fortune to have been able to work with these people.

APPENDIX

Workshop Program

— Wednesday, October 19 —

INTRODUCTION

Harry A. Schafft, National Bureau of Standards

SESSION I: MICROCALORIMETRIC MEASUREMENTS

Chairperson: M. Mosharrafa (Cardiac Pacemakers, Inc.)

Presentations

Pacemaker Battery Microcalorimetry
William S. Holmes (Wilson Greatbatch Ltd.)

The Characterization of Internal Power Losses in Pacemaker Batteries by Calorimetry
L. H. Hansen (Brigham Young University) and R. M. Hart (Tronac, Inc.)

Microcalorimetry: A Tool for the Assessment of Self-Discharge Processes in Batteries
D. F. Untereker and B. B. Owens (Medtronic, Inc.)

A Microcalorimeter for Measuring Characteristics of Pacemaker Batteries
Edward J. Prosen and Jennifer C. Colbert (NBS)

SESSION II: BATTERY CHARACTERIZATION AND QUALITY CONTROL

Chairperson: W. R. Grace (American Pacemaker Corp.)

Presentations

End-of-Life Characteristics of the Lithium-Iodine Cell
A. A. Schneider and F. E. Kraus (Catalyst Research Corp.)

Statistical Projections of Battery Longevity from Accelerated Discharge Data on Lithium-Iodide Power Cells
Douglas J. Gerrard and Boone Owens (Medtronic, Inc.)

Qualification Procedures for Lithium-Iodine Pacemaker Cells and Cell Components
F. E. Kraus, M. V. Tyler, and A. A. Schneider (Catalyst Research Corporation)

Lithium-Thionyl Chloride Battery for Implantable Cardiac Pacemakers
James Epstein (GTE Laboratories)

The SAFT Lithium Battery - Quality System
G. Lehmann and J. P. Rivault (SAFT Departement Piles)

The Interrogation of Lithium Iodide Pacemaker Power Sources with Neutron Radiography
Donald A. Garrett (NBS)

SESSION III: MOISTURE AND RELIABILITY

Chairperson: G. Heenan (Medtronic, Inc.)

Presentations

Moisture Measurements and Reliability - An Overview
Robert W. Thomas (Rome Air Development Center)

Overview of Methods for Reducing Moisture Levels in Hermetically Sealed Pulse Generators
Frank J. Wilary and Arthur W. Burnham (Medtronic, Inc.)

SESSION III: MOISTURE AND RELIABILITY (continued)

The Effects of Moisture on the Reliability of Implantable Pacemakers
Lloyd A. Ferreira (Telectronics Proprietary Ltd.)

Moisture Measurement, Leak Rate, and Reliability - A Status Report
Robert E. Sulouff (Martin Marietta Aerospace)

Experimental and Theoretical Analyses of the Rate of Water Vapor Penetration into Non-Hermetic Enclosures
Aaron Der Marderosian (Raytheon Company)

Moisture Measurement Studies
Kenneth L. Perkins (Rockwell International)

Humidity Calibration Facilities at the National Bureau of Standards
Saburo Hasegawa (NBS)

GROUP ENCOUNTERS*

SESSION IV: TESTING AND RELIABILITY

Chairperson: S. Kolenik (ARCO Medical Products Co.)

Presentations

Electrostatic Damage to Semiconductor Devices
Roy Walker (Reliability Analysis Center)

Procuring High Reliability Hybrid Circuits for Use in Cardiac Pacemakers
Warren A. Gerz (Cordis Corp.)

Reliability Trends of Semiconductor Components for Cardiac Pacemakers
Francesco Blanco (SGS-ATES Componenti Elettronici SpA)

Recent Advances in Automated Testing of Pacemakers
Harold R. Meyering (Custom Devices, Inc.)

An Actuarial Analysis of Lead and Pacemaker Failure
Philip Hurzeler, Richard L. Whitman, and Seymour Furman (Montefiore Hospital and Medical Center)

Panel and Open Discussions

ADJOURN

— Thursday, October 20 —

SESSION V: MATERIALS AND PROCESSES

Chairperson: S. Saulson (Cordis Corp.)

Presentations

Factors to Consider in the Selection of a Welding Process for the Welding of Cardiac Pacemaker Enclosures
E. R. Bangs (IIT Research Institute)

High Energy Beam Welding as an Aid to More Reliable Pacemakers
Steven A. Llewellyn (EBTEC Corp.)

---

* Speaker Groups:
1. Holmes, Hansen, Untereker, Prosen
2. Schneider, Gerrard
3. Kraus, Epstein, Lehmann, Garrett
4. Thomas, Wilary, Ferreira, Sulouff, Der Marderosian, Perkins, Hasegawa.

SESSION V: MATERIALS AND PROCESSES (continued)

Measurement of Surface Contamination Using a Contact Angle Goniometer
Byron Gilman (Medtronic, Inc.)

Corrosion and Accelerated Tests for Metallic Materials in the Encapsulation of Long-Term Pacemakers
M. Schaldach and R. Thull (Zentralinstitut für Biomedizinische Technik der Universität Erlangen-Nürnberg)

Conformal Coatings for Pacemaker Applications
Arnold Thornton (Cardiac Pacemakers, Inc.)

GROUP ENCOUNTERS*

SESSION VI: GROUP ENCOUNTER SUMMARIES

SESSION VII: ISSUES OF CONCERN

Chairperson: Harry A. Schafft (NBS)

ADJOURN

---

* Speaker Groups:
5. Bangs, Llewellyn
6. Gilman, Schaldach, Thornton
7. Walker, Meyering
8. Gerz, Blanco, Hurzeler

NBS-114A (REV. 9-78)

U.S. DEPT. OF COMM. BIBLIOGRAPHIC DATA SHEET	1. PUBLICATION OR REPORT NO. Spec. Publ. 400-50	2. Gov't. Accession No.	3. Recipient's Accession No.

4. TITLE AND SUBTITLE

Semiconductor Measurement Technology: Reliability Technology for Cardiac Pacemakers III — A Workshop Report

5. Publication Date June 1979

6. Performing Organization Code

7. AUTHOR(S) Harry A. Schafft, Editor

8. Performing Organ. Report No.

9. PERFORMING ORGANIZATION NAME AND ADDRESS

NATIONAL BUREAU OF STANDARDS
DEPARTMENT OF COMMERCE
WASHINGTON, DC 20234

10. Project/Task/Work Unit No.

11. Contract/Grant No.

12. SPONSORING ORGANIZATION NAME AND COMPLETE ADDRESS *(Street, City, State, ZIP)*

Same as item 9.

13. Type of Report & Period Covered Final

14. Sponsoring Agency Code

15. SUPPLEMENTARY NOTES

Library of Congress Catalog Card Number: 78-600158

☐ Document describes a computer program; SF-185, FIPS Software Summary, is attached.

16. ABSTRACT *(A 200-word or less factual summary of most significant information. If document includes a significant bibliography or literature survey, mention it here.)*

The workshop, third in a series, served as a forum for pacemaker manufacturers and other interested parties to address technical questions relevant to the enhancement and assurance of cardiac pacemaker reliability. Extended summaries are provided of 27 talks and of eight sets of group encounter discussions on the following topic areas: microcalorimetric measurements to evaluate nondestructively batteries used in pacemakers; qualification procedures, end-of-life prediction, and neutron radiography interrogation of lithium-based batteries; measurement of moisture; moisture effects on the reliability of pacemakers and components; electrostatic-induced damage to semiconductor devices; procurement of high reliability semiconductor components; automated testing of pacemakers; actuarial analyses of lead and pacemaker failures; pacemaker case welding processes; surface contamination measurements; corrosion and accelerated tests for metallic materials; and conformal coatings for pacemaker applications.

17. KEY WORDS *(six to twelve entries; alphabetical order; capitalize only the first letter of the first key word unless a proper name; separated by semicolons)*

Automated testing; batteries; cardiac pacemakers; contamination; corrosion; electrostatic-induced damage; hermeticity; hybrid devices; leak testing; measurement technology; microcalorimetry; moisture; nondestructive testing; pacemaker leads; process control; reliability; semiconductor devices; welding.

18. AVAILABILITY ☒ Unlimited

☐ For Official Distribution. Do Not Release to NTIS

☒ Order From Sup. of Doc., U.S. Government Printing Office, Washington, DC 20402, SD Stock No. SN003-003-02076-1

☐ Order From National Technical Information Service (NTIS), Springfield, VA. 22161

19. SECURITY CLASS (THIS REPORT)	21. NO. OF PRINTED PAGES
UNCLASSIFIED	134
20. SECURITY CLASS (THIS PAGE)	**22. Price**
UNCLASSIFIED	$4.50

USCOMM-DC

☆ U.S. GOVERNMENT PRINTING OFFICE : 1979 O—294-228

NBS TECHNICAL PUBLICATIONS

PERIODICALS

JOURNAL OF RESEARCH—The Journal of Research of the National Bureau of Standards reports NBS research and development in those disciplines of the physical and engineering sciences in which the Bureau is active. These include physics, chemistry, engineering, mathematics, and computer sciences. Papers cover a broad range of subjects, with major emphasis on measurement methodology, and the basic technology underlying standardization. Also included from time to time are survey articles on topics closely related to the Bureau's technical and scientific programs. As a special service to subscribers each issue contains complete citations to all recent NBS publications in NBS and non-NBS media. Issued six times a year. Annual subscription: domestic $17.00; foreign $21.25. Single copy, $3.00 domestic; $3.75 foreign.

Note: The Journal was formerly published in two sections: Section A "Physics and Chemistry" and Section B "Mathematical Sciences."

DIMENSIONS/NBS

This monthly magazine is published to inform scientists, engineers, businessmen, industry, teachers, students, and consumers of the latest advances in science and technology, with primary emphasis on the work at NBS. The magazine highlights and reviews such issues as energy research, fire protection, building technology, metric conversion, pollution abatement, health and safety, and consumer product performance. In addition, it reports the results of Bureau programs in measurement standards and techniques, properties of matter and materials, engineering standards and services, instrumentation, and automatic data processing.

Annual subscription: Domestic, $11.00; Foreign $13.75

NONPERIODICALS

Monographs—Major contributions to the technical literature on various subjects related to the Bureau's scientific and technical activities.

Handbooks—Recommended codes of engineering and industrial practice (including safety codes) developed in cooperation with interested industries, professional organizations, and regulatory bodies.

Special Publications—Include proceedings of conferences sponsored by NBS, NBS annual reports, and other special publications appropriate to this grouping such as wall charts, pocket cards, and bibliographies.

Applied Mathematics Series—Mathematical tables, manuals, and studies of special interest to physicists, engineers, chemists, biologists, mathematicians, computer programmers, and others engaged in scientific and technical work.

National Standard Reference Data Series—Provides quantitative data on the physical and chemical properties of materials, compiled from the world's literature and critically evaluated. Developed under a world-wide program coordinated by NBS. Program under authority of National Standard Data Act (Public Law 90-396).

NOTE: At present the principal publication outlet for these data is the Journal of Physical and Chemical Reference Data (JPCRD) published quarterly for NBS by the American Chemical Society (ACS) and the American Institute of Physics (AIP). Subscriptions, reprints, and supplements available from ACS, 1155 Sixteenth St. N.W., Wash., D.C. 20056.

Building Science Series—Disseminates technical information developed at the Bureau on building materials, components, systems, and whole structures. The series presents research results, test methods, and performance criteria related to the structural and environmental functions and the durability and safety characteristics of building elements and systems.

Technical Notes—Studies or reports which are complete in themselves but restrictive in their treatment of a subject. Analogous to monographs but not so comprehensive in scope or definitive in treatment of the subject area. Often serve as a vehicle for final reports of work performed at NBS under the sponsorship of other government agencies.

Voluntary Product Standards—Developed under procedures published by the Department of Commerce in Part 10, Title 15, of the Code of Federal Regulations. The purpose of the standards is to establish nationally recognized requirements for products, and to provide all concerned interests with a basis for common understanding of the characteristics of the products. NBS administers this program as a supplement to the activities of the private sector standardizing organizations.

Consumer Information Series—Practical information, based on NBS research and experience, covering areas of interest to the consumer. Easily understandable language and illustrations provide useful background knowledge for shopping in today's technological marketplace.

Order **above** *NBS publications from: Superintendent of Documents, Government Printing Office, Washington, D.C. 20402.*

Order **following** *NBS publications—NBSIR's and FIPS from the National Technical Information Services, Springfield, Va. 22161.*

Federal Information Processing Standards Publications (FIPS PUB)—Publications in this series collectively constitute the Federal Information Processing Standards Register. Register serves as the official source of information in the Federal Government regarding standards issued by NBS pursuant to the Federal Property and Administrative Services Act of 1949 as amended, Public Law 89-306 (79 Stat. 1127), and as implemented by Executive Order 11717 (38 FR 12315, dated May 11, 1973) and Part 6 of Title 15 CFR (Code of Federal Regulations).

NBS Interagency Reports (NBSIR)—A special series of interim or final reports on work performed by NBS for outside sponsors (both government and non-government). In general, initial distribution is handled by the sponsor; public distribution is by the National Technical Information Services (Springfield, Va. 22161) in paper copy or microfiche form.

BIBLIOGRAPHIC SUBSCRIPTION SERVICES

The following current-awareness and literature-survey bibliographies are issued periodically by the Bureau:

Cryogenic Data Center Current Awareness Service. A literature survey issued biweekly. Annual subscription: Domestic, $25.00; Foreign, $30.00.

Liquified Natural Gas. A literature survey issued quarterly. Annual subscription: $20.00.

Superconducting Devices and Materials. A literature survey issued quarterly. Annual subscription: $30.00. Send subscription orders and remittances for the preceding bibliographic services to National Bureau of Standards, Cryogenic Data Center (275.02) Boulder, Colorado 80302.

U.S. DEPARTMENT OF COMMERCE
National Bureau of Standards
Washington, D.C. 20234

OFFICIAL BUSINESS

Penalty for Private Use, $300

POSTAGE AND FEES PAID
U.S. DEPARTMENT OF COMMERCE
COM-215

SPECIAL FOURTH-CLASS RATE
BOOK